Escola d'Enginyeria de Telecomunicació i Aeroespacial de Castelldefels
UNIVERSITAT POLITÈCNICA DE CATALUNYA

MASTER THESIS

TITLE: Next-Generation Optical Access Networks Based on Orthogonal Frequency Division Multiplexing

MASTER DEGREE: Master of Science in Telecommunication Engineering and Management

AUTHOR: Marçal de las Heras Mandome

DIRECTOR: Concepción Santos Blanco

DATE: September 30th 2011

Title: Next-Generation Optical Access Networks Based on Orthogonal Frequency Division Multiplexing

Author: Marçal de las Heras Mandome

Director: Concepción Santos Blanco

Date: September 30th 2011

Overview

Orthogonal Frequency Division Multiplexing (OFDM) is a robust modulation and multiplexing format which is at the base of many present communication standards.

The interest of the OFDM application in optical fiber deployments is quite recent. As the next generation of Passive Optical Networks (NG-PONs) is envisioned, targeting greater capacity and user counts, the limitations of TDMA (Time Division Multiplexing Access) approaches to meet the expected increase in requirements becomes evident and therefore new technologies are being explored. Optical OFDMA is an emerging technology which can be a promising candidate.

The main goal of this Master Thesis is to study the problem of users multiplexing in access networks, using OFDM as a technology to transmit the user information data. This work has focused in the uplink study of the network, because it is the most challenging part of the network to design.

The studies have been conducted both in a theoretical way and also by simulating the targeted environments by means of a fiber optics transmission simulation tool. *Virtual Photonics Integrated* (VPI) is the software selected for the simulations. This tool is specially designed to simulate optical transmission system environments.

The analysis of the Optical Beat Interference, which is a critical impairment in optical carrier multiplexing schemes, is the most important part of the user multiplexing study.

“Primerament, vull donar les gràcies a la Conchi per la forma en què s’ha dut a terme aquesta col·laboració, pel seu tracte i per les seves contagioses ganes d’aprendre i ensenyar.

Hi ha moments en que t’adones de les persones que realment paguen la pena. Aquest Projecte de Final de Carrera el vull dedicar a l’Edurne i a l’Alfonso; ells ja saben perquè…”

INDEX

CHAPTER 1. INTRODUCTION

Orthogonal Frequency Division Multiplexing (OFDM) is a promising modulation and multiplexing format that has proven successful in a variety of communications applications such as wireless local area network (WLAN), Wi-Fi and WiMAX standards (IEEE 802.11 and IEEE 802.16 respectively). In addition, the OFDM concept is the basis for the Digital Subscriber Line family standards (xDSL) as a modulation and multiplexing technique. In this case, however, is called Discrete Multi-Tone (DMT) due to different details in the application.

Despite the advantages that OFDM provides in other fields, the interest in optical fiber deployments is quite recent because it is just now that the performance in silicon signal processing CMOS circuits are capable of meeting the requirements of high-speed optical communications systems.

The deployment of fiber-optic technology over the past two decades has lead to a significant bandwidth growth in backbone telecommunications networks [P0] However, access networks, which cover the last-mile areas and serve numerous residential and small business users, have not been scaled up commensurately. Mostly, the local subscriber lines are still using twisted pairs and coaxial cables [P0] As the demand for access bandwidth increases with emerging high-bandwidth applications, those access networks have become a bandwidth bottleneck in the current telecommunications infrastructure.

Although fiber-optic systems excel in high-bandwidth applications, optical fiber has been slow to achieve its goal of fiber to the premises or to solve the last mile problem. However, as bandwidth demand increases, significant progress towards this goal can be observed.

Regarding the infrastructure expansion, Figure 1.1 shows the evolution of Fiber to the House/Building (FTTH/B) deployments. The Spanish performance is quite poor as compared to the majority of the European countries.

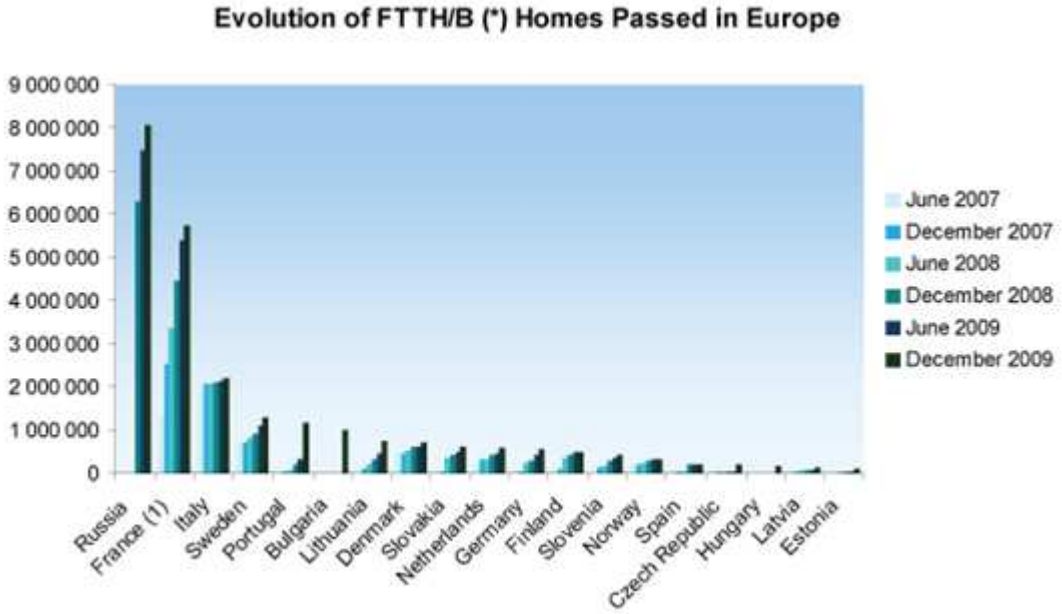

Figure 1.1. European countries FTTH/B home-deployments comparison

As seen, there is a generic trend towards increasing the fiber optic infrastructure with different intensity depending on the country. As the new generation of fiber optic networks is targeted with greater user count, greater reach and greater velocities, new technologies need to be explored and their potential assessed to tackle the next step and finally see a true take off of fiber optic technology towards the users home.

As the next generation of Passive Optical Networks (NG-PON) is envisioned, targeting greater capacity and user counts, the limitations of present TDMA (Time Division Multiplexing Access) approaches to meet the expected increase in requirements becomes evident and therefore new technologies are being explored. Optical OFDMA (Orthogonal Frequency Division Multiple Access) is an emerging technology which can be a promising candidate.

Currently, the main reasons to spend effort in the study of electrical sub-carrier multiplexing for optical fiber deployments are related to the TDM drawbacks. First of all, TDMA-PON has an energetically inefficient performance in some deployments, despite the latest researches introducing *sleep-mode* in the Optical Network Units (ONUs) using fast clock recovery circuits, among other methods. Secondly, the current TDMA-PON have limited scalability capacity.

OFDMA with its dynamic subcarrier assignment capability is expected to allow a more efficient sharing of network resources and also better network re-configurability and adaptability to changing conditions. It further provides simple scaling to multilevel formats, which increase the spectral efficiency for offering higher data rates without increasing the bandwidth requirements.

Another point where advances are expected is in networks convergence. Mobile communications are responsible for a great amount of the networks traffic. Traditionally the mobile backhaul is handled by a separate network. Important

benefits can be derived from the synergic convergence of home networks and mobile backhaul. It is then worth exploring technologies that may allow the routing of both types of traffic in a unified network in a simple and cost-effective way. Since mobile networks are based on OFDMA protocols, the use of that technology in the converged network can be an advantage towards that direction.

Assessment of the potential of OFDMA technologies for new generation optical access networks and for network convergence are the two basic building blocks of *Accordance*, which is an important research and development European project in which our University takes part.

The A*ccordance* project is composed by partners from around Europe. Its investigations are related to a new paradigm for the access networks, trying to develop a new concept facing the future needs of the next generation connectivity. Its main goal is the introduction of OFDMA into PON architectures.

Accordance introduces a novel high-capacity extended-reach optical access network architecture, based on OFDMA technology. This proposed architecture is not only intended to offer improved performance compared to evolving TDMA-PON solutions, but it also provides convergence between optical- radio- and copper-based access[I1].

This project has been conducted under the supervision of the Signal Theory and Communications department at UPC. The research within this Master Thesis is added to the collaboration of the UPC into the *Accordance* project.

The main goal of this Master Thesis is to study the basis of users multiplexing in access networks, using OFDM as a technology to transmit the user information data. Note that this work has been focused in the uplink, in other words, the direction in which the customer equipments send the information to the service head-end. The studies have been conducted both in a theoretical way and also by simulating the targeted environments by means of a fiber optics transmission simulation tool.

The starting point of this work is a brief chapter about the study of basic concepts of OFDM. At the same time, the main features of OFDM transmission systems based on optical fiber are treated.

The following chapter is dedicated to explain the basic aspects of optical transmission systems. The chromatic dispersion and the basis of optical modulation and detection techniques are treated in depth. Then, the software used to carry out the simulations of this Master thesis is introduced: *Virtual Photonics Integrated* (VPI). This tool is specially designed to simulate transmission system environments. Moreover, it has some transmission system templates. A point-to-point long-haul OFDM optical fiber system template has been used as a basis for further developments.

Studies about specific features of OFDM point-to-point optical transmission systems have been undertaken through the VPI tool, such as the use of

guardbands and optical filters. In order to do that, the point-to-point template included in VPI for the simulation of long-haul optical OFDM links has been modified to fulfill the access networks characteristics

In the last chapter lies the most important contribution of this work, which is the study of an important impairment in optical carrier multiplexing schemes, the Optical Beat Interference (OBI) present when information from different sources is detected in the same photodiode receiver.

Finally, in the last chapter, the main conclusions that can derived from the work carried out are summarized and also, the future research lines in this field are outlined according to the results.

CHAPTER 2. OFDM BASICS

The main goal of this chapter is to establish the basis of Orthogonal Frequency Division Multiplexing technique. Based on the analysis carried out in this chapter along with the basis of optical transmission systems that are explained in the next chapter, the different optical OFDM proposals contained in CHAPTER 4 can be understood.

2.1 FDM Systems

The Frequency Division Multiplexing (FDM) scheme is defined by the fact that the data symbols to be sent are assigned to a set of frequencies known as subcarriers and sent in parallel. See Figure 2.1.

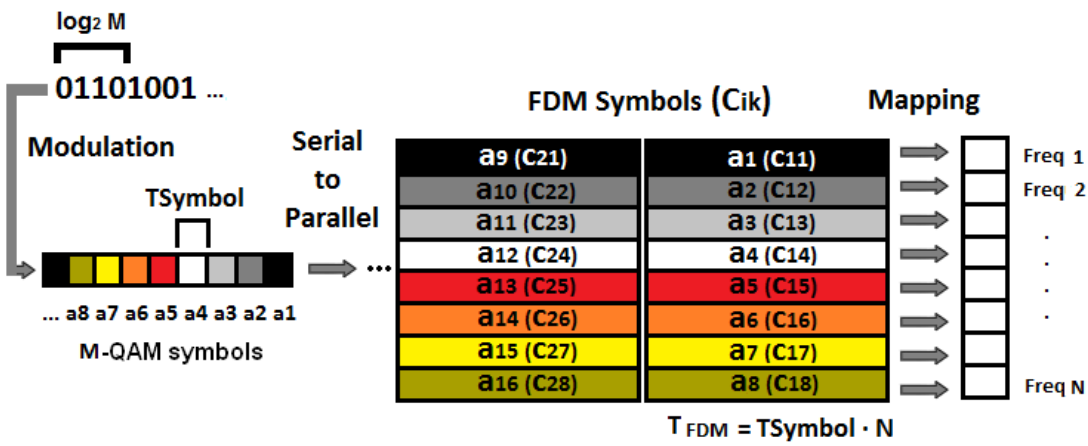

Figure 2.1. FDM mapping scheme

As seen, the original bit sequence is mapped into complex data symbols, usually following a M-QAM format, with M the number of QAM levels, meaning that for any $log_2(M)$ bits a complex M-QAM symbol is obtained. Then the serial symbol sequence is converted to a N-parallel sequence, with N the number of subcarriers, where each parallel channel is assigned to a different frequency subcarrier. Since N symbols are required to form an OFDM frame, each OFDM symbol is N times longer than each of the individual QAM symbols, and the data rate is reduced by a factor *N*.
Mathematically, the resulting complex signal can be written as follows:

$$X(t) = \sum_{i=0}^{N_{FDM}} \sum_{k=0}^{N-1} C_{ik} \cdot e^{j2\pi k\Delta f t} \cdot p(t - iT_{FDM}) \qquad \textbf{(E2.1)}$$

Being *N the* number of subcarriers and *kΔf* the frequency of each subcarrier. N_{FDM} represents the FDM frames. The expression ***P(t - i·T$_{FDM}$)*** represents the frame pulse with duration ***Tfdm= N·Tsymbol***. In the ideal case it is a squared pulse.

The principal advantage of this modulation scheme is that when selective frequency fading occurs, only the data contained in the subcarriers affected by the fading is lost, whereas in single-carrier systems the whole stream of symbols is affected.

Since the individual QAM symbols are complex numbers, the usual way to modulate them into the corresponding subcarrier frequencies is to assign respectively the real and imaginary parts of each symbol to the phase and quadrature components of each frequency. See Figure 2.2.
.

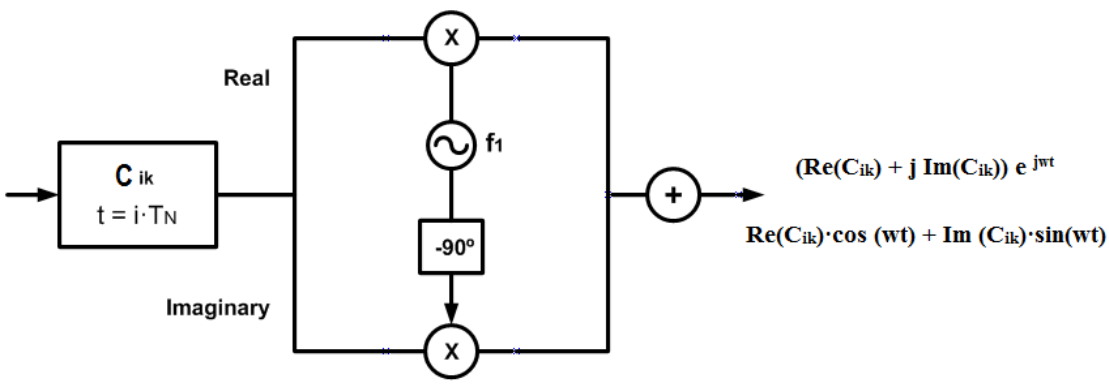

Figure 2.2. FDM transmitter

The resulting signal is:

$$Xsent(t) = \sum_{i=0}^{N_{OFDM}} \sum_{k=0}^{N-1} \left[[\mathrm{Re}]C_{ik} \cdot \cos(2\pi f_k t) + [\mathrm{Im}]C_{ik} \cdot \sin(2\pi f_k t) \right] \qquad \textbf{(E 2.2)}$$

At the receiver side, in order to recover the original symbols a technique to separate the information carried by each subcarrier is required. This technique is based on electrical mixers acting as down-converters and low pass filtering. See Figure 2.3.

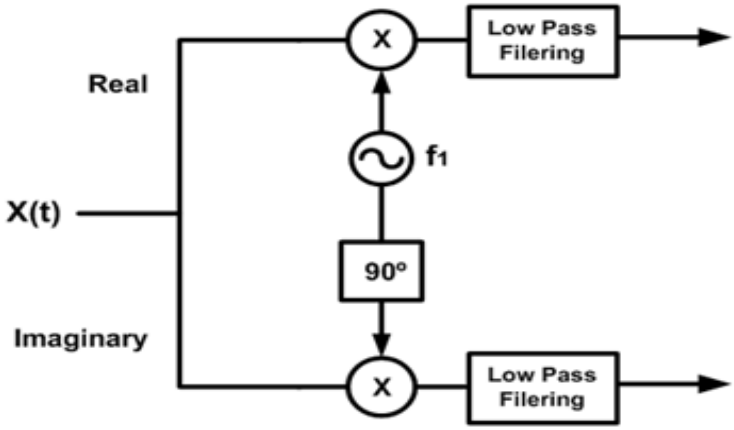

Figure 2.3. FDM Receiver

Of course for the filters to properly separate the information contained into each frequency wide enough frequency guard bands among subcarriers are required which entail a loss of spectral efficiency.

In order to improve the spectral efficiency, in OFDM the individual subcarrier spectra are allowed to overlap, because they can be recovered thanks to the orthogonality condition as explained into the next section.

2.2 OFDM Systems: Orthogonality

To fulfill the orthogonality condition among the subcarriers, the frequency spacing between them is selected so that the FDM symbol comprises a complete number of subcarrier periods, i. e.

$$\Delta f = \frac{1}{To_{FDM}} \qquad \textbf{(E2.3)}$$

Being T_{OFDM} the OFDM symbol duration. The Figure 2.4 shows the shape of an OFDM signal in the time domain. It is shown the proportionality in the period of the signals.

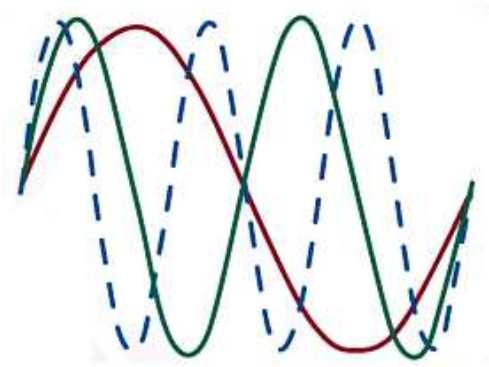

Figure 2.4. OFDM signal in time domain [I1]

Then, a receiver such as the one shown in Figure 2.3 will allow to recover the information in any subcarrier, despite the spectral overlap among the subcarriers.

From a spectral viewpoint, the orthogonality condition applied to proper recovery of symbols in reception is understood as a frequency down-conversion of the OFDM signal such that the required subcarrier falls at zero frequency. The zero frequency value of the down converted signal corresponds to the symbol in the targeted subcarrier since all other subcarrier contributions go to zero at zero frequency. Figure 2.5 is a graphical representation of the process of symbol recovery in the spectral domain.

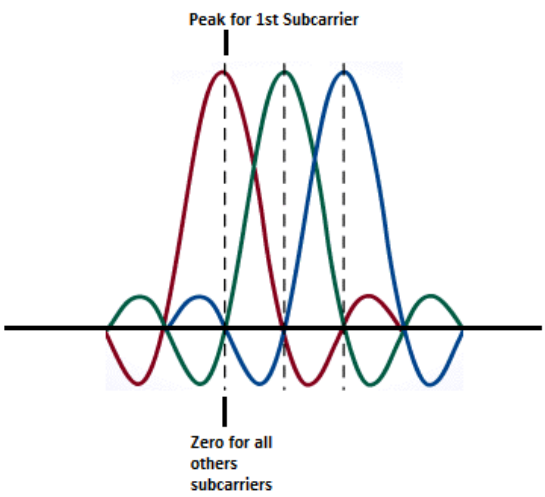

Figure 2.5. Graphical representation of the OFDM recovery of symbol *k* in the frequency domain [I1]

Mathematically, the spectrum in the frequency domain of one OFDM symbol obeys the following expression:

$$X(\omega) = \sum_{i=0}^{N_{OFDM}} \sum_{k=0}^{N-1} C_{ik} \cdot P(\omega - 2\pi k\Delta f) \cdot e^{-j\omega i T_{OFDM}} \quad \textbf{(E 2.4)}$$

Where the pulse described in (E 2.4 is defined in the ideal case by a *sinc* shape according to:

$$Sinc\left(\frac{\omega - 2\pi k\Delta f}{2\Delta f}\right) \quad \textbf{(E 2.5)}$$

Summarizing, in Figure 2.6 a comparison between FDM and OFDM in terms of spectrum shows the better spectral efficiency of OFDM.

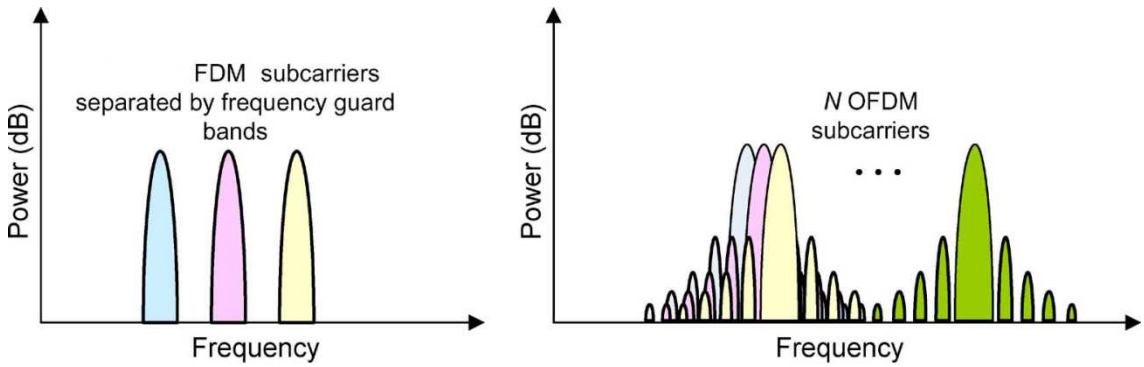

Figure 2.6. Spectrum efficiency comparison between FDM signals and OFDM signals

For an analogue OFDM transmission system, a set of oscillators and low-pass filters is required at reception for each subcarrier (Figure 2.7). Likewise, the generation of subcarriers at the transmission side has to be handled separately, resulting in a complex system in terms of hardware.

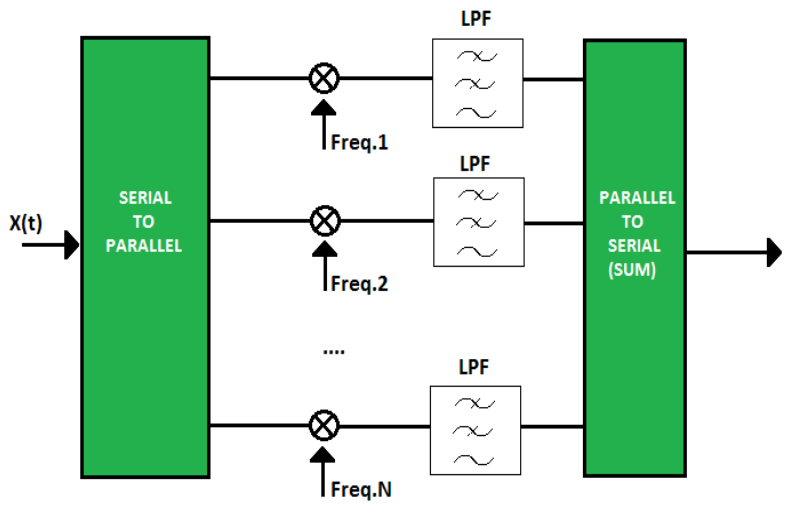

Figure 2.7. FDM Analogue receiver schematic

2.3 Digital generation of subcarriers

The conclusion of the preceding sections is that OFDM systems can provide an efficient way of dealing with frequency selective channels with good spectral efficiency, but they involve a high hardware complexity since for every subcarrier a complete set of IQ modulator/demodulator is required. The real take off of OFDM systems was enabled by the digital implementation. The procedure consists basically in taking the temporal expression of (E2.1 and considering it is sampled every T_{symbol}.

$$X(nTsymbol) = \sum_{k=0}^{N-1} C_{ik} \cdot e^{j2\pi k \cdot \frac{1}{N \cdot Tsymbol} n \cdot Tsymbol} = \sum_{k=0}^{N-1} a_{ik} \cdot e^{\frac{j2\pi Kn}{N}} \quad \textbf{(E2.6)}$$

With n an integer number, (E2.6 represents the Inverse Fast Fourier Transform (IFFT) of an OFDM symbol. Thus, in a digital OFDM system, the IFFT is performed in the transmitter module after the QAM *mapping* process. In other words, the modulation stage involves the IFFT application [P0]

For the parallel demodulation of all subcarriers at the receiver side, the procedure involves the subcarrier detection in the digital domain using the Fast Fourier Transform (FFT) [P2]. As important benefits, the digital system is able to avoid the RF hardware complexity but it introduces the use of digital-to-analogue conversion and analogue-to-digital conversion .Finally, the analogue filtering to separate the subcarriers is not required in the digital system [P0]
Thus, it is possible to avoid the system complexity allowing cost-effective implementations.

2.4 Digital to Analogue converter

As introduced previously, in the transmission, a digital-to-analogue converter (from now on, DAC) is necessary to transform the digital signal into the analogue domain. Specifically, the DAC is needed to convert the discrete values of $X(nTsymbol)$ to a continuous analogue signal.

During the sampling process, some alias of the signal will appear in the frequency domain. By means of filtering, which is the spectral analog of the pulse shaping of the DAC, those undesired alias will be removed.

The need for filtering in the digital-to-analogue conversion stage implies making the signal fit in its suitable frequency band. The output spectrum of the signal will be determined by the pulse shaping filter used at the transmitter, which is an intrinsic part of the DAC. The output of the filter will be determined by the convolution of the impulse response of the filter (called pulse shape) and the symbols at the input.

2.5 Analogue to Digital converter

An analogue-to-digital converter (from now on ADC) is needed to convert the continuous received signal to discrete samples. At the receiver side, an ADC and then FFT are used to recover the signal.

Aliasing is the effect that causes continuous signals to become indistinguishable when they are digitally sampled. When this happens, the original signal cannot be reconstructed from the digital signal. This effect is present when the analogue band-limited signal is sampled below its *Nyquist* frequency. In the analogue-to-digital conversion stage performed in the receiver side, the filter previous to the ADC has to be designed according to an antialiasing procedure. The frequencies which do not fulfill the *Nyquist* criterion have to be filtered out, limiting the bandwidth of the signal.

2.6 Pulse shaping

The pulse shaping filter needed in an OFDM system should be an ideal low-pass filter with a *sinc* impulse response. As a realistic approach in our studies the raised-cosine filter is used.

The raised-cosine filter with a roll-off factor can be used to model the pulse shaping process in both transmitter and receiver modules of the transmission system (see Figure 4.3 and Figure 4.4). In Figure 2.8, the transfer function and the impulse response of the raised-cosine filter is shown.

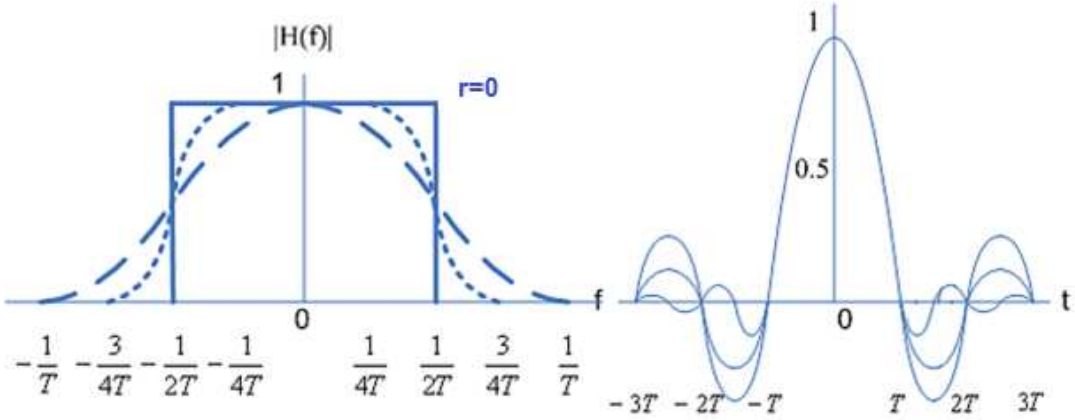

Figure 2.8. OFDM raised cosine filter. System transfer function and System impulse response with different roll-off factor [I2]

The transfer function of the raised cosine filter can be expressed as [I2]:

$$h(t) = 2Wo \cdot \sin c(2Wo \cdot t)\frac{\cos\left[2\pi(W - Wo)t\right]}{1-\left[4(W - Wo)t\right]^2} \qquad \textbf{(E2.7)}$$

$$H(f) = \begin{cases} 1 & |f| < 2Wo - W \\ \cos^2\left(\frac{\pi}{4}\frac{|f| + W - 2W0}{W - W0}\right) & 2Wo - W < |f| < Wa \\ 0 & |f > W| \end{cases} \qquad \textbf{(E2.8)}$$

Where *W* is the absolute Bandwidth. W_o = *1/(2T)* represents the minimum bandwidth for the rectangular spectrum and the -6dB bandwidth. The roll-off factor is defined as:

$$r = \frac{W - Wo}{Wo} \qquad \textbf{(E2.9)}$$

The roll-off factor is going to be an important feature to take into account in the simulations. The typical value used is r=0.2. As shown in Figure 2.8, the roll-off factor r=0 represents an ideal squared pulse.

2.7 Oversampling and zero padding

As it is shown in the Figure 2.9, the output signal at the IFFT block has to be sampled by the DAC. Ideally, the sampling frequency has to fulfill the *Nyquist criterion*, but in practice some oversampling is required in order to reduce undesired effects coming from non-ideal DAC pulse shaping.
The sampling process will create spectral alias. In order to properly eliminate the residual alias after non-ideal pulse shaping, low pass filtering is applied after the DAC. As seen in the figure, more efficient alias removal is allowed by setting to zero some subcarriers at the edges of the signal spectrum (zero padding).

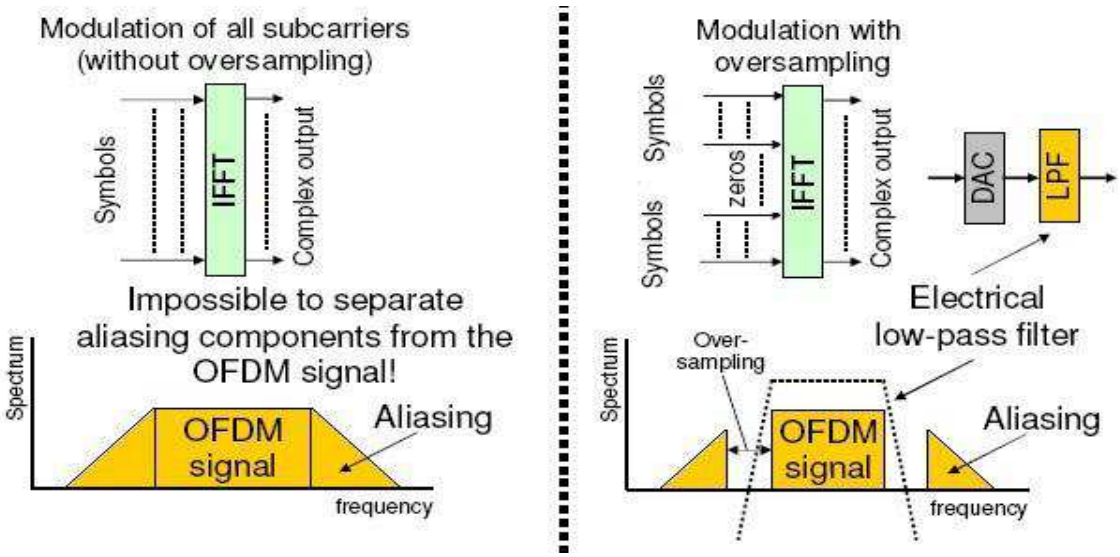

Figure 2.9. Oversampling requirements [P2]

According to the following figure, due to the periodical nature of the FFT, the subcarriers at the spectrum edges are those in the middle of the sequence.

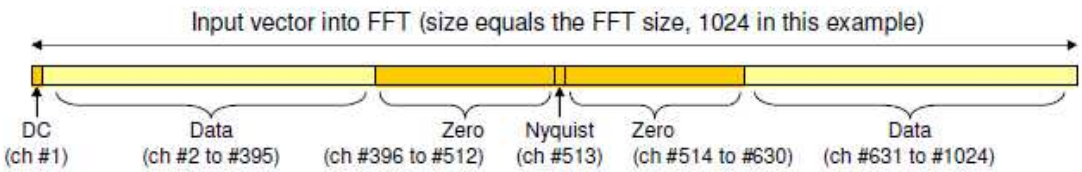

Figure 2.10. Input vector FFT/IFFT [P2]

2.8 Cyclic prefix

The Cyclic Prefix is a guard time inserted at the beginning or at the end of each OFDM symbol after the IFFT. It is shown in Figure 2.11:

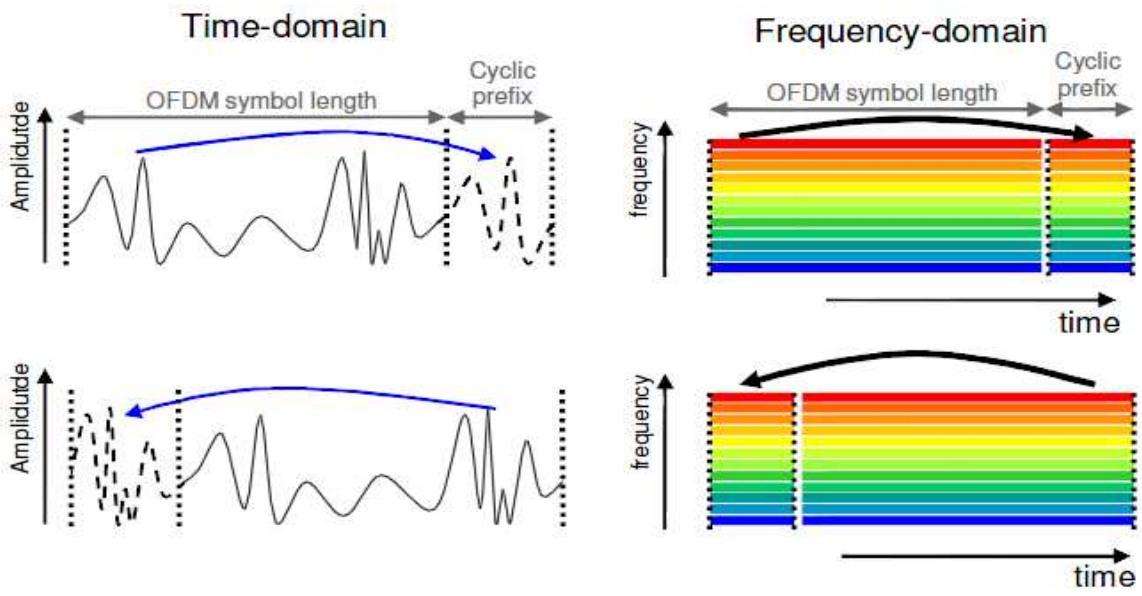

Figure 2.11. Cyclic Prefix [P2]

With cyclic prefix, the OFDM symbol is extended by reinserting the beginning of the symbol to the end (or vice versa). Mostly the chromatic dispersion causes the subcarriers to drift relatively to each other. As a result a cyclic prefix is required to prevent power leakage from neighboring OFDM symbols [P2]. The cyclic prefix reduces the data rate. Typically, the cyclic prefix duration is determined by the expected duration of the channel delay spread in the operating environment.

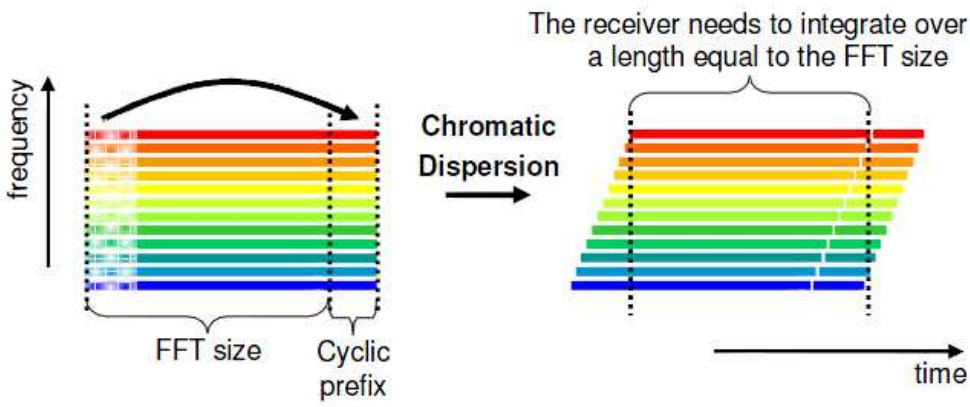

Figure 2.12. Cyclic Prefix [P2]

Note that as long as the number of carriers increases the percentage of overhead decreases because the guard time required for the cyclic prefix only depends on the channel characteristics and therefore it remains the same.

2.9 Equalization and training

The digital data processing has the drawback of requiring DAC/ADC conversion, but it allows for straightforward equalization in the digital domain. In the specific case of OFDM if the subcarrier channels are made sufficiently narrow, the channel behavior can be considered constant for each subcarrier and simple one-tap equalization is feasible. In the temporal domain that is equivalent to considering that the symbol is made long enough so that Inter Symbol Interference (ISI) affects one neighboring symbol at most. Training sequences and pilot tones are the usual means for the channel estimation and for calculation of the equalizer coefficients.

2.10 OFDM transmitter and receiver module

Finally, all concepts explained until now about an OFDM transmission system are depicted in the following figure. The optical modulation/demodulation stages are shown as *black boxes* in Figure 2.13 and will be the subject of the next chapter.

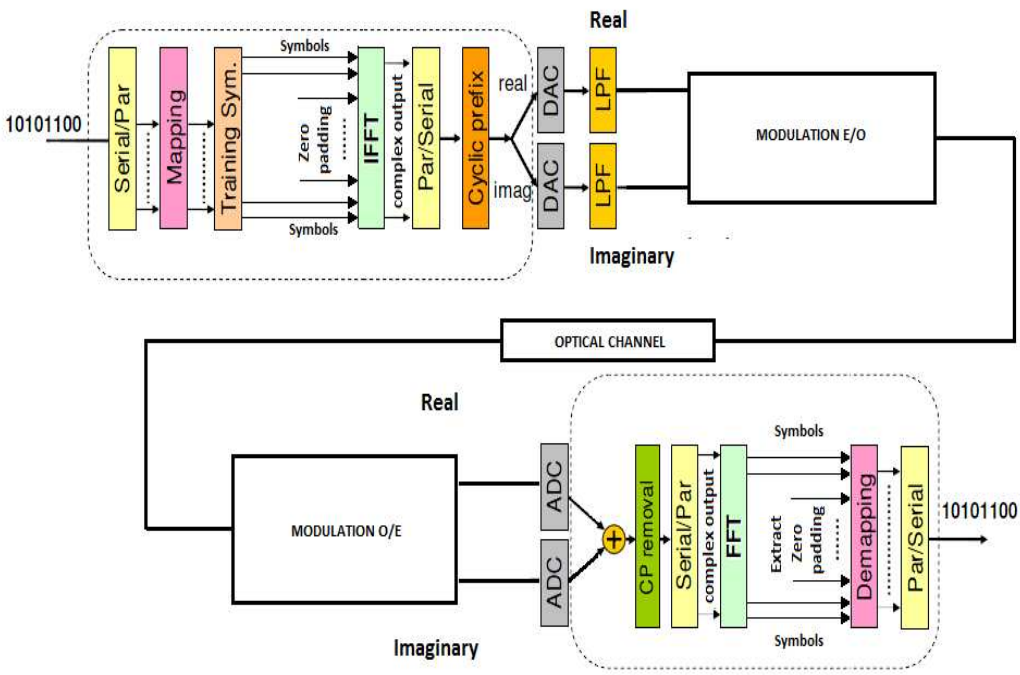

Figure 2.13. OFDM transmission system [P2]

As seen, the input of the transmitter is the bits to be sent. Then, the data is modulated onto symbols according to the selected M-QAM modulation. Afterwards, the symbols are mapped into the different subcarriers.

Then, the training symbols are injected so that the channel transfer function can be estimated. The input of the IFFT block is composed by the symbols coming from all subcarriers and the zero padding data inserted at the suitable place to obtain an oversampled OFDM signal. After taking the IFFT, the complex output has to be serialized and then converted to an analogue continuous signal in order to be sent. The cyclic prefix is inserted in the middle of those two processes. The analogue to digital conversion is applied separately to the real and imaginary parts.

At this point, the real and imaginary parts of the OFDM signal must be encoded into the signal to be sent. In our case, we have to modulate the two parts of the signals over an optical carrier. As it will be seen, there are different techniques to modulate and detect an OFDM signal transmitted over an optical carrier. In this work the focus will be on the IM/DD with RF up and down conversion scheme. See 4.1.

At the receiver side, the received signal is divided again into real and imaginary parts which are digitally converted by two analogue-to-digital converters. Then, the cyclic prefix is removed. The result has to be parallelized in order to be injected into the FFT demodulation block. After the FFT, the zero padding is extracted and then the result is unmapped and serialized, obtaining the information bits.

Regarding the OFDM adaptation to optical fiber based transmission systems, it is important to emphasize two aspects:

- Both real and imaginary parts of the OFDM signal need to be sent [P1]

- It is necessary a linear channel so that equalizations is effective [P1]

These two extremes will be taken into account in the next chapter, where a classification of optical OFDM systems will be made.

CHAPTER 3. OPTICAL SYSTEMS BACKGROUND

Basic concepts of optical communications are described in this chapter focusing in traditional Intensity Modulation with Direct Detection (IM/DD) transmission systems, which at present are the most cost-effective solutions for optical fiber deployments. In order to know the advantages of IM/DD systems in this field, other systems will be explained and compared with IM/DD.

First of all, the optical channel is presented and analyzed. Then, the transmission systems will be the focus of the chapter. The chromatic dispersion, as the most important impairment in fiber transmission systems, is going to be explained in depth.

In the framework of optical access networks, the focus of this Master Thesis is the uplink study because it is the most challenging part of the access networks design.

In addition, the optical access networks and its main components are introduced as a basis for the further advances in following chapters. In this scheme, the main modules studied are:

- Terminal service equipment, acting as service head-end.
- Customer terminal equipments, acting as network transceivers.

Cost effective solutions have been studied for the customer terminal equipments. By contrast, since the head-end equipment is shared by many users, this solution can be more expensive.

Several solutions including those not based upon IM/DD schemes will be analyzed and a classification has been done in order to know all the possibilities to consider, with their respective advantages and drawbacks. In the chapter 4, the system to be further analyzed will be presented.

Finally, the software used to carry out the simulations of this Master thesis is introduced along with its basic transmission system templates.

3.1 The optical channel: chromatic dispersion

The chromatic dispersion is the main limiting effect in optical fiber communications. In addition, there are other impairments such as the nonlinear effects which arise for very high fiber launch powers. The launching powers considered throughout this Master Thesis are low enough to consider nonlinear effects negligible.

The effects of the chromatic dispersion when a signal is transmitted through a single mode optical fiber can be represented by the expression of (E3.1:

$$X_{out}(\omega) = X_{in}(\omega) \cdot e^{-j\beta(\omega)z} \quad \textbf{(E3.1)}$$

Where $X_{in}(\omega)$, $X_{out}(\omega)$ are respectively the input and the output signals in the frequency domain, β is the propagation mode phase constant and Z is the fiber length.

Ideally, the dependence between the phase constant and frequency is linear. Therefore, all spectral components suffer the same propagation delay. However, in a dispersive channel the phase constant has a nonlinear dependence with frequency. So, the different frequency components undergo different delays and consequently, the received signal differs from the transmitted signal [T3].

The propagation constant of a pulse centered at frequency ω_o, which is propagated on a dispersive channel can be approximated by a *Taylor series* [T3], assuming the phase constant varies slowly in the frequency bandwidth of interest ($\Delta\omega = \omega - \omega o << \omega o$), the resulting expression is:

$$\beta(\omega) \approx \beta_o + \Delta\omega\beta_1 + \frac{\Delta\omega^2}{2}\beta_2 \quad \textbf{(E3.2)}$$

Where:

- β_o is related to the phase velocity concept (v_{ph}). The phase velocity is defined as the rate at which the carrier signal is propagated. It is given by the following expression:

$$\beta_o = \beta(\omega_0) \leftrightarrow v_{ph} = \frac{\omega_o}{\beta_o} \quad \textbf{(E3.3)}$$

- β_1 is related to the group velocity concept (v_g), defined as follows:

$$\beta_1 = \left.\frac{\partial\beta}{\partial\omega}\right|_{\omega=\omega_0} = \frac{1}{v_g} = \tau_g \quad \textbf{(E3.4)}$$

The group velocity is the varying rate of the wave envelope when it is propagated. This effect gives the information about the actual delay of the information [T3].

- β_2 is related to the Group Delay Dispersion (GDD). It is defined as follows:

$$\beta_2 = \left.\frac{\partial \beta_1}{\partial \omega}\right|_{\omega=\omega_0} = \frac{\partial \tau_g}{\partial \omega} \qquad \textbf{(E3.5)}$$

The Group Delay τ_g in (E3.4 and (E3.5 is given in seconds over fiber length; it expresses the delay experienced by 1 Km of an envelope signal centered at frequency ω_0. In practice, the chromatic dispersion is characterized by the parameter D, which gives the group delay variation in reference to the wavelength. It is related to the GDD as [T3]:

$$D = \left.\frac{d\tau_g}{d\lambda}\right|_{\lambda=\lambda o} = \left.\frac{d\omega}{d\lambda}\right|_{\lambda=\lambda o} \cdot \beta_2 = \frac{d\lambda \cdot \left(-2\pi c/\lambda^2\right)}{d\lambda}\beta_2 = \frac{-2\pi c}{\lambda^2}\beta_2 \qquad \textbf{(E3.6)}$$

Where:

$$\lambda o = \frac{2\pi c}{\omega o} \qquad \textbf{(E 3.7)}$$

The delay difference between any two subcarriers will depend on the difference in wavelengths, the value of D and the propagated length. It is illustrated in Figure 3.1. In this Thesis, considering the typical wavelength of optical access networks (1.55µm, third window), the typical D value has been set to *17ps/nm per Km*.

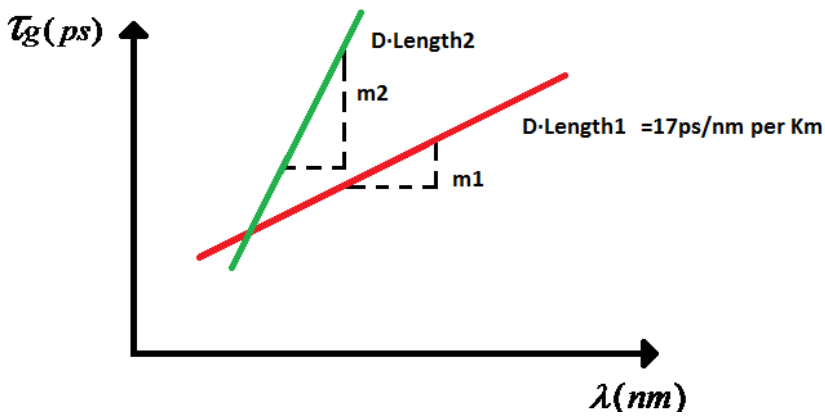

Figure 3.1. D value behavior depending on the fiber length.

3.2 Optical modulation techniques

This subchapter introduces the optical modulation, which is the process of impressing information on a light carrier. It involves varying one or more features that define the optical wave, such as its power level, frequency, phase or polarization.
The phenomena of light emission and detection in optical communications are based on photon-electron exchanges taking place in certain materials and devices. First of all, the photons emission results from the injection of electrons in the optical sources. In the other side, the absorption of photons by the optical detectors results in an electrical current.
Therefore the name Intensity Modulation (IM) applied to conventional modulation techniques, since it is indeed the optical intensity (not the field amplitude) the one that follows the variations of the signal.

In what follows the two basic kinds of IM will be presented: Directly Modulated Laser (DML) and Mach-Zehnder Modulation (MZM) in its quadrature point. Due to its cost-effectiveness the DML will be the one treated in more depth into the following chapters.

3.2.1 Directly Modulated Laser (DML)

With the direct modulation of a laser source, the amount of light power (P_o) that emerges from the laser diode depends linearly on the electric current injected into it for currents above a certain threshold. By adding a bias current, the information signal variations are directly translated into variations of light intensity. This is known as intensity modulation (IM) and it is the simplest way to transmit information through an optical fiber [T2]. Figure 3.6 shows a scheme of a laser diode, where P_o and I_T are, respectively, the optical output power and the feeding current (see also Figure 3.6).

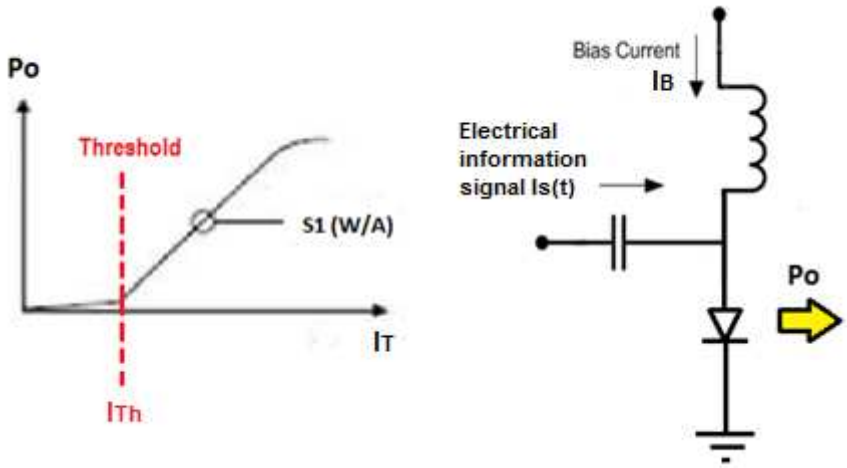

Figure 3.2. Characteristic curve and schematic of a laser diode

3.2.2 External modulator: MZM

The operating principle of the Mach-Zehnder is based on the electro optical effect that occurs in some crystals such as lithium niobate ($LiNbO_3$). This effect makes the optical signal sensitive to a refraction index whose value depends on the electrical field (*E)* applied
The three electrodes depicted in Figure 3.3 induce the electrical field which depends on the RF signal applied. The optical signal will be amplitude-modulated owing to the phase difference between the two modulator branches. In the usual IM mode, the MZM modulator is polarized where its optical power over voltage response is linear, referred as the quadrature point.

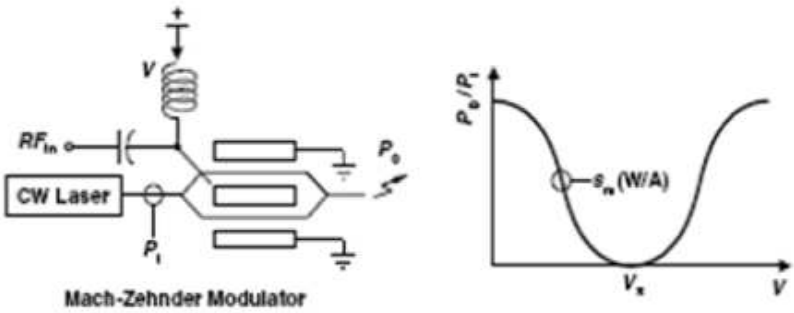

Figure 3.3. Mach Zehnder Modulator intensity modulation scheme and its quadrature point

The output optical power of the MZM can be expressed mathematically as follows:

$$P_{out}(t) = P_{in}(t)\cos^2[\Delta\Phi(t)]$$
$$\Delta\Phi(t) = \frac{\Delta\Phi_1(t) - \Delta\Phi_2(t)}{2} \qquad \textbf{(E3.8)}$$

Being *Δ* the phase difference between the two MZM branches, which is proportional to the electrodes driving amplitude. By using a MZM biased at its null transmission point (see Figure 3.4) a field amplitude modulation with suppressed carrier is obtained.

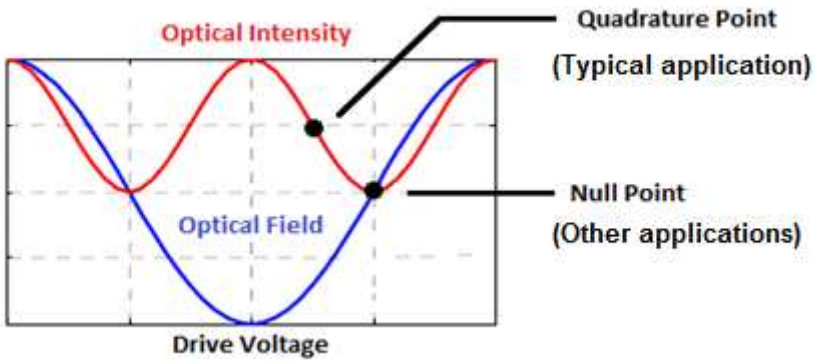

Figure 3.4. Mach-Zenhder optical modulation curve

The characteristic Mach-Zehnder modulator curve is given by the Figure 3.4, in which the bias points for quadrature and null points are shown respectively. The output electric field of the Mach-Zehnder has a cosine shape; by modulating it in the null point the relation between the electric field and the voltage becomes linear.

3.3 Optical detection techniques

There are basically two techniques that allow the detection of an optical OFDM signal at the receiver side, the direct detection (DD) and the coherent detection (CO-D).

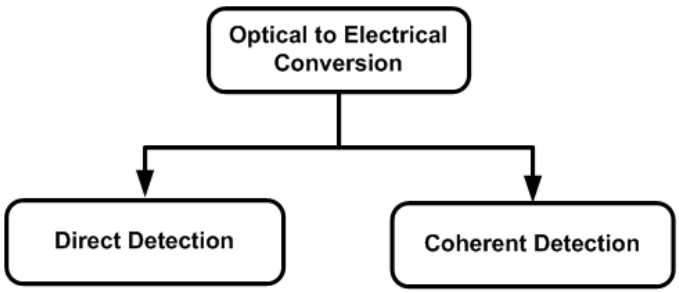

Figure 3.5. Optical detection classification

The direct detection is the simplest and more cost-effective optical detection method. Coherent detection-based systems have a better sensitivity and their spectral efficiency is higher. They allow compensation of linear channel impairments such as chromatic dispersion because the detected photocurrent is proportional to the optical field amplitude. However, the main drawback of the systems based on coherent detection is the complex requirements in the receiver design.
This Master Thesis focuses on direct detection receivers. These detectors are usually PIN diodes, which carry out the inverse function of the transmitter power detecting and transforming intensity power changes into proportional current variations. Mathematically, the detected photocurrent is obtained by applying the square modulus operation over the low-pass equivalent of the incoming optical field:

$$I(t) \propto \left|E(t)\right|^2 \qquad \textbf{(E3.9)}$$

Therefore, the system selected for further analysis will be composed by an intensity modulation scheme at the transmitter side combined with a direct detection scheme at the receiver side (IM/DD).

3.4 IM/DD optical transmission system analysis

A mathematical IM/DD system analysis has been developed based in DML because of its cost-effectiveness and low complexity compared with MZM.

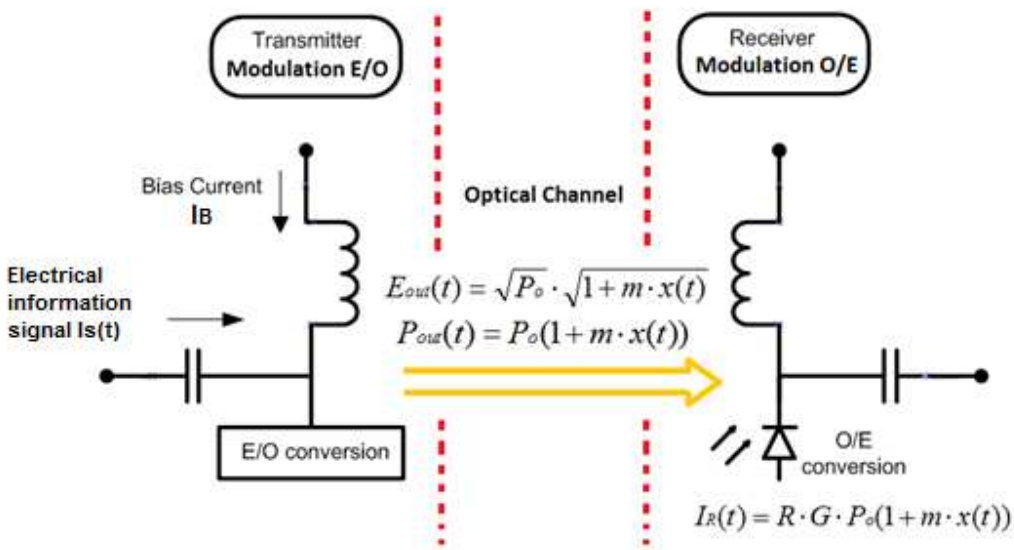

Figure 3.6. Intensity Modulation with Direct Detection schematic

According to Figure 3.6 and Figure 3.2, I_T is defined as:

$$I_T(t) = I_B + I_s(t) \quad \textbf{(E 3.10)}$$

The optical power at the output of the optical transmitter is [T2]:

$$P_{out}(t) = S \cdot \left| I_T(t) - I_{Th} \right| \quad \textbf{(E3.11)}$$

Being *S* the slope efficiency of the laser and $I_T(t)$ the current associated to the sent message. I_{th} is the current threshold shown in Figure 3.2. According to (E3.12, *Is(t)* is described as the product of the peak amplitude of the current (I_m) and the signal *x(t)* normalized to unity.

$$I_s(t) = \mathrm{I_m} \cdot x(t) \quad \textbf{(E3.12)}$$

Finally, the expression of the optical power at the output of the laser is:

$$P_{out}(t) = S(I_B - I_{Th})(1 + \frac{I_s(t)}{(I_B - I_{Th})}) = P_o(1 + m \cdot x(t)) \quad \textbf{(E3.13)}$$

Where *m* is defined as:

$$m = \frac{\mathrm{I_m}}{I_B - I_{Th}} \quad \textbf{(3.14)}$$

The received intensity (in an ideal channel) is a function of the PIN diode responsivity *R* and the gains of the amplifier devices in reception (*G*):

$$I_R(t) = R \cdot G \cdot P_o(1 + m \cdot x(t)) \quad \textbf{(E3.15)}$$

The detection is done directly by means squared law detectors, according to the expression in E 3.9.

3.4.1 IM/DD spectrum and guardbands

Starting from the expression of the output power of IM modulation ((E3.13), the output field is given by:

$$E_{out}(t) = \sqrt{P_o} \cdot \sqrt{1 + m \cdot x(t)} \qquad \textbf{(E3.16)}$$

Moreover, to gain insight into the spectral content of the signal, we consider the Taylor series expansion of E 3.17:

$$E_{out}(t) = 1 + \frac{m}{2} x(t) - \frac{m^2}{8} x^2(t) - \frac{m^3}{16} x^3(t) - \ldots \qquad \textbf{(E 3.17)}$$

The different orders of the polynomial will basically give rise to different harmonics of the modulated passband signal x(t).
When modulating the intensity or the optical power, the spectrum of the modulated optical signal will be composed by the optical carrier and several sidebands which are higher order replicas of the original signal at both sides of the optical carrier (Figure 3.7). This effect is due to the fact that it is the optical intensity and not directly the amplitude of the electrical field of the optical wave the magnitude that is proportional to the information signal.

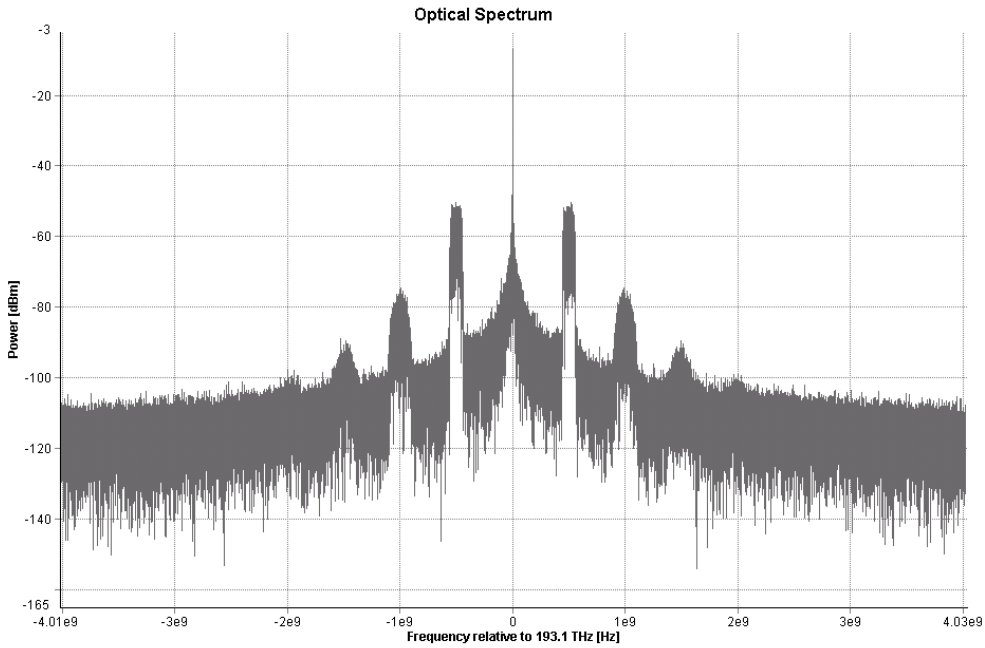

Figure 3.7. Signal with higher-order sidebands. Graphic with OFDM signal at 1 Gbps with a 4QAM modulation, 500MHz as carrier frequency composed by 64 subcarriers. 2km fiber length

Ideally, the spectral components of the signal amplitudes and phases are precise for contributions coming from the mix in a square-law detector of higher order sidebands to mutually cancel. But if the amplitudes and phases of spectral components undergo variations in their propagation through the fiber as a consequence of chromatic dispersion for example, cancellations may not be complete and **nonlinear distortions** will appear at the receiver end [T2].

3.4.2 Guard Bands

To avoid **nonlinear distortion** produced by the chromatic dispersion, the use of guard bands between the optical carrier and the OFDM information signal is needed in both modulation and in detection stages. In the IM modulation so that higher-order spectral sidebands do not overlap and also in the direct detection so that mixing of intraband components fall within the guardband and can be filtered out. The required spectral guard band is of a size at least equal to the signal bandwidth and it ensures that the linearity of the transmission is preserved when using IM/DD optical transmission systems. Figure 3.8 shows the intermodulation products in the receiver side falling inside the guardband.

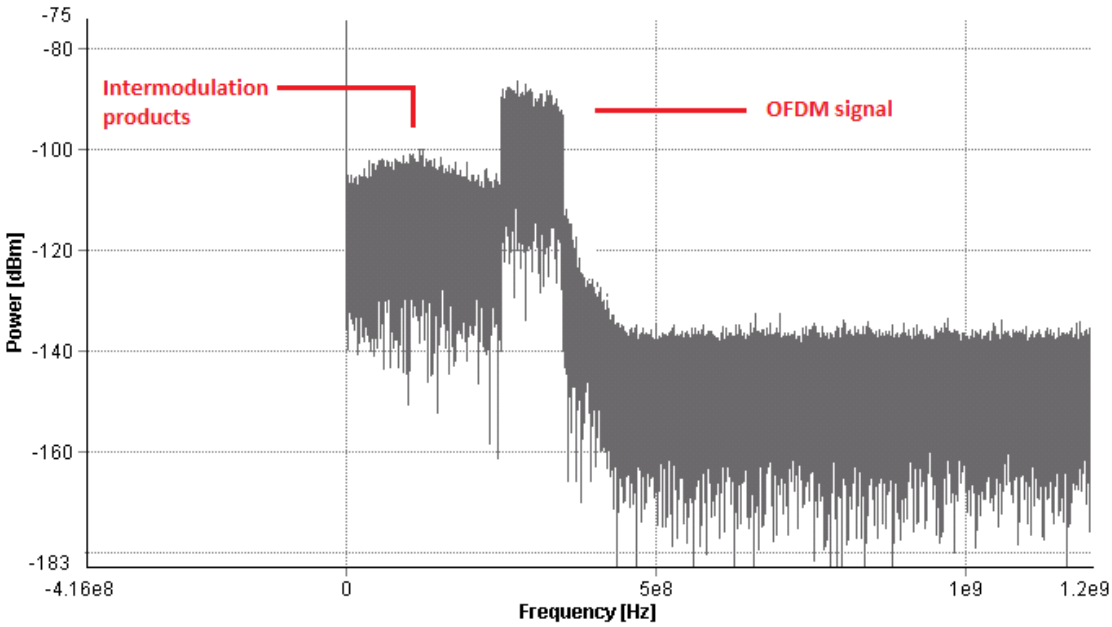

Figure 3.8. Detected OFDM signal with guard band in electrical domain

3.4.3 Single Sideband Filtering (SSB)

Even when the systems linearity is preserved by means of spectral guarbands still the optical modulated signal is naturally a dual sideband signal with two spectral bands at each side of the carrier. Through the direct detection process, these two bands mix with the optical carrier and fall in the same electrical frequency band. Since chromatic dispersion has a different effect on each one, the two bands may interfere causing amplitude fading. This is avoided by eliminating one of the sidebands by SSB optical filtering. The effect is analogous to the image frequency effect that takes place in the process of up and down conversion with frequency mixers in RF transmission systems. In this case, the optical carrier plays the role of the local oscillator.

When the chromatic dispersion effects are small, such as in short-distance/low bit-rate transmission systems, since the expected fading will have little importance, it is possible to consider solutions with double sideband so that the optical filter is spared, entailing not only lower cost and greater power budget but also wavelength independency (colorless operation), which is a much valued feature in optical carrier networks.

3.4.4 Non desired effects in IM-DD systems

In summary as non desired impairments related to chromatic dispersion, we can identify the following:

- **Nonlinear distortion in IM-DD systems:** Avoided by means of guard bands between the optical carrier and the information OFDM signals.

- **Carrier fading:** Related to the image frequency effect as in a RF mixing. This effect is avoided by means of optical SSB filtering.

To give a clear example of generic dispersion effects, in Figure 3.9 it is shown a 4-QAM constellation at the receiver side without dispersion effects in the optical channel (left). The same constellation affected by dispersion is shown at the right side.

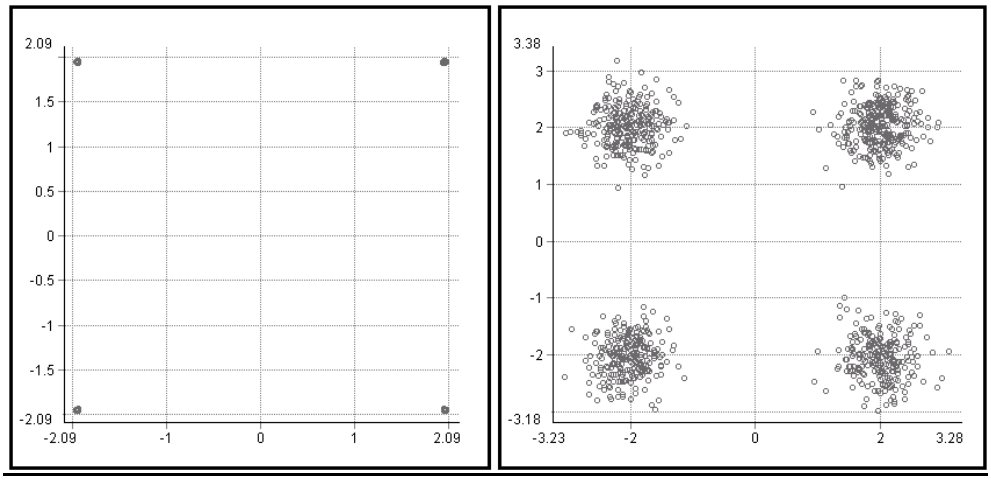

Figure 3.9. Dispersion effect (2km fiber length *vs* 100 km fiber length). No optical filter. Data rate: 1Gbps

3.5 Classification of optical OFDM systems

From the analysis of the basic features of optical systems and the review of OFDM transmission systems, a general classification of Optical-OFDM transmission systems has been proposed.

As explained in 2.10, two are mainly the points to be considering when modulating an electrical OFDM signal over an optical carrier:

1. OFDM signals usually have two components, real and imaginary, while optical modulation techniques usually act over the intensity of the optical signal only.

2. Electro-optical conversions usually have a square-law nature and are hence non-linear, which means that channel equalization strategies based on linear channel behavior need to be adapted. As seen above, spectral guardbands are usually the means to achieve linearity in IM/DD systems.

In what follows several strategies to deal with these two issues are presented and analyzed and a general classification of the more important optical OFDM modulation and detection techniques is proposed. In Figure 3.11 it is seen how different modulation techniques may be combined with different detection strategies.

If IM is chosen as the optical modulation format, it can be achieved by DML, MZM-QP or Electro-Absorption Modulation (EAM). On the other hand, the Hermitian Symmetry (HS) among the subcarriers can be used so that the OFDM signal is purely real and it is modulated on the intensity of the signal.
If a guardband wants to be allocated in order to preserve linearity, then some carriers will have to be set to zero so that it can be considered effectively a field modulation. In the classification it corresponds to the zero-padding label under the Field Modulation branch. This is illustrated in Figure 3.10.

Also an IM modulator may be used in conjunction with electrical IQ upconversion so that both the real and the imaginary parts of the OFDM signal can be modulated over the intensity of the optical signal, and thus HS is not required and all carriers may transmit an information symbol. The RF upconversion frequency may be chosen so that a proper guard band is allocated in order to preserve nonlinearity, i. e. f_{RF} = 1.5BW, being BW the OFDM signal bandwidth.

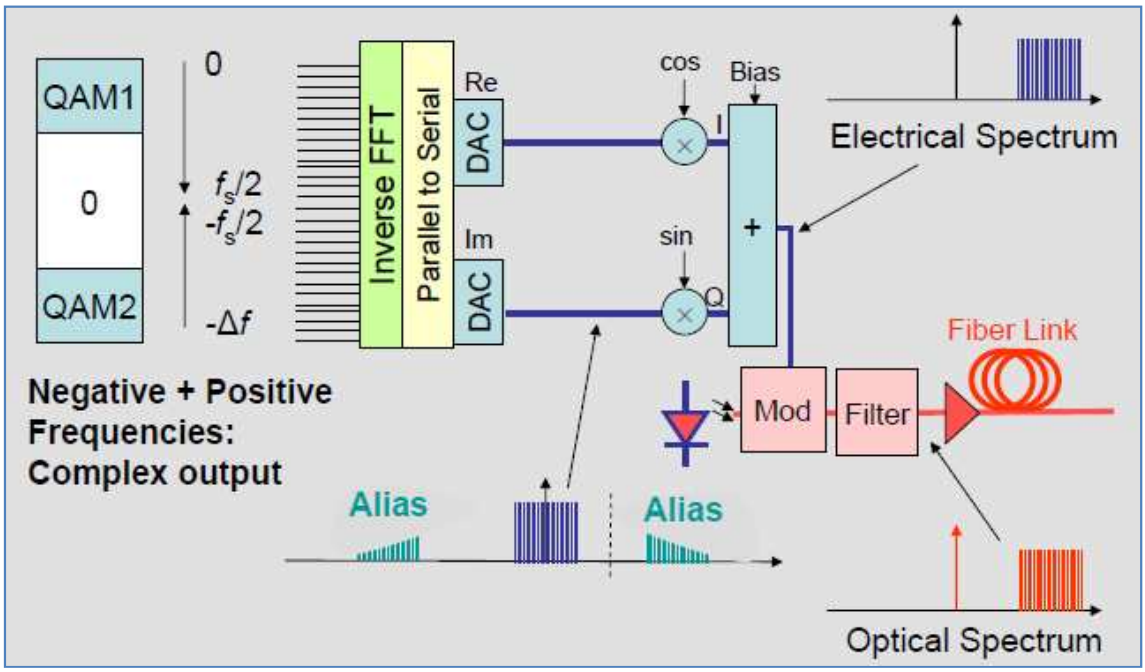

Figure 3.10. Carrier zero-padding setting

On the other hand, field modulation techniques may rely either on a MZM biased at the null point or in an IM with guardbands. In order to be able to modulate the complex OFDM signal, an optical IQ modulator based on nested MZM may be used.

As compared with the electrical IQ technique, the Hermitian Symmetry plus zero padding technique allows to spare the RF up/down conversion stage but requires 4 times the system capacity to transmit the same effective data rate.

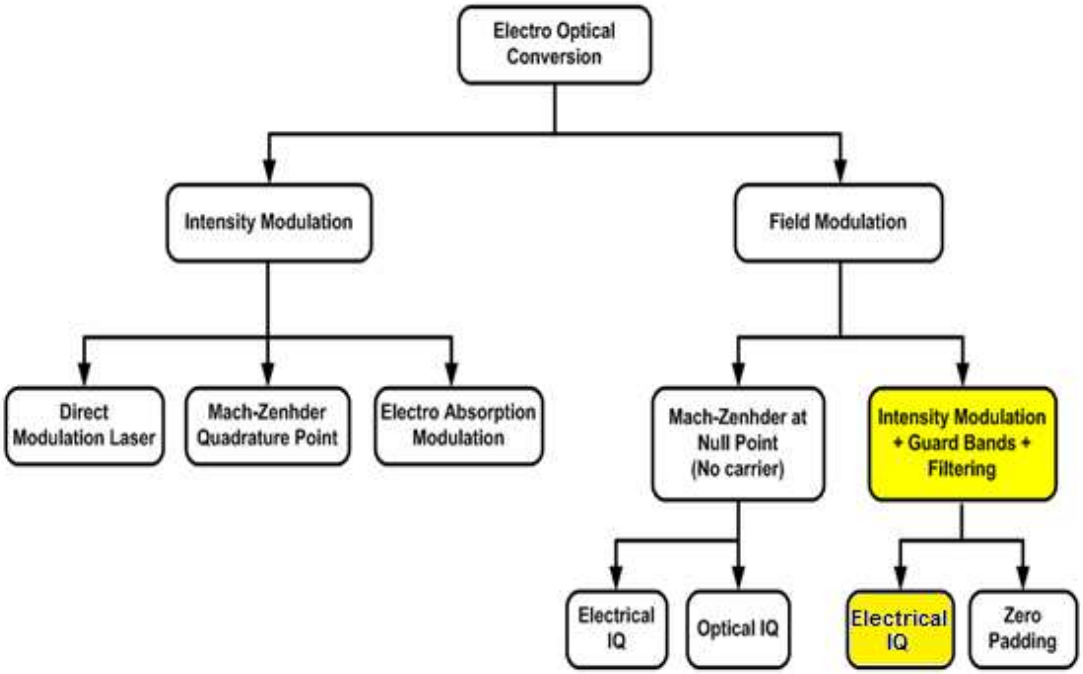

Figure 3.11. Optical Modulation classification

Due to its cost-effectiveness the works within this Thesis will focus on the field modulation scheme based on IM-DD and guard-bands. As compared to the Hermitian Symmetry scheme, the RF upconversion will be considered due to its better bit rate efficiency allowing for lower speed DACs at the user premises, and also due to its higher flexibility for the management of multiuser access through dynamical selection of the RF frequency.

3.6 Optical access networks basis

In this subchapter, basic concepts about optical networks are given as a basis for the next further advances in the optical access networks design. The Figure 3.12 shows an architecture example of a metropolitan optical network implementation.

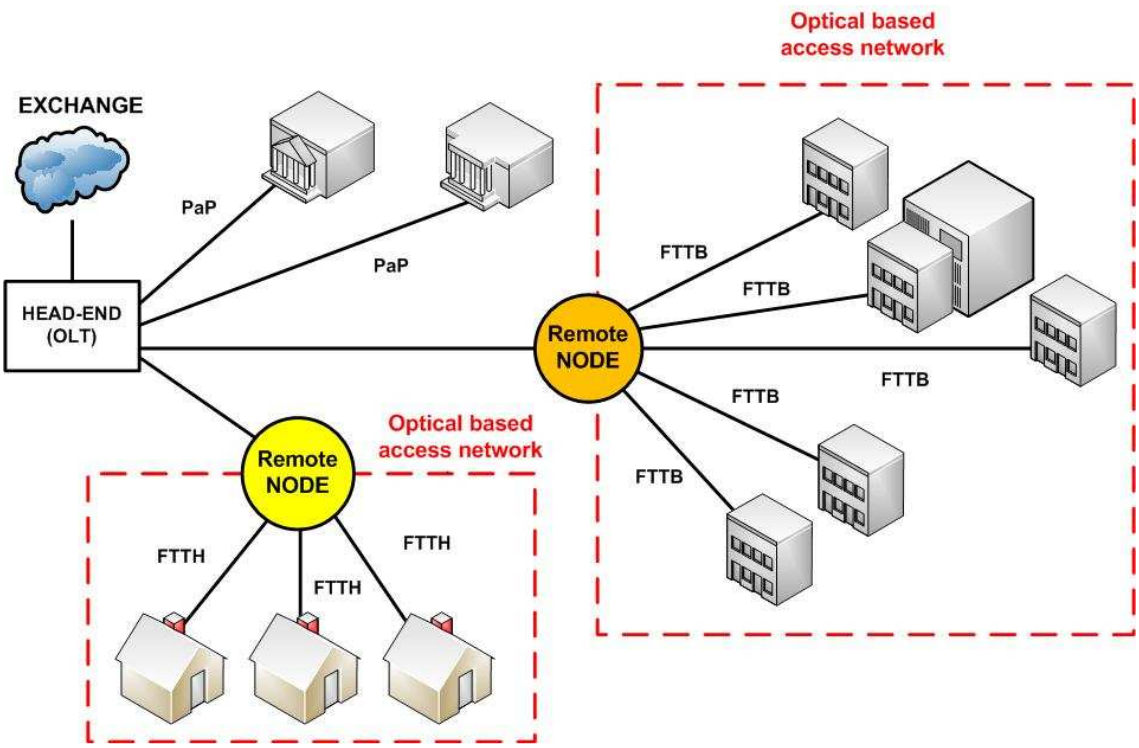

Figure 3.12. Metropolitan optical telecommunication network

The uplink is the term used in a communication link for transmission of information signals from the customer terminal equipments to the service head-end. An uplink is the inverse concept of a downlink, representing the opposite direction of the information flow.

In Figure 3.12 several network elements are identified:

- **OLT:** Optical Line terminal, which is a device that acts as a service provider endpoint in an optical network. It performs conversion between the electrical signals used by the service provider equipment and the optical signals transmitted/received to/from the users. In addition, it coordinates the signal multiplexing process of the customer terminal equipments.

- **ONU:** Optical network unit, placed at the customer side, is the device responsible of the down-conversion of incoming optical signals into electronics at the customer premises in order to provide communication services over an optical fiber network in downlink. Also, it modulates the user information into an optical signal in uplink.

- **Remote Nodes:** According to the previous figure, the topology of the optical network as a star implies the use of intermediate nodes which optimize the optical fiber distribution over the customers, avoiding higher

expenses in materials such as optical fiber and amplifiers. The remote nodes are responsible for covering the access networks area and must be placed strategically covering neighborhoods or business centers. Their capacity will depend on the number of residential or business customers to serve.

Passive Optical Networks deployments are presently taking-off on a global scale. Those deployments are based on time-division multiplexing access with standardized Ethernet-PON (EPON) and Gigabit-capable-PON (GPON) solutions [P11].

Proposing a new paradigm, several studies have focused in frequency multiplexing deployments [I5]. Figure 3.13 shows a block diagram of a bidirectional optical network based on subcarrier multiplexing, assigning different subcarrier frequencies to each ONU.

In the model of Figure 3.13, the ONUs share the same optical channel from the optical coupler *1:N* to the head-end. Each ONU uses an optical carrier to transmit the information in the uplink channel. This optical carrier may be locally generated or remotely sent through the network. On the other hand, an optical receiver is placed in each ONU to receive the transmitted information from the head-end in the downlink channel.

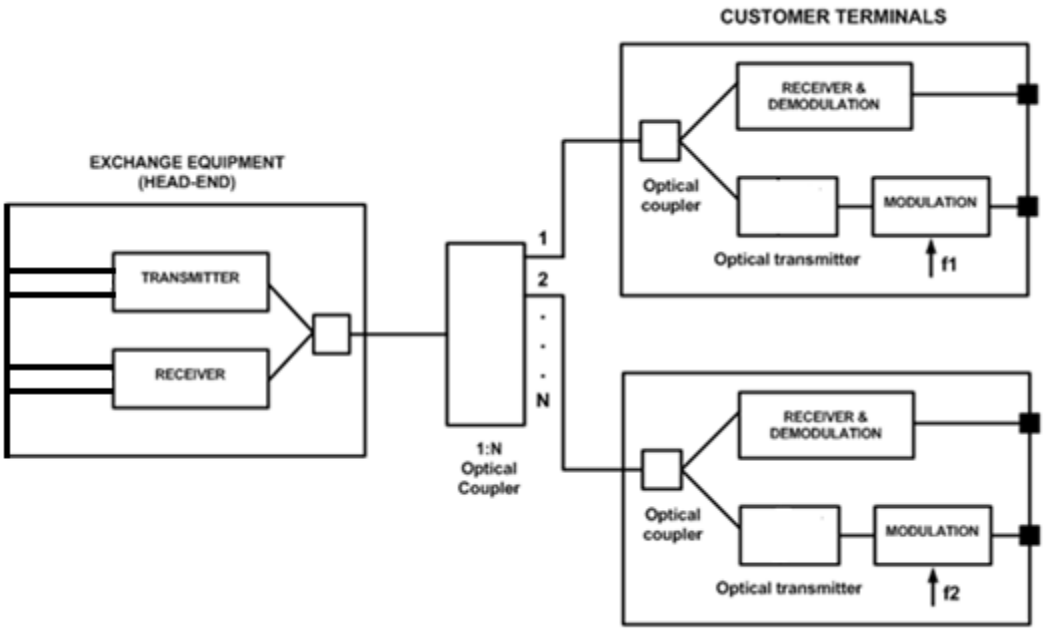

Figure 3.13. Bidirectional optical carrier modulation system [P6]. Direct detection assumed

Due to its higher spectral efficiency, OFDM is selected for the frequency multiplexing of the users signals. In this sense, taking into account the specifics

of the above discussed modulation/detection techniques of OFDM signals onto optical carriers some **Uplink strategies** can be considered:

1. IM/DD strategies:

These formats add in modulation and also require in detection an optical carrier to be sent along with the OFDM sideband. Basically two different cases can be distinguished depending on the choice of the optical wavelength of the optical carrier added at each ONU site.

Same wavelength: When trying to optimize the spectrum available it would be desirable to use the same optical channel for all the ONUs on a segment. If IM is used as a low-cost alternative, all users information will be modulated over an optical carrier with the same wavelength and at the OLT side, the information signals coming from the different users will be detected in different electrical bands. The optical carrier can be generated locally in the ONUs (local sources) or can be sent from the OLT and remodulated in the ONUs (seeded approach) using Semiconductor Optical Amplifiers or Electro-Absortion Modulators. Both solutions are challenging from a practical viewpoint.

- Local generation of the optical carrier needs stringent requirements on the laser frequency stability control in order to maintain the subcarrrier orthogonality.

- The seeded approach on its side, suffers from Rayleigh backscattering issues and also from limited power budget owing to the fact that the optical carrier has to cover twice the distance between the OLT and the ONU. Amplifiers are then required at the ONU side, increasing the cost.

With regard to these solutions, it should be noted that in either case the optical carriers even when they have the exact same center wavelength will have lost coherence at the receiver side. As a consequence, the mixing of data sidebands with carriers coming from a different users will be out of phase and give rise to OBI as it is explained in CHAPTER 5.

Wavelengths at safety distance: As a cost-effective option, also based in an IM/DD with RF upconversion scheme, free-running lasers can be considered in each ONU, with a wide enough spectral gap between their wavelengths so that interfering mixing products among spectral components are kept below a quality threshold.

2. Non IM/DD alternatives:

Another option to consider is a deployment with optical carrier suppression using MZM as a modulation technique. It should be noted that this configuration is too complex and costly for the ONU as

compared with the previous options and would require the addition of a carrier for direct detection or the use of coherent detection at the OLT. This alternative is not going to be considered in this Thesis.

Since the focus is the uplink, the studies within this Master Thesis will consider two options for the multiuser integration, both based in IM/DD schemes with RF upconversion. Both options differ in the wavelength assigned to the optical carrier coming from different users. According to the classification above, the first option considers all users sharing the **same wavelength**. From now on, we will refer to this first option as the **Spectral-Efficient approach.** In the second option, **enough frequency separation** has to be maintained between the wavelengths of the optical carriers belonging to different users in order to guarantee an acceptable Carrier-to-Interference Ratio (CIR). In next chapters, we will refer to this second option as the **Low-cost Approach**.

On the other hand, a practical example has been introduced following the Low-cost approach.

In the proposed model of Figure 3.13, the head end receiver is based in a photo-detector which has to be able to retrieve the transmitted data from all the users. Before the optical conversion at the transmitter uplink side, the modulated RF signals of each ONU are placed in different frequencies (in the electrical domain), avoiding overlaps between each other. Each RF signal is modulated in a different optical carrier. The example below shows three optical carriers (representing three ONUs) transmitting in different wavelengths their corresponding RF signals at different electrical frequency bands.

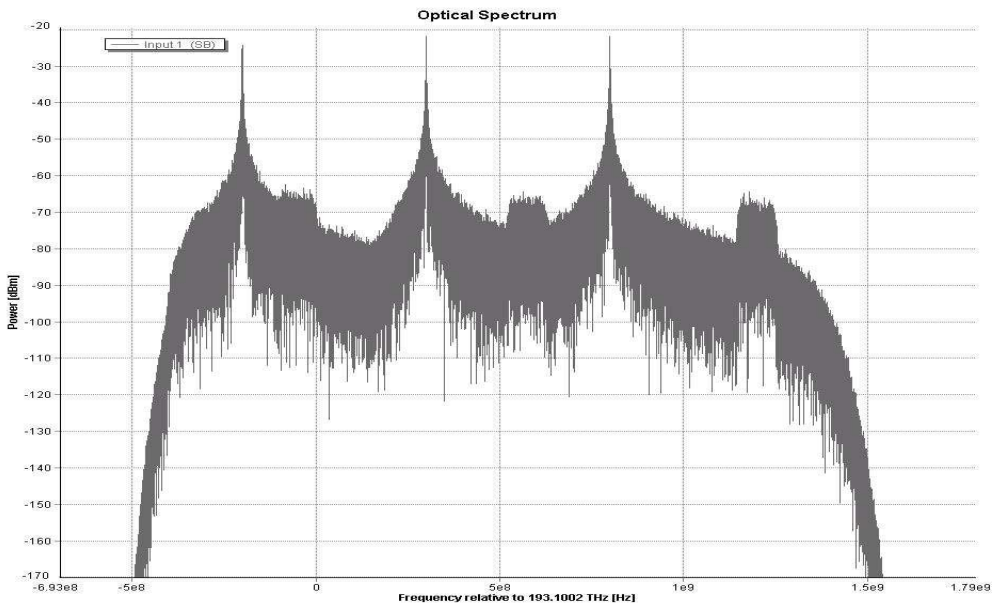

Figure 3.14. Optical spectrum of optical carriers with their RF signals. The bandwidth of the electrical OFDM signals is 100MHz. The optical carriers are spaced 500MHz among them.

Thus, after the optical to electrical conversion at the head-end side, the RF signals can be retrieved in different frequency bands. In Figure 3.15 a plot of the received information after the optical to electrical conversion at the head end photo-detector is shown. The bandwidth has been set equal for all the customers. The spectra shown at the right side of the RF signals represents useless information from the beating among the optical carriers and the RF signals. When some of this energy falls into the signal band we talk about Optical Beat Interference (OBI).

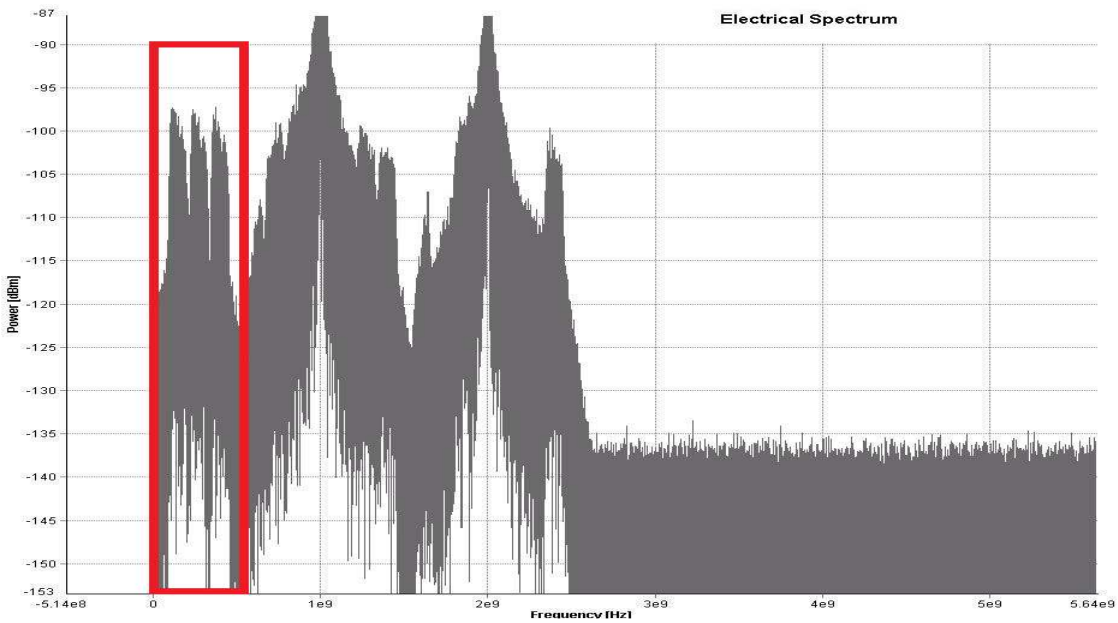

Figure 3.15. Received information after the optical to electrical conversion at the head end photo-detector for three simultaneous users in the OFDM network. The bandwidth of the electrical OFDM signals is 100MHz and the space between them is 50MHz.

The aim of the following chapters is the study in depth of the interferences encountered in the uplink user-multiplexing design of optical access networks.

3.7 VPI Basics

For the simulations of this Master Thesis the VPI software has been used. This Software is the suitable tool to simulate optical transmission systems.

The *Virtual Photonics Integrated* software is the tool pack used in this project to simulate the fiber optic transmission systems. *VPItransmission Maker for Optical Systems* (from now on VPI) allows us to design access networks based on optical systems [I3]. The tool includes design templates as a base for further developments. The simulation results are displayed by means the *VPI Photonics Analyzer* tool, which is automatically executed after the simulation. VPI is based on the interconnection of modules to design and simulate the

operational characteristics of systems. Those modules, and its parameters, are organized following a hierarchy [P9].

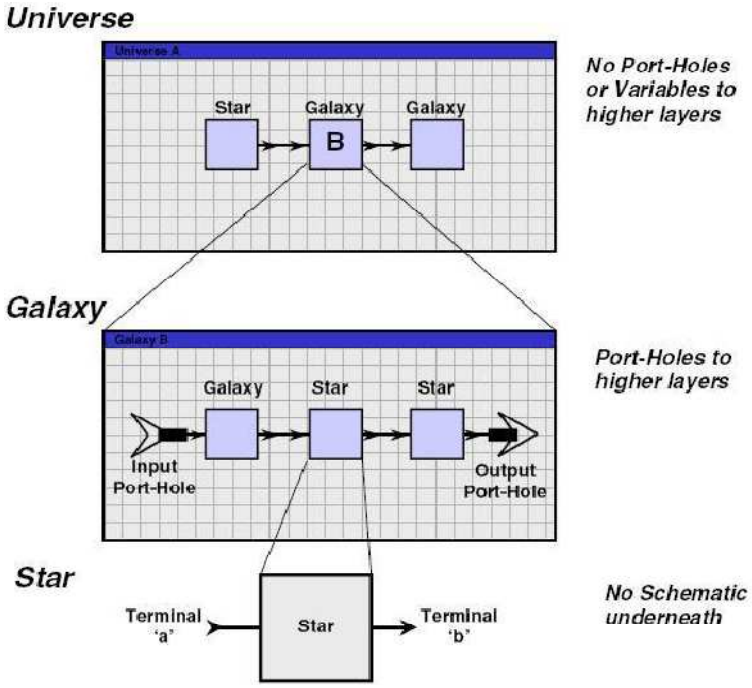

Figure 3.16. VPI hierarchy [P9]

As seen, we can design a simulation organizing the single modules (stars) into a galaxy (in order to build a complex module from stars) or directly in a universe (main simulation frame). The universe will be composed either by stars and galaxies, the latter presented as modules in the main simulation frame or universe. In order to analyze or modify the structure of the galaxies, we can access them by clicking in their *look inside* feature, placed in their right-click menu. Then, the galaxy is displayed in another window. The stars inside the galaxies can share some parameters which can become a single global parameter of the galaxy. By default, VPI has a set of global defined parameters for the universes. The most important parameters are:

- ***TimeWindow*:** this parameter sets the period in which a block of data is represented. This time will fix the spectral resolution of the simulated signals.

- ***SampleRateDefault*:** It is defined as the number of samples taken by second and determines the maximum frequency that can be simulated and the temporal resolution (time between temporal samples).

- ***BitRateDefault*:** it defines the transmission bit rate by setting the BitRate parameter of emitters, bit generators, etc. to BitRateDefault.

There are restrictions setting the values of the global parameters. First at all, since the simulator is based on the FFT algorithm, the sample rate of the simulation by the time windows has to be a power of two:

$$SampleRate \cdot TimeWindow = 2^n \quad \textbf{(E3.18)}$$

Then, the bit rate by the time window has to be a power of two as well:

$$BitRate \cdot TimeWindow = 2^n \quad \textbf{(E3.19)}$$

Finally, the sample rate (include the number of symbols) is defined as:

$$SampleRate = 2^n \cdot BitRate \quad \textbf{(E3.20)}$$

In general, we can also conclude that:

$$\frac{BitRate}{2^n \cdot BitRate} = N \quad \textbf{(E 3.21)}$$

Being N a natural number.

3.7.1 VPI Sweeps

Some of the studies in this project have required a systematic variation of a parameter of the simulated system. The VPI controls that allow the continuous analysis of the system parameters are the *sweep* controls. There are two equivalent ways to perform a *sweep*.

The first one is shown in Figure 3.17. The control components in the system design are:

- Value to sweep
- Ramp to follow by the value
- Value adaptation to further stages

As seen, this method needs the introduction of extra modules in the simulation frame. This solution is useful in cases when the output values of the sweep

have to be combined with other module output values, for instance, to make a chart. In addition, when the value to sweep belongs to a module placed inside a galaxy, this is the only way to make a sweep.

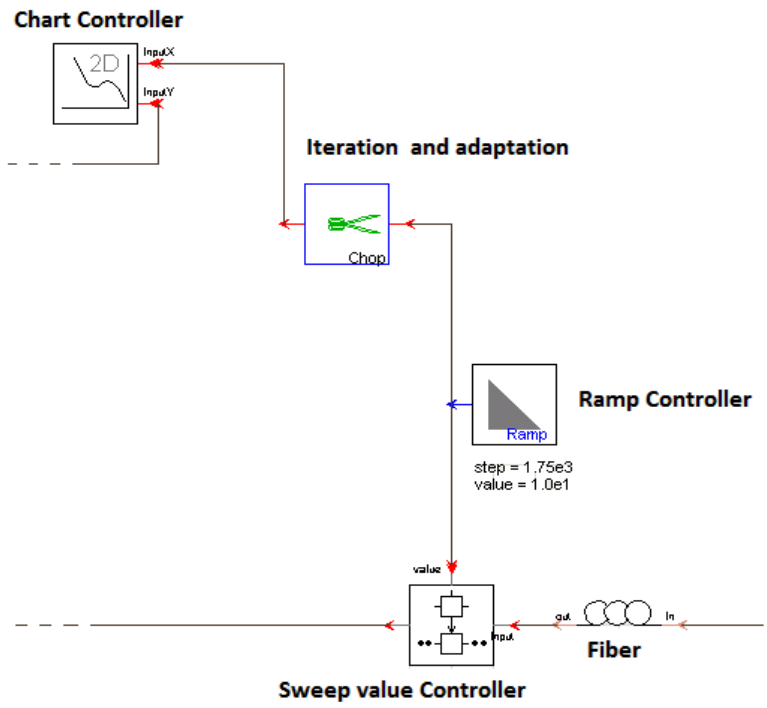

Figure 3.17. Sweep establishment 1

The *sweep ramp* module configures the step value. Some other modules are needed such as the *chop*, in which the number of iterations is indicated. The signal repetitions value is set by the signal repeater (sweep value controller) module according to the iterations number. By means of the plot modules, the data is presented graphically.

By contrast, the other method to establish a continuous sweep analysis does not need the introduction of extra modules in the system design. So, it is the easiest way to analyze a system trough a sweep. It is necessary to configure a control by setting the value to sweep, the value range of the parameter and finally, the scale between them.
This feature is accessed by right-clicking in the module and selecting the *edit parameters* menu. Once the parameter to sweep is selected by clicking over its own textbox, it is necessary a right-click and the selection of the *create Sweep control* option:

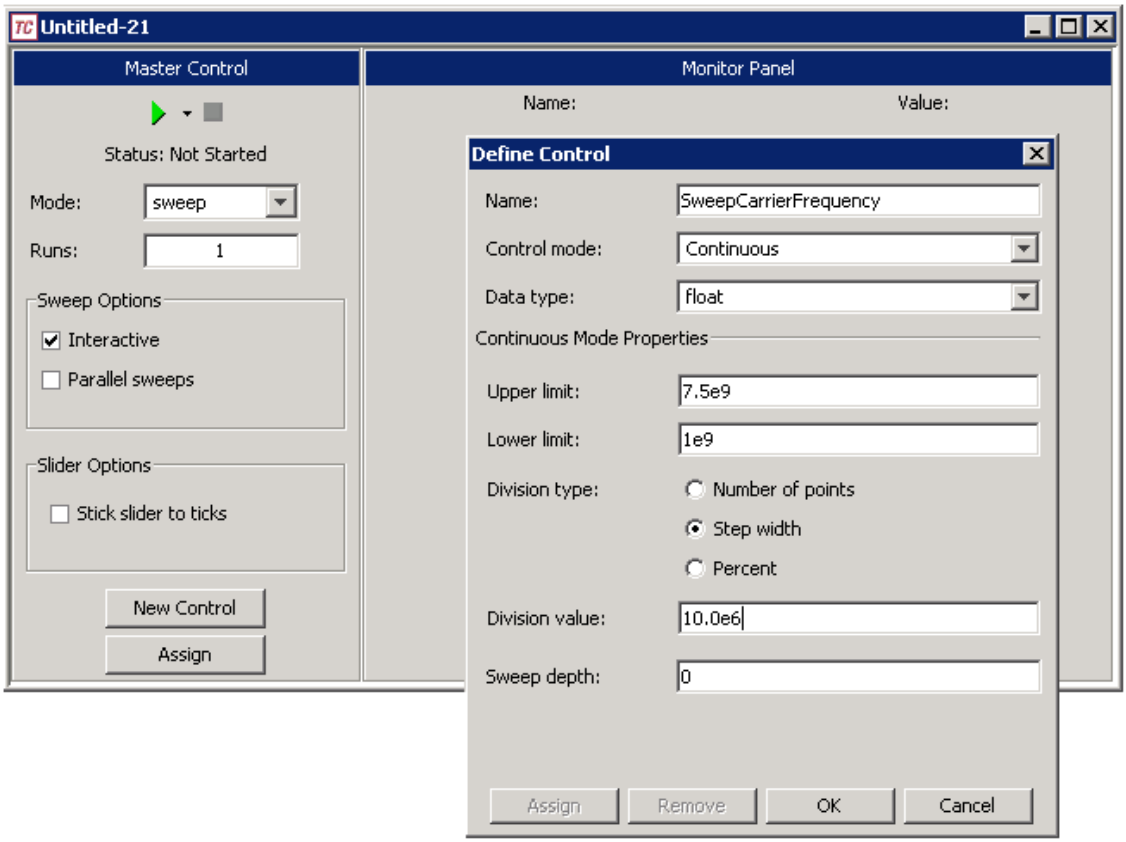

Figure 3.18. Sweep establishment 2

CHAPTER 4. POINT-TO-POINT OFDM SYSTEMS (UPLINK ANALYSIS)

After the analysis of the previous chapters with regard to OFDM and optical transmission systems, the selected IM/DD system is specified in this chapter.

As a first step towards the study of uplink multiuser integration strategies in IM/DD systems (introduced in 3.6), we explore in this chapter some issues related to the uplink point-to-point system. Thus, VPI setups and scenarios have been performed in order to study the key requirements of the optical access networks.

We take as starting point a VPI template that illustrates the simulation of the IM/DD with RF upconversion optical OFDM scheme. This template focuses on long-haul optical OFDM systems and therefore it uses a MZM. MZMs are at the present time, too costly and too difficult to operate to be used in the ONU. Since we focus in the uplink, and seek cost-effective solutions, our first task has been to adapt the optical OFDM system to use a DML as a modulating technique.

As a second task, the use SSB filters in order to avoid chromatic dispersion amplitude fadings for moderate fiber distances/data rates has been studied.

The amount of amplitude fading experienced by the signal increases with distance and therefore for the short distances required in access networks it could be tolerable and justified by the colorless operation the elimination of the optical filter enables.

As a third task, the amount of spectral guardband which is actually necessary to maintain the quality of the transmission has been assessed as a function of the fiber length.

Given the fact that in absence of chromatic dispersion the IM/DD system can recover the sent signal without nonlinear distortion and also considering that the level of intermodulation products generated decreases with frequency inside the guardband, one can expect the required guardband to decrease for small quantities of chromatic dispersion and to be zero in the limiting case when no fiber is considered. Within this task, the size of the guardband with respect to the fiber length will be obtained for representative cases.

4.1 IM/DD with RF-Upconversion optical OFDM transmission system

After the study of the OFDM multiplexing technique performed in the second chapter of this Thesis, the study of the optical channel and finally the modulation and demodulation schemes considered in the third chapter, inside the framework of the IM/DD systems presented in 3.5 , an IM/DD system based on RF-upconversion has been selected. This will be the system considered from now on in the setups.

After the OFDM modulation process described in Figure 2.13, the real and imaginary parts of the OFDM signals have to be treated separately before the IM modulation. Both real and imaginary parts of the OFDM signal are up-converted in order to be sent, as shown in Figure 4.1. The chosen RF frequency is 1.5BW, with BW the bandwidth of the OFDM signal, as required by the linearity criterion.

Moreover, the IM modulation can be performed by means of an external Mach-Zehnder modulator at quadrature point or modulating directly a laser source. Since this Master Thesis is focused in the uplink network design, and cost-effective solutions are preferred in the ONUs, the **Direct Modulation Laser** technique has been selected as IM modulation scheme.

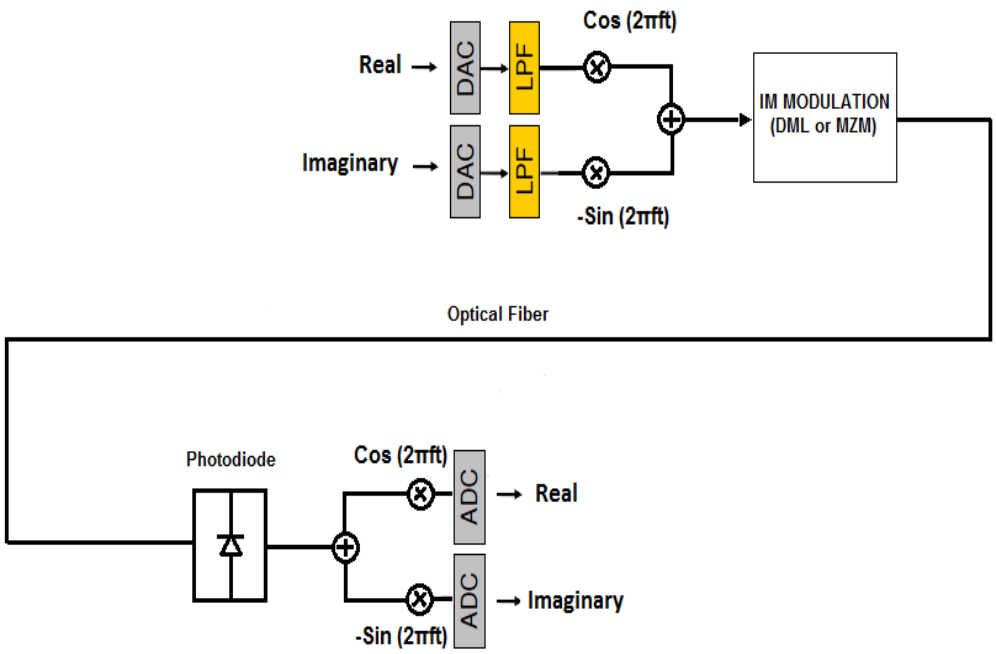

Figure 4.1. IM/DD with RF up-conversion optical OFDM transmission system

4.2 Description of the VPI template for OFDM Long-Haul

The starting point of the following studies is an optical long-haul transmission VPI template.

This template is based on the IM/DD with RF upconversion optical OFDM scheme. The universe is shown in Figure 4.2. The electrical part of the TX and RX is organized into galaxies.
As seen, once the RF OFDM upconversion has been achieved in the OFDM transmitter galaxy, the signal is applied to a MZM through a voltage driver. Thus, the IM optical modulation is performed by means of a Mach-Zehnder external modulator biased at its quadrature point. In the scheme we can also see an SSB filter and the means for displaying the results after the OFDM demodulator at the output of the photodiode.

As seen in Figure 4.2, three different of output results are offered: the received constellation, the spectrum at the receiver input and the error vector magnitude (EVM) at the receiver output (inside RX OFDM galaxy). The EVM can be considered as an indicator of the transmission quality (see ANNEXES C).

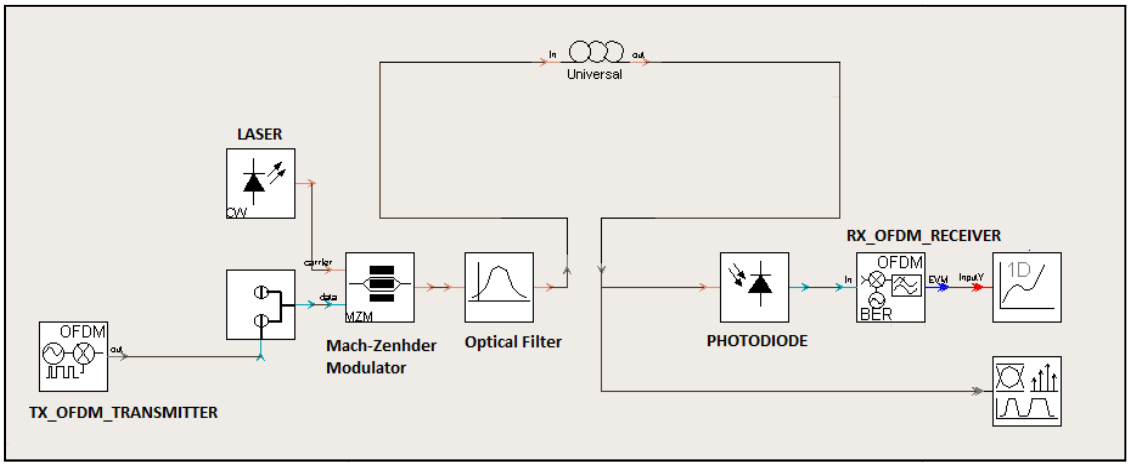

Figure 4.2. Optical transmission system template

We observe that several global parameters have been defined in the universe; according to 3.7 the most important are:

- Time window
- Bit rate
- Sample rate
- Bits per symbol (modulation)

The TX module is arranged as a VPI galaxy. By clicking on the *Look Inside* property of the galaxy we can see its internal structure.

By having a look at the TX galaxy (Figure 4.3) we see it first starts with the bit sequence generator. The Pseudo Random Bit Sequence (PRBS) of length *TimeWindow*BitRate* is fed to the OFDM coder. Two outputs carrying respectively the real and imaginary parts of the OFDM signal are upconverted at an RF frequency using an electrical IQ scheme. Inside this module all the functions described in CHAPTER 2 such as Cyclic Prefix, Zero Padding, QAM modulation etc. take place and can be set to the desired value through the parameter editor of the galaxy; the main configurable parameters are described following Figure 4.3.

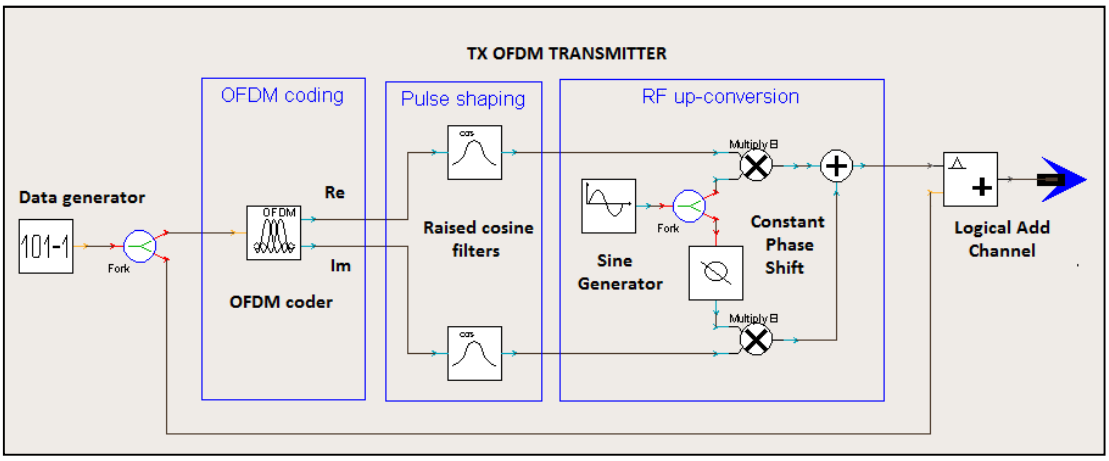

Figure 4.3. OFDM Transmitter module.

We can stand out some configurable key parameters of this galaxy such as:

- Roll-off factor: belonging to the Raised cosine filter module, which mainly performs the Pulse shaping stage. The Roll-off factor defines the grade of accuracy of the filter. It is zero in the ideal case, when all the subcarriers are perfectly orthogonal. This value is set to 0.18 to simulate a more realistic DAC conversion.

- Carrier Frequency: configurable in the sine generator module, allocates the OFDM signal in their corresponding band. This signal defines the central frequency of the OFDM signal with regard to the optical carrier. In a multiuser scenario, this value will depend on the carrier frequency value of the other transmitter modules in order to do not overlap the OFDM signals among each other.

- Number of carriers: belonging to the OFDM Coder module, define the number of carriers to transmit the OFDM frame. This value is set to 64.

- Cyclic prefix: configurable in the OFDM coding module. According to 2.8, The CP is added in the sequence to avoid ISI. By default, 0.2% of the

number of FFT samples is copied from the end to the sequence to the beginning.

- Logical Channel: Galaxy parameter. Assigns the logical channels stored in a global list to the signal. This is performed by adding the label of the logical channel to the label set of the signal. Those labels are useful to differentiate the channels in a multi-user environment.

Aside the modules explained before, the OFDM receiver galaxy is based on the following modules:

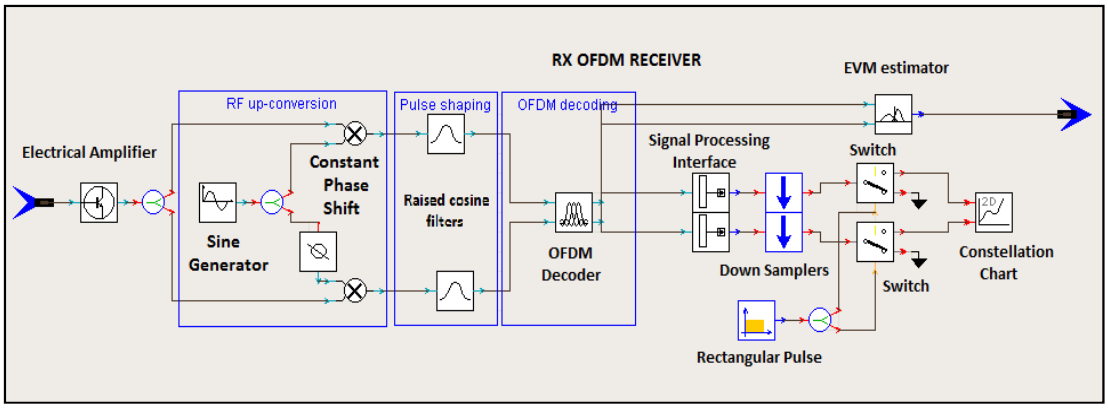

Figure 4.4. OFDM Receiver module

In the receiver module after the optical to electrical conversion, the complementary operations to those in the TX are found in the reverse order. First the electrical IQ downconversion and antialising filtering are performed prior to ADC and OFDM demodulation. The real and imaginary outputs that contain the demodulated QAM symbols are used to calculate the EVM and to show the constellation.

In order to display the received QAM constellation first the signal is converted from electrical to numerical type of data, then downsampled to obtain from the VPI samples the symbols. This conversion can be thought as the simulation analogous to the ADC conversion in a practical system. Then, two switches connected to a rectangular pulse generator select the information symbols and discard the redundant information.

Once the VPI Long-Haul template has been described, the adaptation of some of its features to the optical access networks requirements are explained in the next subchapter

4.3 OFDM LONG HAUL VPI TEMPLATE ADAPTATION

The VPI long-haul template uses 4-QAM as a symbol modulation and OFDM as an electrical carrier multiplexing technique. Obviously, these features remain the same in the adaptation universe (Figure 4.5).

Since basically the uplink is targeted in this work, and according to 4.1, the IM scheme of interest is the **Direct Modulated Laser**. So, the template has been modified according to our needs. The **pulsed laser** is directly modulated by the OFDM transmitter VPI galaxy.

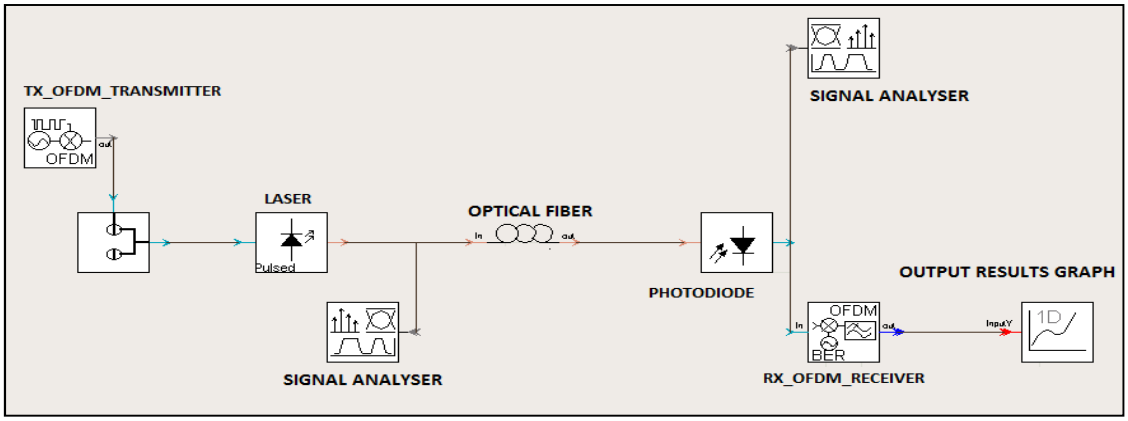

Figure 4.5. Optical transmission system template DML.

From the many laser models available in VPI, the Pulsed Laser module has been selected. This module models a DFB laser with dynamic configurable chirp. It uses behavioral parameters to describe the laser operation.

The laser module parameters have been adjusted so that for low modulation depths, the **Optical Modulation Index** is set by the electrical signal amplitude at the output of the laser driver.

The **Emission Frequency**, in which the laser will work, is set to 193.1THz (third window), this value has not been modified from the original template. Moreover, the **Linewidth** defines the amount of phase noise of the laser source. This feature depends on the quality of the laser. By default, in the simulations the Linewidth value is set to 100KHz except for the simulations performed in 5.3 (because a sweep of this value, see 4.4, has been performed in order to obtain the desirable results). By means of the **Random number seed** value we can configure the decorrelation among the laser sources in a multiuser scenario, setting different integer numbers for each laser, the VPI software performs a simulation with decorrelation among the optical sources.

The **photodiode** used is the same as in the long-haul template. It is based in a PIN diode. As seen, the **optical filter** has been removed in the adaptation model. A particular subchapter has been dedicated to study the optical SSB

filter needed. So, by default, in the other studies of this Master Thesis the SSB filter has been removed according to 3.4.3 and 4.4. It is important to stand out that the considered fiber length is completely different than the used in the long-haul template. According to the access networks requirements, the considered distances cover up to 30 Km (see ANNEXES B). The values of the attenuation and chromatic dispersion coefficient configured in the fiber link are typical for a transmission in 3rd window (α=0.2 dB/Km and D=17ps/nmKm).

Moreover, the Roll-off factor in the pulse shaping stage is set to 0.18, equal to the value of the original template. The Carrier Frequency of the RF upconversion (and downconversion) stage/s has different values depending on each case (see ANNEXES B). The **Number of carriers** value is set to 16, meaning that the OFDM signal is transmitted by less carriers than the original template (64). As said, since the simulations focus is the uplink direction, obviously the ONUs need less subcarriers than the OLT. In the downlink, the OLT must send information to all their associated ONUs, needing more subcarriers to cover their requirements.

The **Cyclic prefix** aggregated to the frame is null in all the setups because we tried to isolate the specific behaviors in each case of study, avoiding influences from other parameters in the analysis. It can also be seen that considering the accumulated dispersion in the fiber lengths and bandwidth used the effect of adding some cyclic prefix is not relevant.

Afterwards, the main default global parameters, common in all simulations universes are:

- Time window
- Bit rate
- Sample rate
- Bits per symbol (modulation)

Moreover, inside the galaxies (i.e. OFDM coder/decoder) several important parameters are shared by more than one module. Thus, those important parameters are configured as general parameters of the galaxy; setting once the value in the general menu of the galaxy, all its internal modules will get the new desired value. The most important global galaxy parameters are:

- Channel Label
- Cyclic Prefix
- Number of carriers
- Carrier Frequency
- Roll-Off factor
- Random number seed

In some cases, it might be necessary to create a new universe parameter. The reason, for instance, can be to perform a sweep of a parameter which is shared by more than one modules or galaxies:

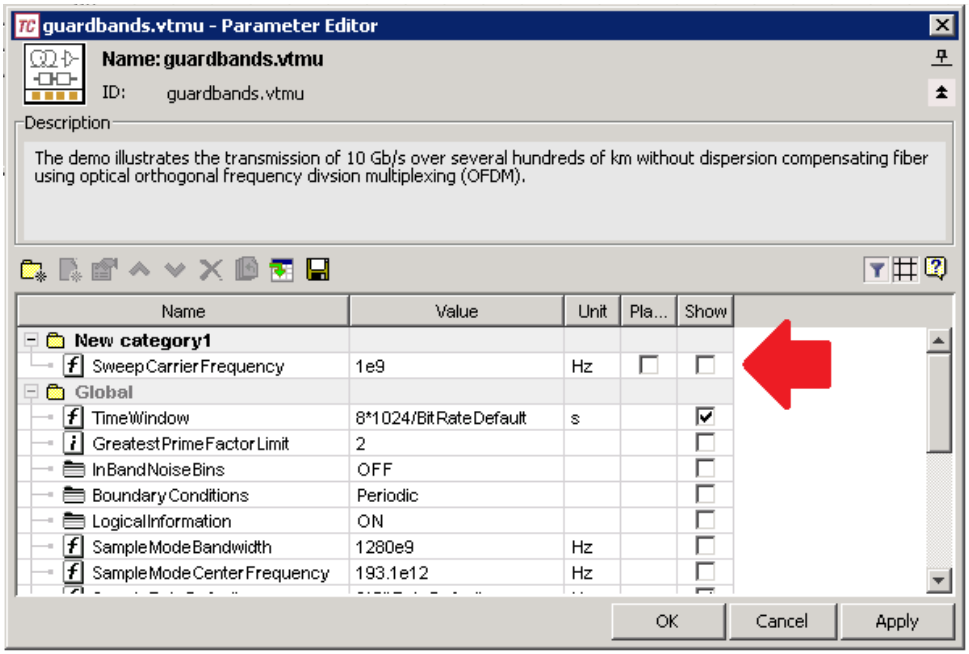

Figure 4.6. New universe parameter definition

Finally, as explained in the introduction of this chapter, the use of SSB filters in order to avoid CD amplitude fadings (low distances) has been studied using the adaptation setup as a starting point. Moreover, the amount of spectral guardband necessary to keep the quality of the transmission has been studied as a function of the fiber length. Both studies are explained in the next subchapters.

4.4 OPTICAL SSB FILTER STUDY

Since the chromatic dispersion effect depends on the frequency and also on the fiber length, for short distances it could be possible to avoid the filter while maintaining a tolerable transmission quality. On the other hand, the system installation without filter, provides flexibility for the optical band used (colorless operation) in a multiple user scenario (uplink sense).

The amplitude fading due to the chromatic dispersion has been the subject of this section. This effect is analogue to the image frequency effect in the RF-upconversion and it is due to the fact that the two frequencies resulting from upconversion (the two optical sidebands) are downconverted to the same RF frequency.

In order to study the concepts above, in the simulation demo of Figure 4.5 an optical filter has been added in order to evaluate empirically the SSB filter need. The parameter to evaluate the quality of the transmission is the EVM of the received 4-QAM constellation (see ANNEXES C).

Based on the previous analysis, in a plot of EVM vs distance, the EVM should increase from zero for no fiber present to untolerable values for a high amount of fiber and the increasing trend should depend on parameters such as the bandwidth, the carrier frequency and bit rate.

It is then of interest to know up to what distance is the EVM low enough to spare the SSB filter, giving flexibility to the system and reducing its cost.
That is why we have built a simulation setup in which a basic uplink OFDM system is presented. The simulation is run with an SSB (image rejection) filter, following the scheme of Figure 4.7.

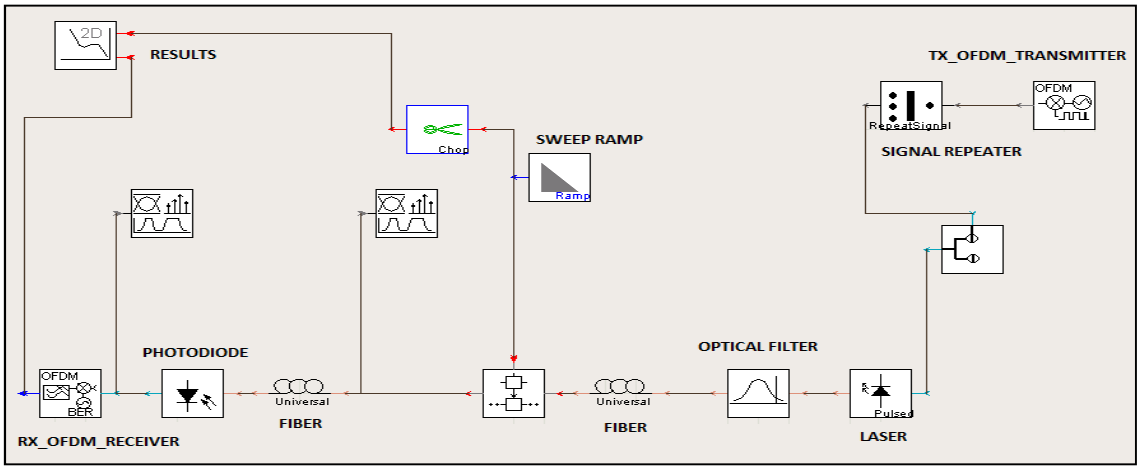

Figure 4.7. Optical filter analysis scenario

As seen, besides the optical filter, some extra modules have been added. Those modules are necessary in order to perform a sweep of the fiber length parameter (see 3.7.1). Specifically, this simulation consists in a sweep of the fiber length. This is achieved in the VPI software by making use of the sweep ramp indicating the step value (1.75 Km). The iterations number is 40. By means of the plot modules, the data is presented graphically.

Two simulations have been performed as a function of the fiber length. The first one with the optical SSB filter module enabled, the second, disabled. Both cases will be compared in order to know when it is possible to spare the SSB filter.

The main parameters of the scenario are:

- Laser central frequency: 193.1THz
- Iterations: 40
- Ramp value fiber: 1.75Km
- Fiber length starting value : 1m
- Carrier Frequency OFDM signal: 1 GHz

- Bandwidth OFDM signal: 100MHz
- OFDM Carriers: 16
- Bit Rate: 200 Mbps
- Roll-off factor= 0.18

The EVM always increases with the iterations. In other words, the EVM at the receiver side increases with the fiber length growth as expected, since chromatic dispersion increases the phase difference among the subcarriers. In Chart 4.1 the results of the EVM against the fiber length with the optical filter installed are presented.

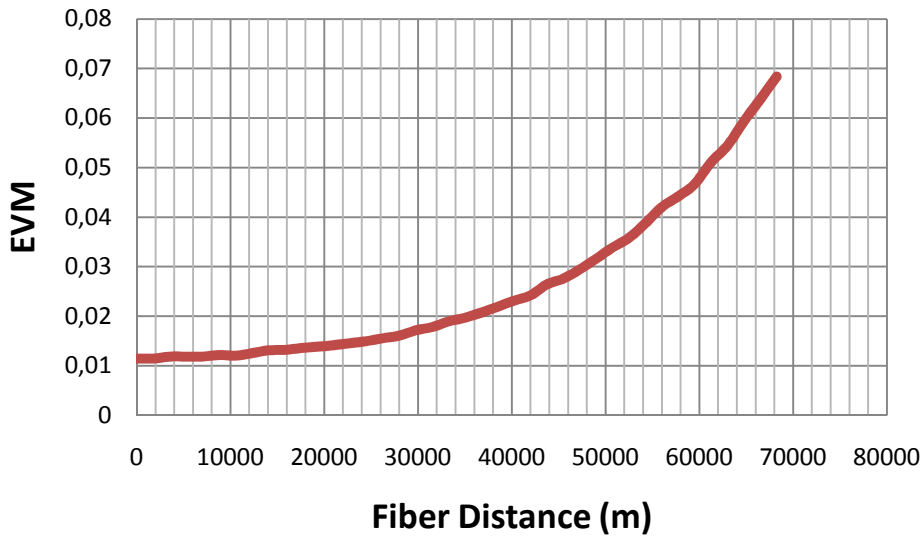

Chart 4.1. EVM versus fiber length with optical filter

Complementing the previous analysis, some plots of the received constellations have been taken for different distances of fiber (Figure 4.8):

- A= 3.5 Km.
- B= 21 Km.
- C= 50 Km.
- D= 69 Km.

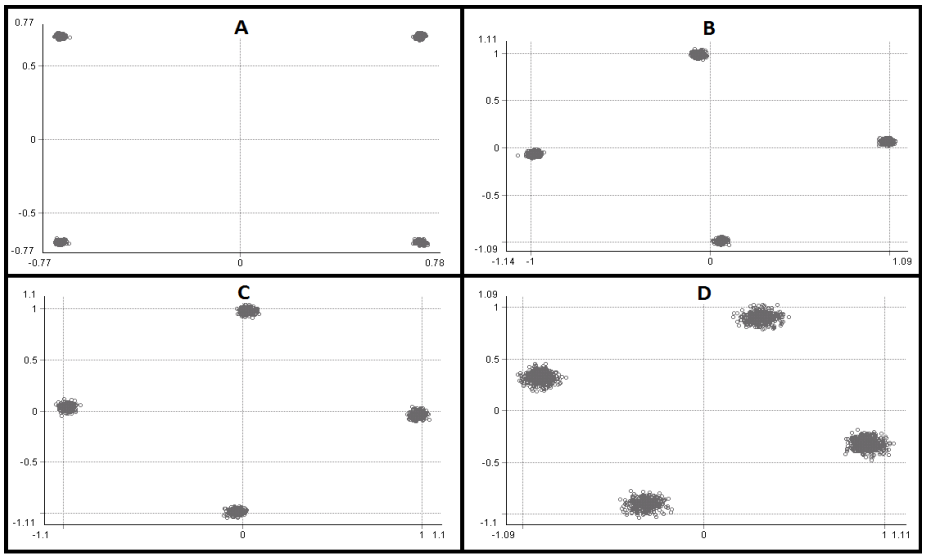

Figure 4.8. Received Constellation evolution with filter 1

The rotation experienced is due to the fiber length and the choice of the fiber reference frequency. This effect is known as a Common Phase Error and can be recovered with equalization. Note that the EVM estimator is able to compensate this rotation of the constellation when it calculates the EVM.

The fiber reference frequency is a parameter of the simulator that in the presence of chromatic dispersion indicates the frequency at which the group delay is considered zero. In other words, it indicates which spectral component is the first to appear in the temporal time window considered in the simulator. In practice, this reference frequency choice corresponds to a proper synchronization of the incoming signal at reception.

According to [T4], in this optical OFDM scheme it has been proven that the correct reference frequency choice is

$$\omega_{ref} = (\omega_0 + \omega_{RF}) \qquad \textbf{(E 4.1)}$$

Being ω_0 the frequency of the laser source and ω_{RF} the central frequency of the OFDM electrical signal in the RF upconversion scheme that is the focus of this work. As seen, the reference frequency has to be placed in the center of the OFDM signal.

In the Chart 4.2 we present the results of the EVM against the fiber length without the optical filter. When the fiber length increases, the amplitude is reduced by destructive interferences among the upper and lower sidebands. This is the reason of the EVM increasing. Then, after 39 Km the interference becomes constructive (360º phase shift) and the amplitude grows again. This gives in fact a semi-periodical evolution of the EVM against fiber length (losses are not periodical) due to the periodicity of the phase shift induced by chromatic dispersion.

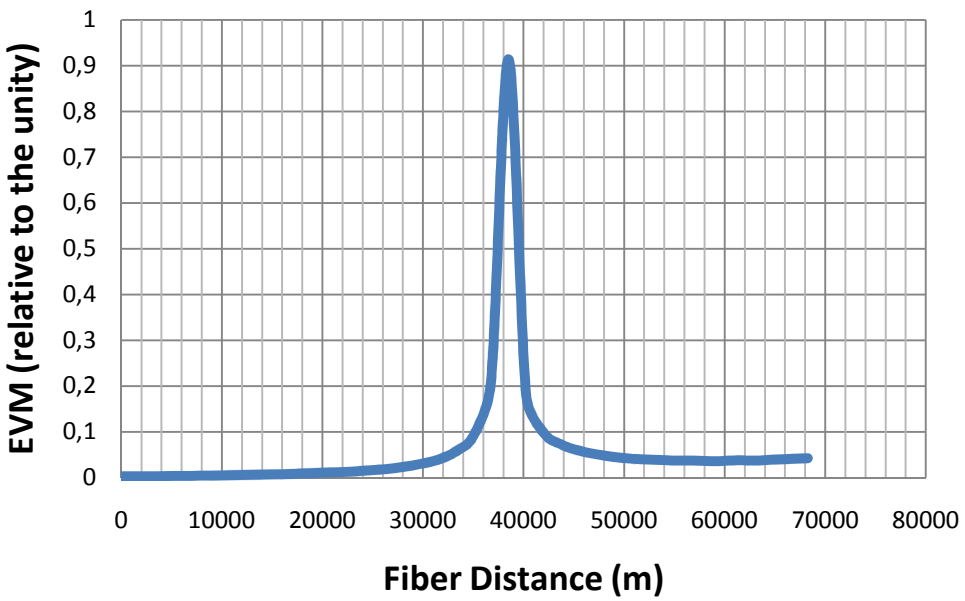

Chart 4.2. EVM versus fiber length without optical filter

Complementing the previous analysis, some plots of the received constellations have been taken in different distances of fiber (Figure 4.9):

- A= 3.5 Km.
- B= 21 Km.
- C= 50 Km.
- D= 69 Km.

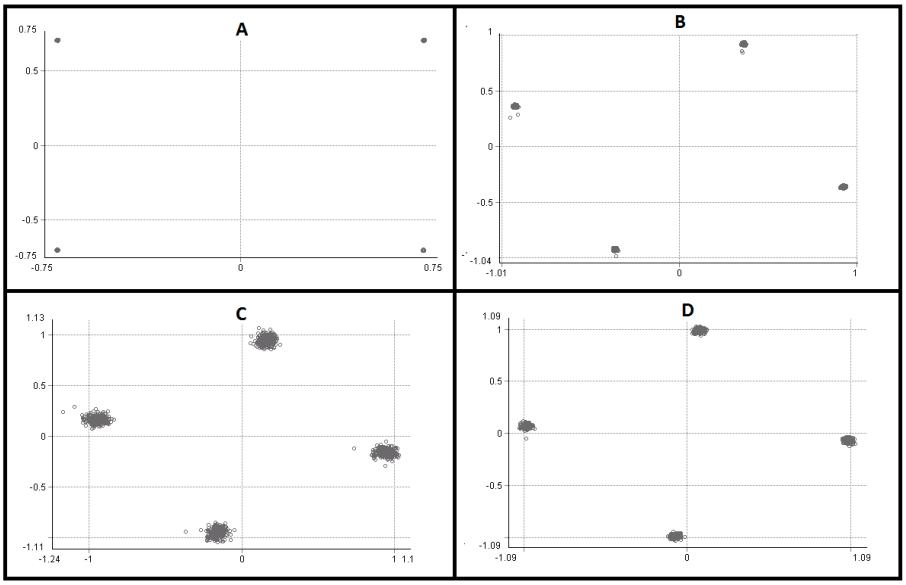

Figure 4.9. Received Constellation evolution without filter

The constellation of the Figure 4.10 A has been taken when the maximum error appears, specifically at 39 Km.

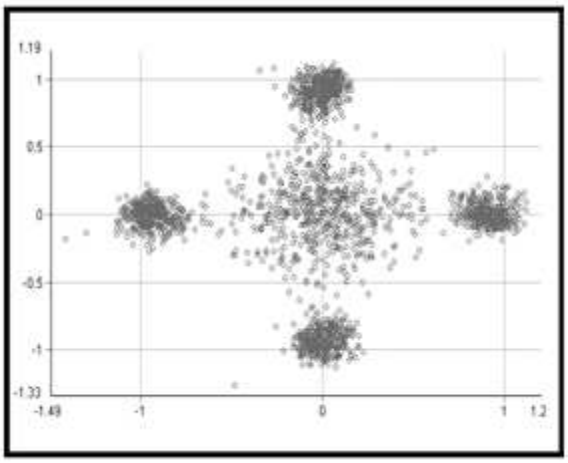

Figure 4.10. Error at 39 Km and received constellation evolution without filter 2

In Figure 4.10 some points are seen to fall close to the constellation center as a consequence of several subcarriers suffering from important amplitude fadings. Finally, a comparison between both cases has been done (Chart 4.3), being the blue curve the analysis without filter and the red one with filter. As a conclusion, it is possible to consider the sparing of the filter installation until 24 Km of fiber length. Moreover, according to the EVM acceptable values presented in Figure C 2 , the sparing of the filter can be considered until 32 Km with tolerable signal degradation.

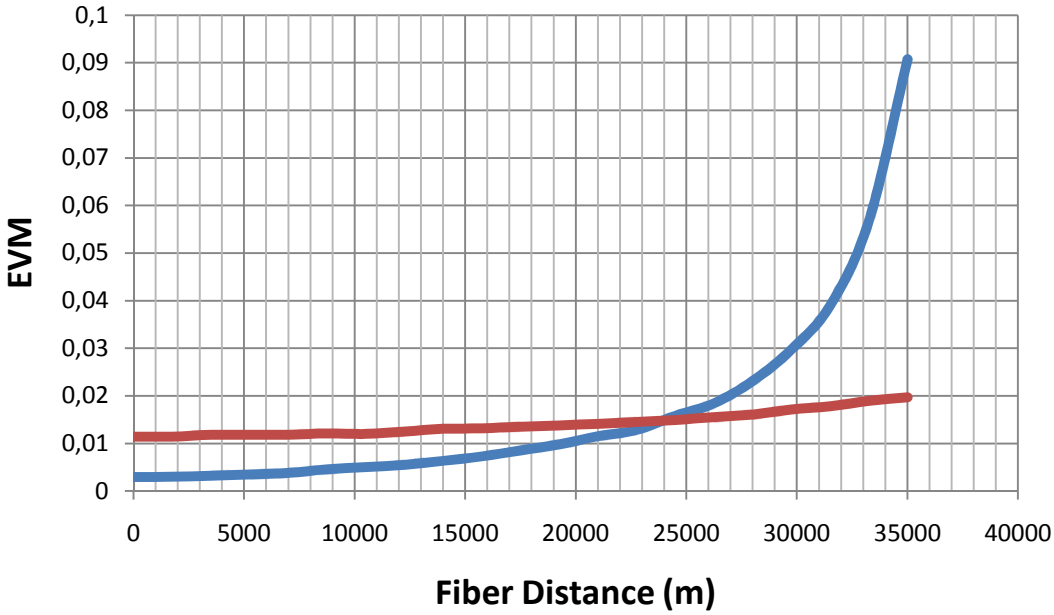

Chart 4.3. Comparison at 200 Mbps

The comparisons above have been done for 200Mbps as a bit rate. The next generation optical access networks will probably need higher data rates per customer, considering both residential and business customers. This is the reason to repeat the analysis for higher data rates. The results for 1 Gbps (Chart 4.4) and 10 Gbps (Chart 4.5) are shown below respectively. For a 1 Gbps link, the fiber threshold distance for the filter sparing is very close (+1Km) to the 200 Mbps analysis. However, according to the tolerable values of Figure C 2, for 10 Gbps, the service can be given until 10 Km approximately without SSB filter.

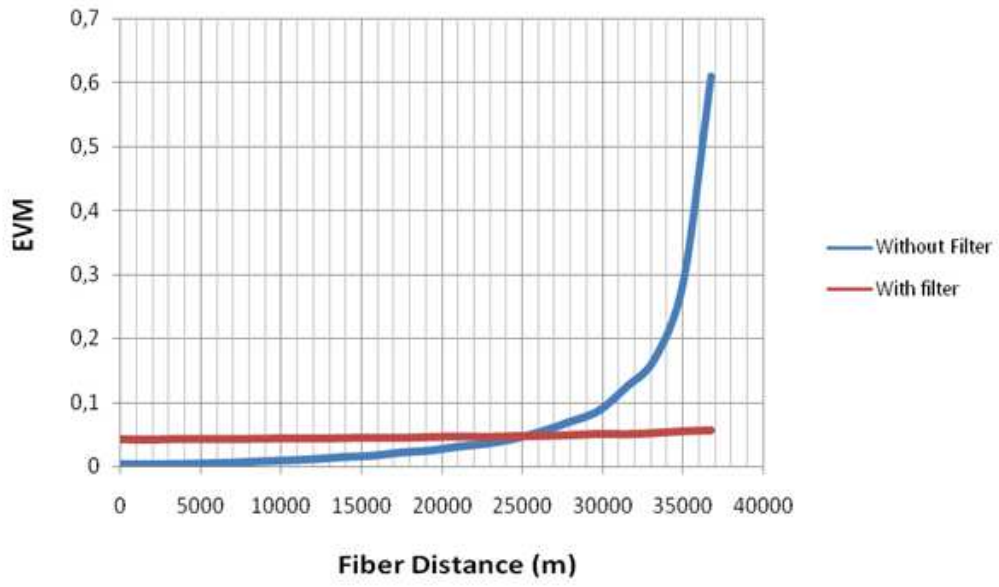

Chart 4.4. Comparison at 1Gbps

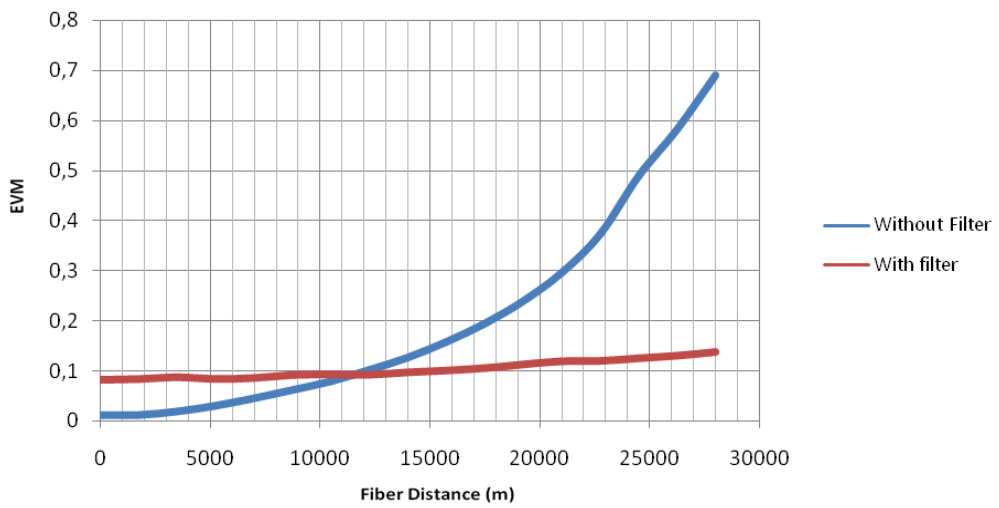

Chart 4.5. Comparison at 10 Gbps

4.5 GUARDBAND STUDY

In this section, the amount of guard band necessary to maintain the quality in the optical transmission has been studied. The goal is to place the OFDM band closer to the carrier in IM/DD schemes yet get a tolerable transmission quality. This study is important from the viewpoint of the spectral efficiency and in order to reduce the modulation/detection bandwidth requirements.

The guardband is required because the different spectral components acquire different delays due to chromatic dispersion which prevent from perfect cancellation of mixing products resulting from square-law detection. To avoid this effect the use of guard bands between the optical carrier and the OFDM information signal is necessary. It is important to find the minimum guard band value to achieve a good performance for the fiber length used.

When chromatic dispersion is low (small fiber distance) some cancellation could still be possible and perhaps the target quality could still be met without guardbands and therefore lowering the requirements in transmission and reception hardware, which is an important factor in the uplink design.

The first step is to analyze a basic transmission (Figure 4.5 demo) without guard band. The Figure 4.11 shows the optical received signal without guard bands and the corresponding 4-QAM constellation. As it is shown, the received 4-QAM constellation is useless for the communication, being impossible to recover it with equalization due to the nonlinearities introduced by the IM/DD with chromatic dispersion system.

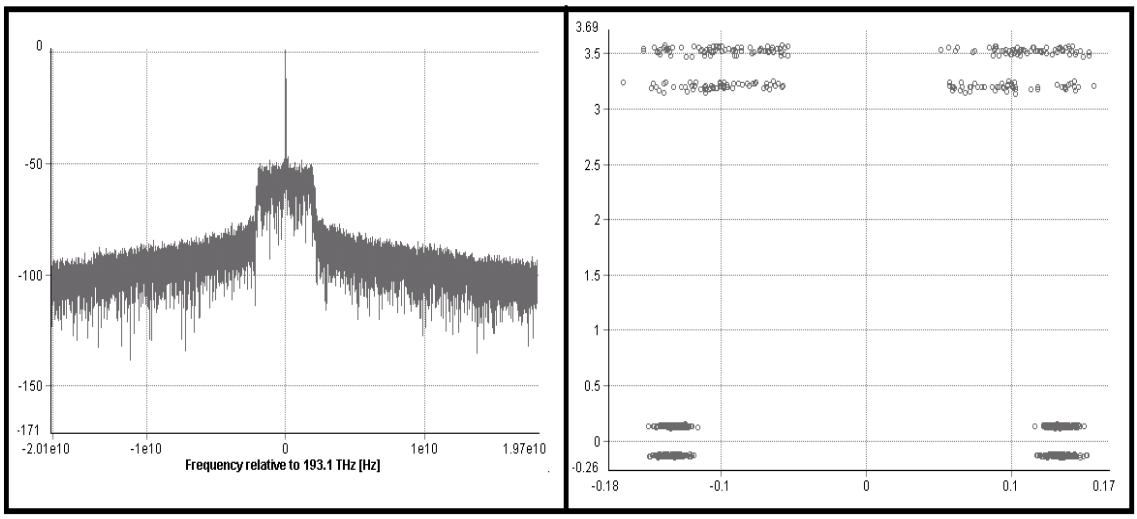

Figure 4.11. 4-QAM received constellations and the optical signal with zero guardband. Fiber length 20 Km.

We see that without any guardbands the received constellation is useless. That justifies the use of a certain amount of guard bands in all the further tests and simulations. In this study, the optical SSB filter has not been used because of the fiber length configured and the selected frequency of the OFDM signal (see

4.4). The simulations have been performed with a basic point-to-point demo (Figure 4.5) and sweeping the central frequency value of the OFDM signal (by consequence modifying the guardband) by means of the second method to sweep a parameter, explained in 3.7.1. Since the parameter to sweep is a parameter used in different galaxies and modules, a new universe global parameter has been defined as shown in Figure 4.6.

In Chart 4.6 the evolution of the Error Vector Magnitude (EVM) against the guard band growth is shown. As a conclusion, from 200 MHz of guard band in advance the EVM value is about 0,014, guaranteeing a good enough quality.

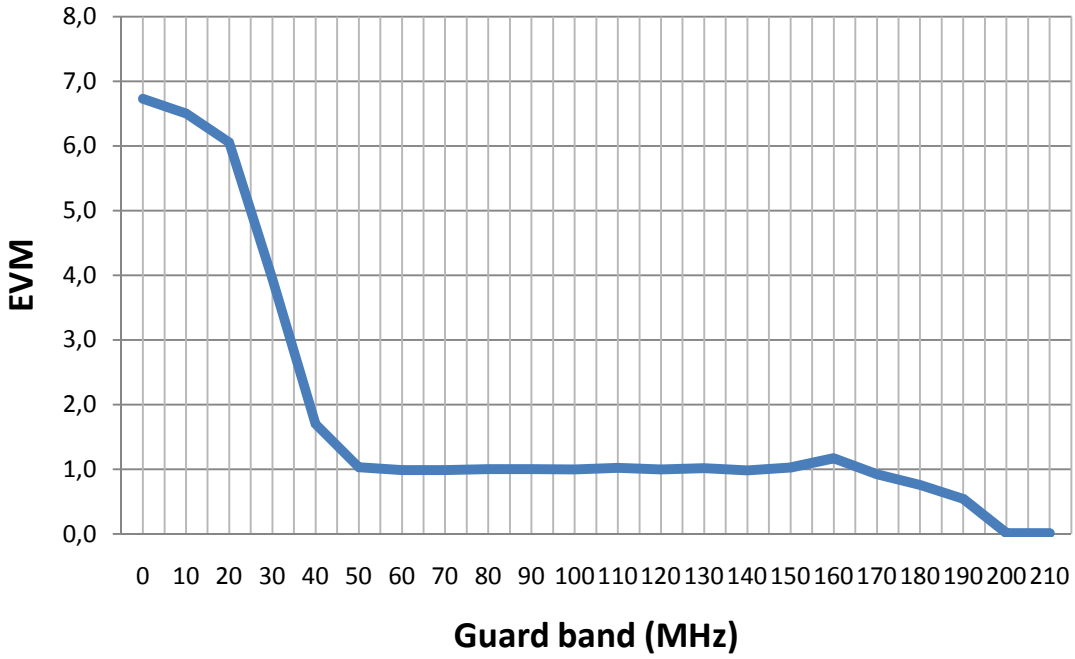

Chart 4.6. EVM evolution due to the configured guard band. Bandwidth 2GHz. 20 Km fiber length.

In addition, it is possible to observe the constellation received with 40 MHz of guard band (20 Km of fiber length) in Figure 4.12. The right plot corresponds to an amplification of the central object in the left plot. We can appreciate that the received constellation is useless.

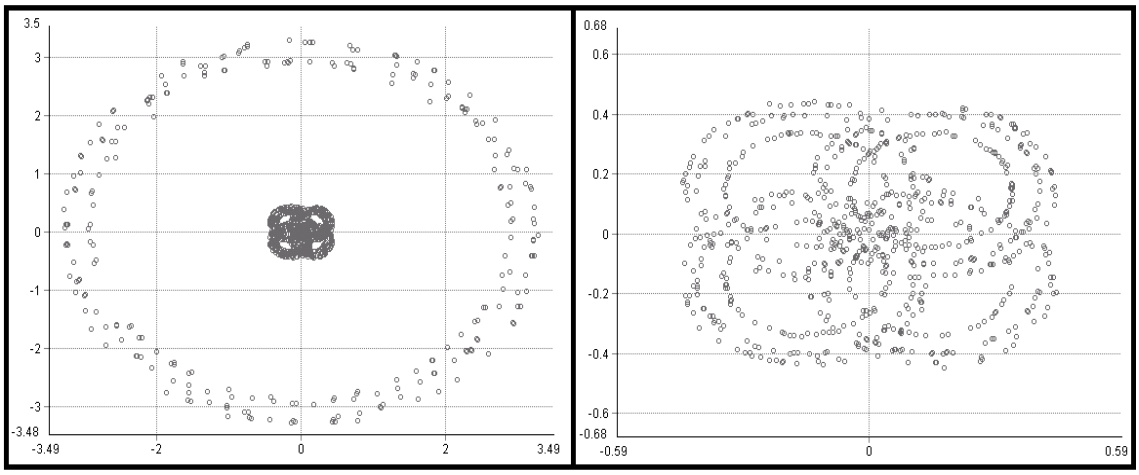

Figure 4.12. 4-QAM received constellations and the optical signal with 40MHz guard band.

The figure below shows the aspect of the received constellations with a guard band of 200 MHz (20 Km of fiber length) in advance (Figure 4.13). As shown, the constellation is received correctly.

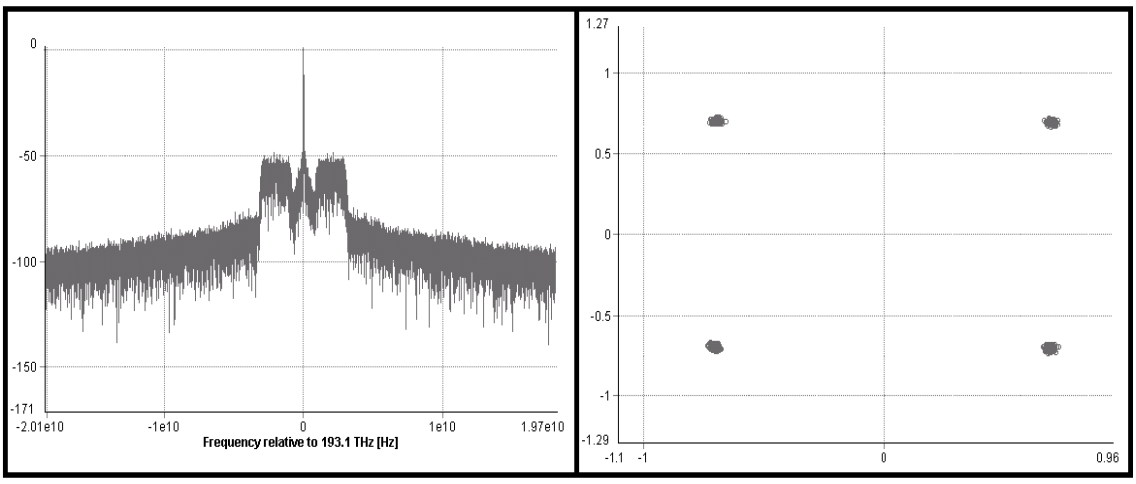

Figure 4.13. 4-QAM received constellations and the optical signal with 200MHz guard band

Finally, we have performed another test with a higher bit rate. The necessary guard band increases lineally with the OFDM bandwidth growth. Specifically, for a 10Gbps as a bit rate, the minimum guard band needed is 500MHz. The fiber length in this simulation has been set at 20 km (Chart 4.7).

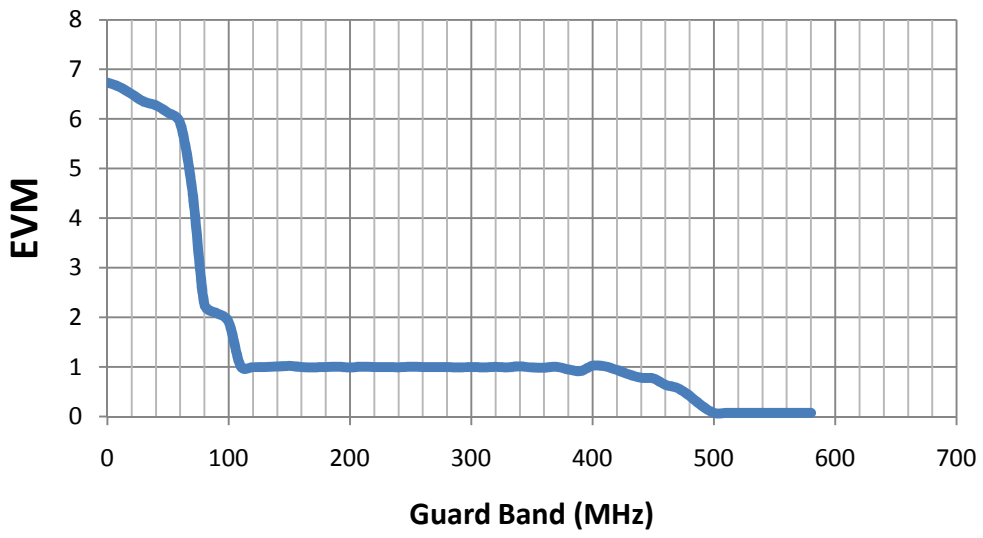

Chart 4.7. EVM evolution due to the configured guard band. Bandwidth 5GHz. 20 Km fiber length.

The results remain the same when the fiber length increases to 60 Km (Chart 4.8). But, the EVM from 500 MHz in advance is higher than in the previous analysis. In fact, it increases with the distance.

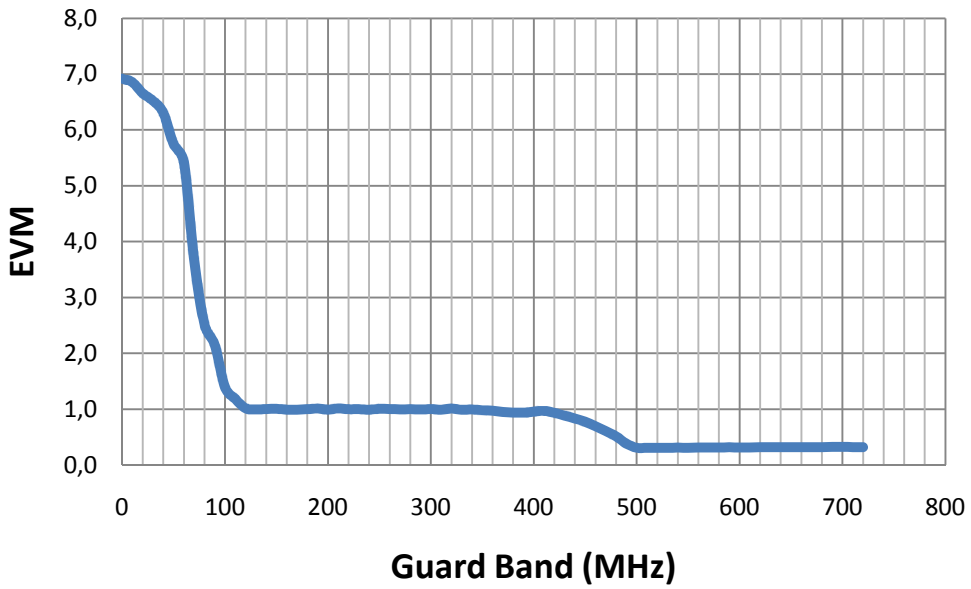

Chart 4.8. EVM evolution due to the configured guard band. Bandwidth 5GHz with 60Km fiber length

The results of the tests prove that the amount of guardband necessary needed does not exceed the 10 percent of the OFDM bandwidth.

It is important to stand out that the obtained results depend on the fiber length used. So, as a conclusion, these results only can be extrapolated to similar scenarios.

CHAPTER 5. USER MULTIPLEXING

5.1 Background

An accurate user multiplexing study is necessary when designing an access network. In optical transmission systems based on OFDM, the correct use of the spectral bandwidth available and the optical multi-user detection are key aspects to analyze.

Following the basic classification of uplink strategies regarding the placement of the optical carrier wavelength of each user in IM/DD schemes (see 3.6), in this chapter, an in-depth analysis of the two introduced strategies, i. e. Spectrally-efficient and Low-cost approaches is performed.

The Optical Beat Interference (OBI) concept is introduced, establishing three basic kinds of OBI depending on how it is generated. Focusing into each one of the two uplink strategies, several simulations and mathematical studies are used to understand the OBI, its drawbacks and the solutions to overcome its deleterious effects.

5.2 Uplink: Optical carriers assignment to ONUs

In this section, the concepts introduced in the optical access network basis subchapter (see 3.6) about uplink strategies are going to be treated in depth.

According to 3.6, for the IM/DD systems considered in this work, two are basically the strategies that can be followed regarding the wavelengths of the optical carriers of the different users:

- **Spectrally efficient approach (SE):** Optical carriers at the same wavelength, it can be achieved by:
    - Local Sources
    - Seeded Approach
- **Low-cost Approach (LC):** Wavelengths separated at a CIR threshold distance
    - Local Free-Running Sources

For spectral efficiency reasons it would be desirable to align the spectra of all the ONUs in the same band, so that optical carriers would be at the same optical wavelength and the data bands at different RF frequencies, see Figure 5.1. This is the SE approach. For putting this approach into practice basically two strategies can be followed: to place local sources at the customer premises,

or to send the optical carrier from the OLT to be remodulated at the ONUs. We assess the implication of each of these two approaches below.

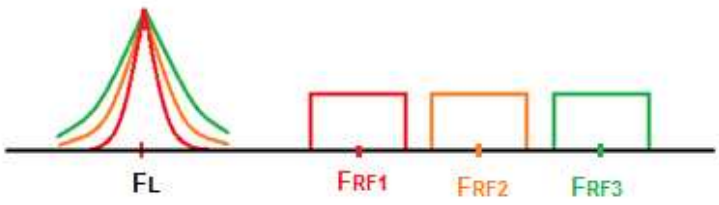

Figure 5.1. Spectrally efficient approach (SE). Optical Carriers at the receiver side with their RF signals

The problem with **local sources** based on lasers placed at each ONU would be to keep all the lasers perfectly aligned in frequency and keep random and temperature frequency drift under control, so that the orthogonality among subcarriers arriving from the different ONUs could be maintained.

The second practical setup considered in the SE approach is the **seeded approach**, in which there is no laser source placed in the ONU. In order to generate an optical carrier, the ONUs have to re-modulate a tone sent by the OLT. Graphically, a schematic is shown in Figure 5.2. The tone is then the same for all ONUs, meaning that all the ONUs use an optical carrier placed at the same optical frequency.

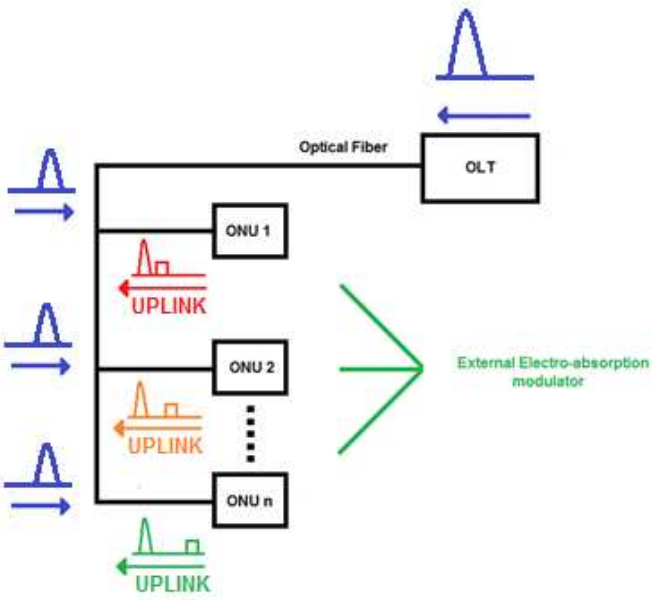

Figure 5.2. Seeded approach schematic

The seeded solution type in the SE approach solves the frequency alignment problem by considering sourceless ONUs that remodulate in a Electro-Absorption Modulators the signal sent from the OLT. The ONUs frequency alignment will thus be solved but still the seeded solution faces problems regarding Rayleigh Backscattering and reduced power budget since the optical carrier needs to cover the ONUs-OLT distance twice.

The second approach considered focuses in low-cost applications (**low-cost approach**) and considers optical carriers in different wavelengths for each ONU. Even when the optical spectrum efficiency is considerably reduced, important benefits can be derived from the processing of the data signals in the electrical domain. The OBI problem in this scenario is the subject of 5.3. There the minimum spectral spacing among optical carriers belonging to different ONUs in order to maintain the transmission quality by reducing the effect of OBI will be obtained.

5.1 Optical Beat Interference: Main Concepts and Types

The concept “Beat Interference” is a natural effect, which can be found in several fields besides optics, such as acoustics.
The Beat Interference in acoustics takes place when two tones very close in frequency are perceived as periodic volume fluctuations of the semi-sum frequency with a period which is the inverse of the frequency semi-difference.

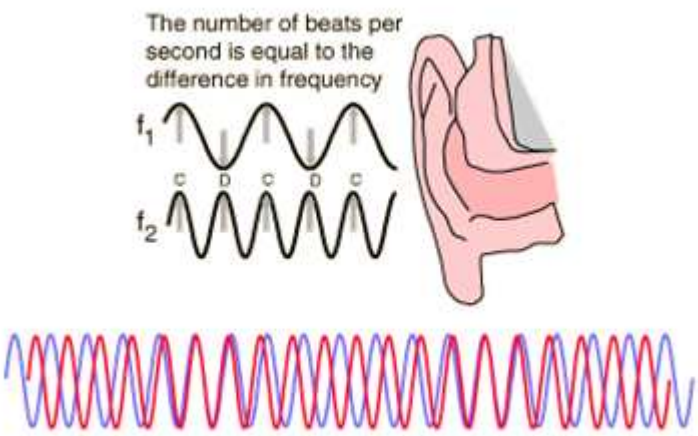

Figure 5.3. Tones mixing at the human ear

As shown in Figure 5.4 and Figure 5.5 the effect produced at the human ear by the mixing of two tones is perceived as amplitude changes of the average frequency.

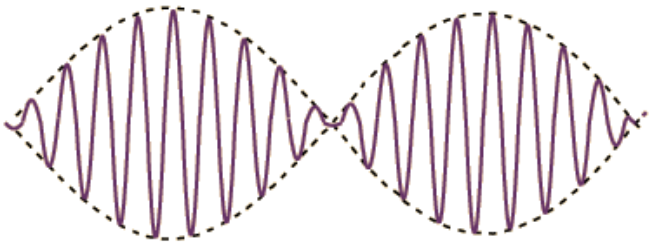

Figure 5.4. Perception amplitude changes

This effect is called *Beat Interference* in the acoustics field. In addition, it can be extrapolated to the effect perceived in optics because both effects share some features.

In optics, the same phenomenon occurs and therefore the periodic amplitude fluctuation found after photo-detection due to the presence of two tones very close in frequency can be understood as *Optical Beat Interference*.

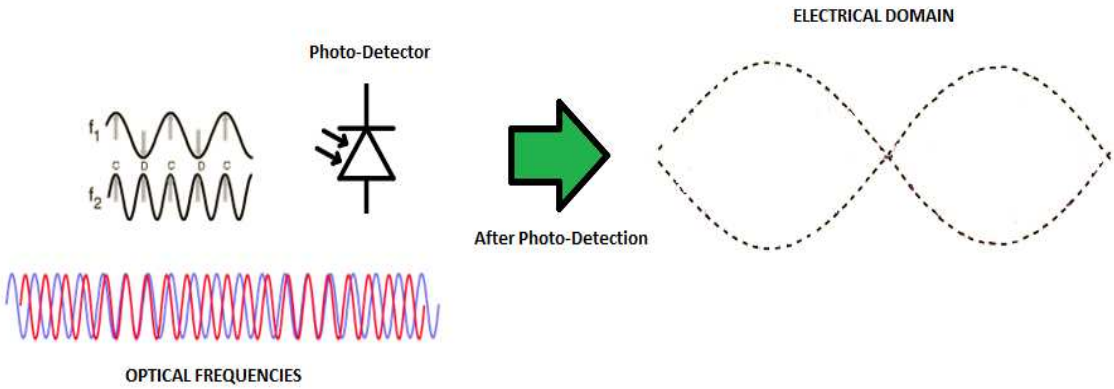

Figure 5.5. Perception amplitude changes in Optics

Mathematically, the expression of the received tones at the input of the photo-detector is:

$$\cos(\omega_1 t) + \cos(\omega_2 t) \qquad \textbf{(E 5.1)}$$

Where ω_1 and ω_2 represent both optical frequencies. After the photo detection stage, the mathematical expression is as follows:

$$\underbrace{\cos\left(\frac{\omega_1 + \omega_2}{2} t\right)}_{TERM\,1} \cdot \underbrace{\cos\left(\frac{\omega_1 - \omega_2}{2} t\right)}_{TERM\,2} \qquad \textbf{(E 5.2)}$$

The first term of E 5.2 is neglected because the photodetector removes the optical frequencies but when the difference between optical frequencies results in an electrical frequency inside the photodetector bandwidth, amplitude fluctuations are perceived in the detected signal.

Comparing Figure 5.4 and Figure 5.5, the difference is the first term suppression after the detection/perceiving stage. In the acoustic field, the frequency (inverse of the frequency semi-difference) inside the periodic volume fluctuation is kept while in the optics field it is suppressed.

From the analogy of the OBI concept in optics and acoustics, we can design a model to particularize the effect in the optical access networks field, focusing in the uplink. Figure 5.6 shows a schematic of a case in which two optical carriers transmit two OFDM signals. Both optical carriers are placed closely in the frequency domain.

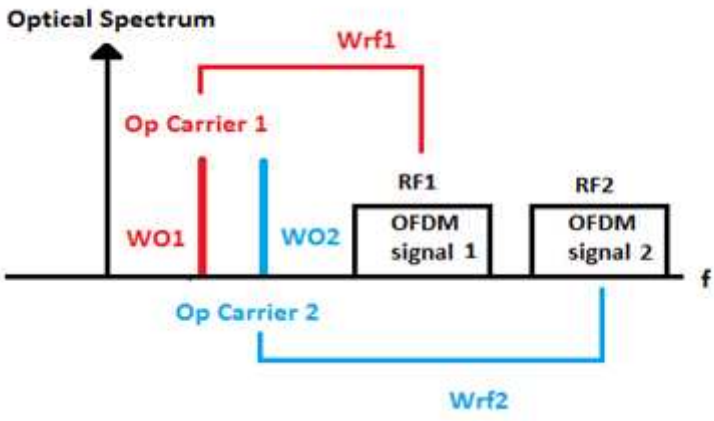

Figure 5.6. OBI Model

Being ω_{01} and ω_{02} the frequencies of the optical carriers and ω_{RF1} and ω_{RF2} the frequencies at which the OFDM signal should be retrieved at the receiver end (Figure 5.6). Following the model of Figure 3.6 and E 3.15, the signal at the input of the receiver would be:

$$\begin{bmatrix} \cos(\omega_{o1}t)\cdot(1+m_1\cdot x_1(t)\cdot e^{j\omega_{RF1}\cdot t})+ \\ +\cos(\omega_{o2}t)\cdot(1+m_2\cdot x_2(t)\cdot e^{j\omega_{RF2}\cdot t}) \end{bmatrix} \quad \textbf{(E 5.3)}$$

When these two optical OFDM signals are directly detected at the same photodetector, the electrical signal current obtained is:

$$i = \left| e^{j\omega_{o1}t} \cdot (1 + m_1 \cdot x_1(t) \cdot e^{j\omega_{RF1} \cdot t}) + e^{j\omega_{o2}t} \cdot (1 + m_2 \cdot x_2(t) \cdot e^{j\omega_{RF2} \cdot t}) \right|^2 \quad \textbf{(E 5.4)}$$

Setting the expression of E5.5 as a common factor, the analysis results in E5.6:

$$e^{j(\frac{\omega_{o1} + \omega_{o2}}{2})t} \quad \textbf{(E 5.5)}$$

$$i = \left| e^{j\frac{\omega_{o1}}{2} - \frac{\omega_{o2}}{2}t} \cdot (1 + m_1 \cdot x_1(t) \cdot e^{j\omega_{RF1} \cdot t}) + e^{j\frac{\omega_{o2}}{2} - \frac{\omega_{o1}}{2}t} \cdot (1 + m_2 \cdot x_2(t) \cdot e^{j\omega_{RF2} \cdot t}) \right|^2 \quad \textbf{(E 5.6)}$$

Finally, the obtained expression is:

$$i = \left| \begin{array}{l} \cos(\frac{-\Delta\omega}{2}t) + m_1 \cdot \cos\left(\frac{\Delta\omega}{2}t\right) \cdot \cos((\omega_{RF1} - \frac{\Delta\omega}{2})t) \cdot x_1(t) + \cos(\frac{\Delta\omega}{2}t) \\ + m_2 \cdot \cos(\frac{\Delta\omega}{2}t) \cdot \cos((\omega_{RF2} - \frac{\Delta\omega}{2})t) \cdot x_2(t) \end{array} \right|^2 \quad \textbf{(E 5.7)}$$

On the other hand, the ideal reception of two tones should be:

$$\begin{array}{l} i = m_1 \cdot x_1(t) \cdot \cos(\omega_{RF1}t) + \\ + m_2 \cdot x_2(t) \cdot \cos(\omega_{RF2}t) \end{array} \quad \textbf{(E 5.8)}$$

Comparing the expressions of both ideal case and actual case, the causes of the OBI can be explained with the first, second and third terms of E 5.9. Note that in expression E 5.9 second order terms in the optical modulation index have been omitted. These terms come from the data-data mixing products and are usually very small as compared to the other OBI terms. They have been referred in other chapters of this Thesis as the intermodulation products. As said before, guardbands are the usual means to get rid of these interfering products, which can also be considered a kind of OBI.

The first term in E 5.9 represents the carrier-carrier interfering mixing products (explained in 5.3). The second term represents amplitude fluctuations, and the third term is referred to frequency change. The second and third terms regard to the OBI effect due to the detection of signal bands by mixing with multiple carriers (carrier-data interfering mixing products).

$$i = \underbrace{\cos^2(\frac{\Delta\omega}{2}t)}_{TERM\,1} + m_1 \cdot \underbrace{\cos(\frac{\Delta\omega}{2}t)}_{TERM\,2} \cdot \cos((\omega_{RF1} - \underbrace{\frac{\Delta\omega}{2}}_{TERM\,3})t) \cdot x_1(t) + \qquad \textbf{(E 5.9)}$$

$$+ m_2 \cdot \underbrace{\cos(\frac{\Delta\omega}{2}t)}_{TERM\,2} \cdot \cos((\omega_{RF2} - \underbrace{\frac{\Delta\omega}{2}}_{TERM\,3})t) \cdot x_2(t)$$

Looking at the above from an intuitive viewpoint, we may think that direct detection is based on the mixing of a carrier with the data signal which in this scheme is located at a RF frequency; these would be the ‘good’ mixing products since they provide in reception the electrical signal that was modulated in the transmitter. In direct-detection OFDMA schemes where the optical signals coming from all the ONUs are detected together in the same photodiode in the OLT, other ‘interfering’ mixing products appear. We will refer to these interfering mixing products with the generic term **OBI (Optical Beat Interference)** since they interfere with the signal when they fall into the signal frequency band.

Among these “interfering” mixing products we can distinguish three different types:

1. **carrier-carrier** interfering mixing products
2. **carrier-data** interfering mixing products
3. **data-data** interfering mixing products

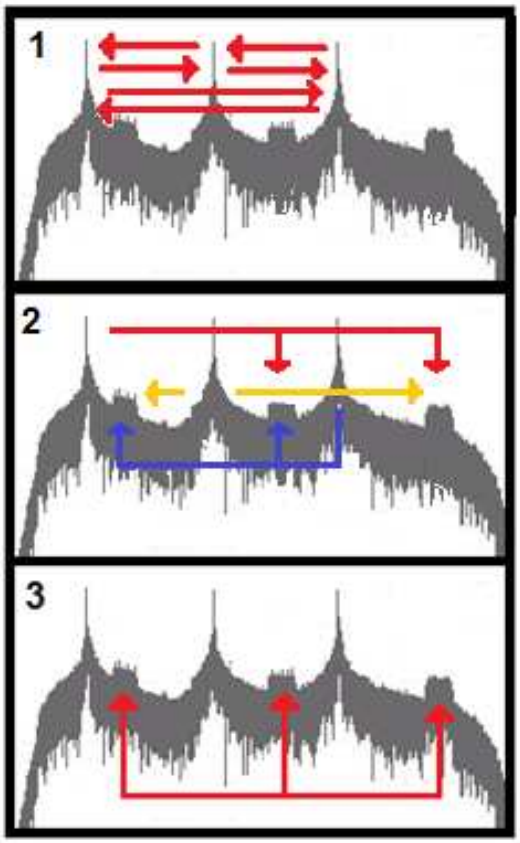

Figure 5.7. OBI Types

In the SE approach since all the carriers are at the same frequency, the carrier-carrier OBI product due to decorrelation of carriers will be restricted to a low frequency bandwidth (approximately equivalent to the linewidth) which is usually left as a security guardband. As said, the data-data OBI is equivalent to the intermodulation products analyzed in section 3.4.2 and the very reason to leave the guardbands and so it can also be eliminated by electrical filtering of the relevant electrical band at the photodetector output. It is finally the carrier-data OBI the one relevant and the one analyzed in more detail in 5.2.

Conversely, in the low-cost approach, practically all OBI products could be relevant but the most powerful are those of the carrier-carrier kind, and therefore these OBI products are the main focus of the study in section 5.3. Specifically, we will see which is the minimum spectral distance between the different ONUs wavelengths to guarantee the transmission quality.

5.2 Carrier - Data OBI. Spectral Efficient Approach

Once the OBI effect has been explained, the next step is to simulate its effects in the VPI tool.

A simulation scenario has been designed with two ONUs which modulate their data following a spectral-efficient approach, over decorrelated optical carriers of the same wavelength and with different electrical frequencies. See next Figure.

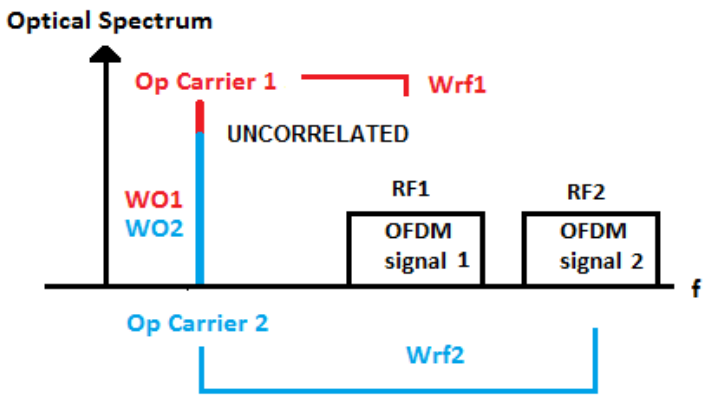

Figure 5.8. Seeded approach scheme

As explained in 5.2, the correlation between the laser sources in the simulations is a key aspect. In fact, depending on this characteristic, the approach of the simulations could vary significantly. In VPI, the correlation among the different laser sources in a simulation has to be set through the *Random Number Seed* option, situated in the laser options menu (Figure 5.9). By setting different numbers for all the laser sources in the simulation, VPI simulates a phase noise uncorrelation among them.

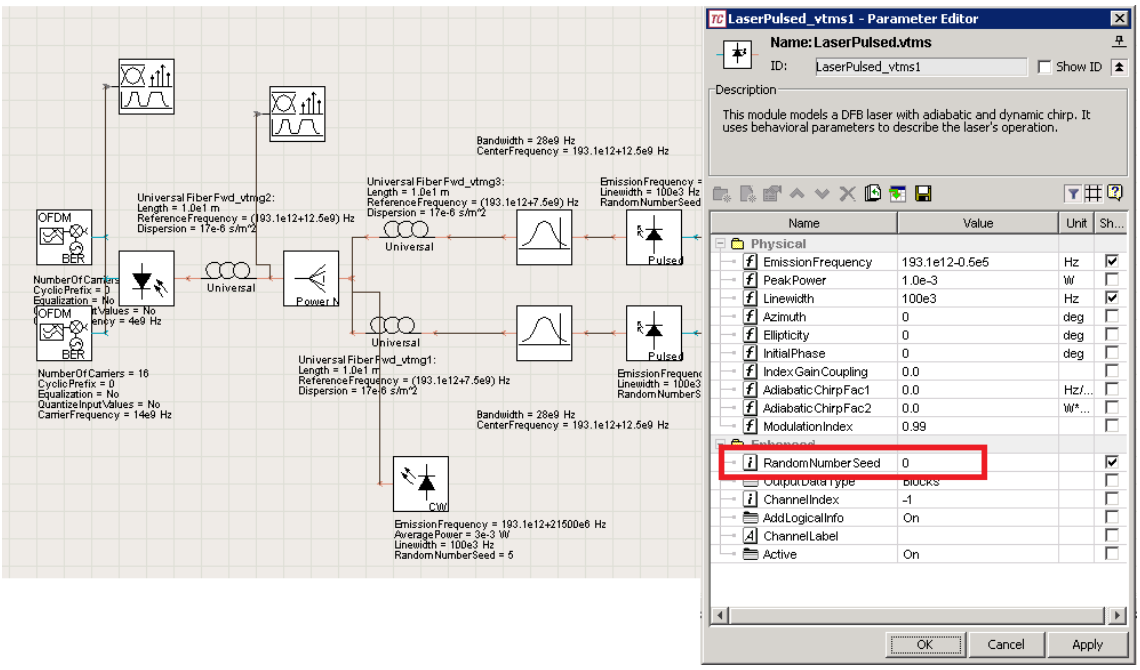

Figure 5.9. Correlation VPI configuration

The simulation setup used is shown in Figure 5.10. This demo is based on the one shown in Figure 4.5 but adding an extra OFDM modulator with its corresponding laser source and voltage driver, simulating a second uplink user. Both optical channels are joint by an **optical coupler** module and their logical bands are mixed in the same channel by means of a **Join bands** module.

As said, there are two laser sources with their corresponding OFDM modulators. By contrast, in this case, only one OFDM demodulator is used because it is only necessary to measure the constellation received by one laser source. The effect produced by the neighbor source is going to be appreciated in the single constellation received.

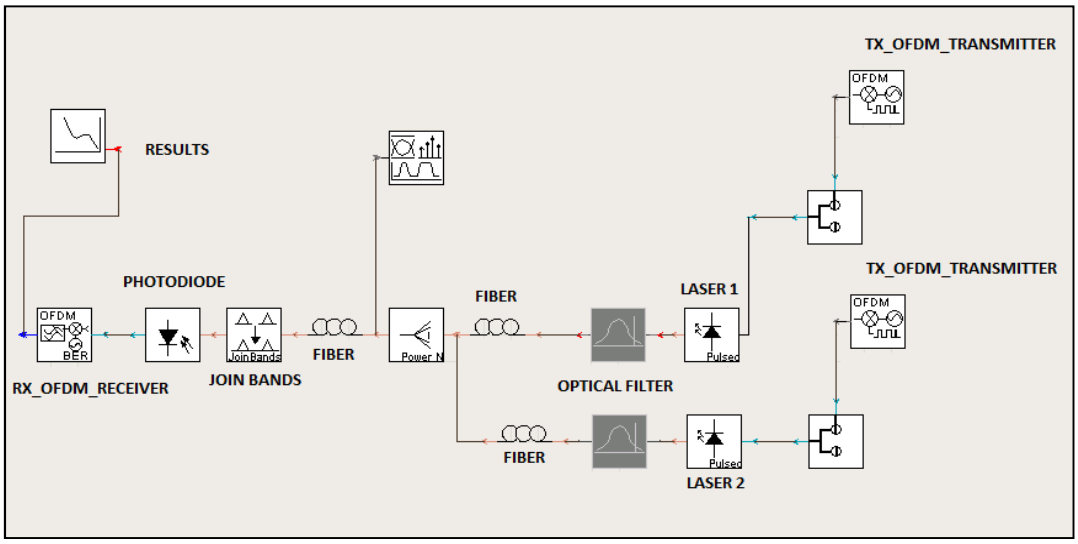

Figure 5.10. Simulation setup scheme

The constellation received for the SE approach showing the effect of the OBI introduced by the second decorrelated optical carrier at the same frequency is shown in Figure 5.11:

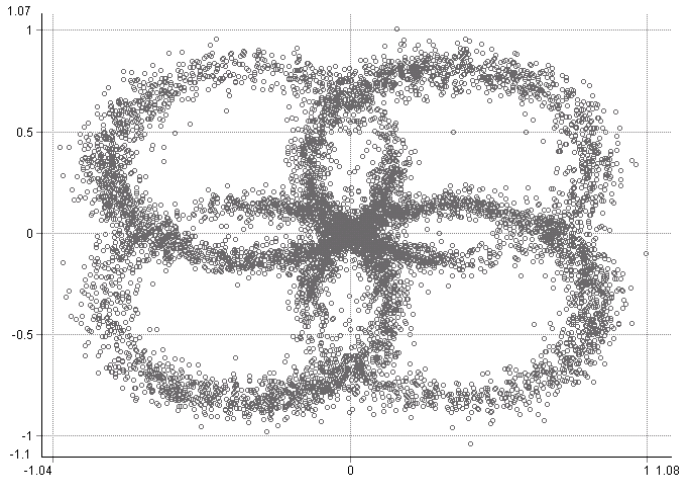

Figure 5.11. Second scenario. Received constellation

Looking closely into this constellation we may infer that the ring-shapes are due to the overlapped reception of two mixing products of the data sideband respectively with each one of the two present carriers. One is the mixing with the sideband with the correlated carrier which would give the correct QAM symbol. On top of that there is the mixing product of the single band with the decorrelated carrier with a random phase and hence following the ring shape.

To verify this extreme we may change the power into the interfering optical carrier to obtain smaller diameter rings. Figure 5.12.

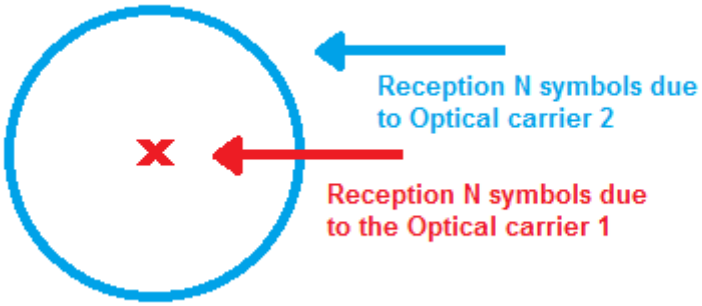

Figure 5.12. Result explanation of a lobe of the received constellation (Figure 5.8)

The following figure explains intuitively the previous explanation. In the detecting process of the OFDM signal, when having several uncorrelated optical carriers at the same frequency there is a **Multi detection** effect which gives errors in the received constellation (see Figure 5.11). These errors are due to the different phase noise from each of the optical carrier. In other words, the OFDM signals are detected N-times with different phase shifts. (Figure 5.13)

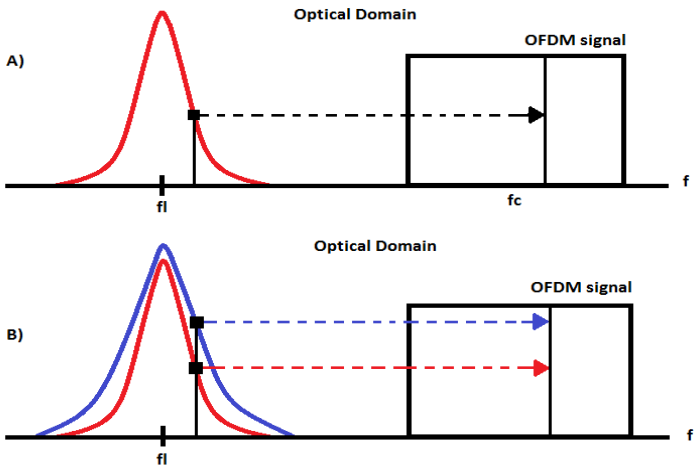

Figure 5.13. Multidetection

5.2.1 Using different optical carriers for TX/RX

In order to prove the multi-detection effect, another scenario has been designed to corroborate the previous explanation. Thus, the detection will be performed by a different optical carrier than the one used in transmission.

One laser source has been set acting as a transmission optical carrier of the OFDM signal. The electrical frequency in the OFDM TX is 500 MHz (BW_{OFDM}=100MHz). According to Figure 5.14, the OFDM will be detected by the second optical carrier with a certain frequency spacing ($\Delta\omega_{1=}$100MHz). Both lasers are uncorrelated. The OFDM RX is configured with an electrical frequency of 400MHz. The optical carrier and electrical carrier frequencies have been selected so that the mixing products with the TX carrier do not interfere with the RX electrical band.

Thus, the scenario of Figure 5.14 represents a model of the multicarrier detection.

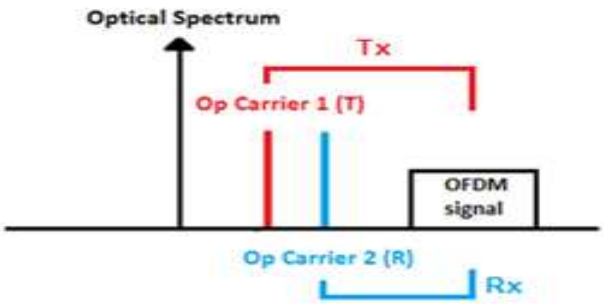

Figure 5.14. Graphical test description.

The optical and electrical (after detection) spectrum of the setup is shown in Figure 5.15. As seen, the optical SSB filter is not active and consequently, the OFDM signal is present with double sideband.

In the electrical spectrum image (Figure 5.15), we distinguish the carrier-carrier OBI at 100MHz (a) and the overlapped detection with each one of the optical carriers.
Specifically, the ‘c’ term represents the detection mix of the original TX carrier with ‘e’ and ‘f’. On the other hand, ‘b’ represents the term resulting from the beat between the RX carrier with ‘f’ (this is the band considered for detection in the constellation of Fig. 5.16), and finally,‘d’ represents the term resulting from the mix between the RX carrier and ‘e’.

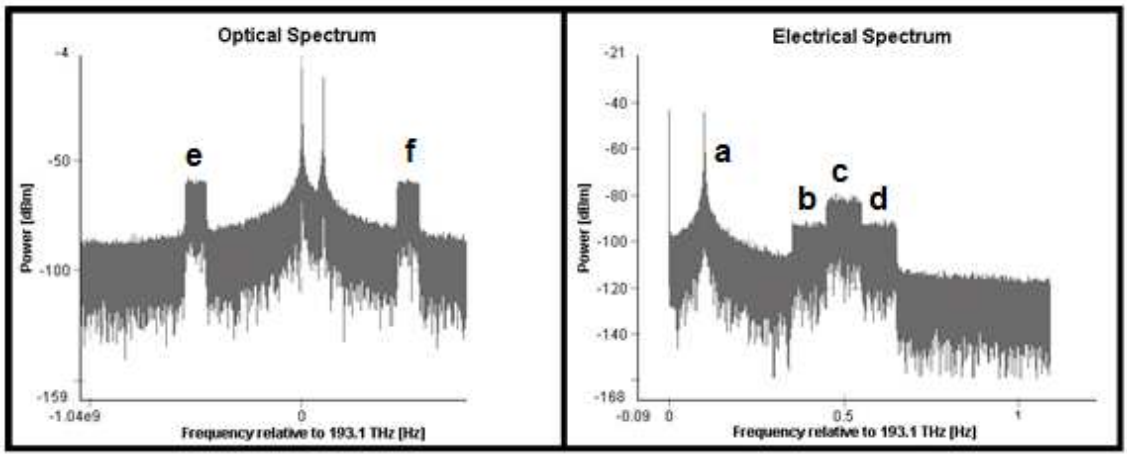

Figure 5.15. Multidetection setup. Optical and Electrical spectrum.

The result of the simulation is shown in Figure 5.16:

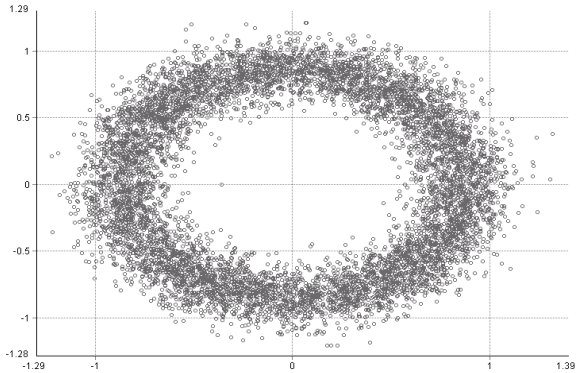

Figure 5.16. Received constellation. Different optical carriers for TX/RX

The round shape of the constellation in Figure 5.16 is due to the phase uncorrelation between the TX and the RX carrier. Since the optical carrier used for the detection comes from a different laser source than the transmission optical carrier, the phase noise difference between both laser sources provokes the mentioned uncorrelation effect.

At this point, a mathematical explanation of the effect shown in Figure 5.16 is necessary. Since the correlation characteristic of the laser sources is an intrinsic feature defined by their phase noise, which is of a random nature the grade of complexity to describe it mathematically is high.

Understanding of the basic phase noise mechanisms behind these ring-shaped constellations (see Figure 5.11 and Figure 5.16) gives us the clue to conclude that a similar constellation would be obtained when correlated but with slightly different wavelength interferring carriers are present. That is indeed the case as it is shown in the next section.

5.2.2 Correlated carriers with a frequency drift

Both optical carriers have been configured as correlated.

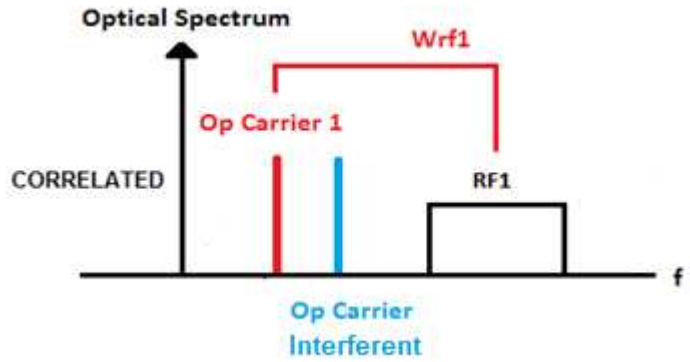

Figure 5.17. Equivalent model with correlation

The received constellation is shown in Figure 5.18:

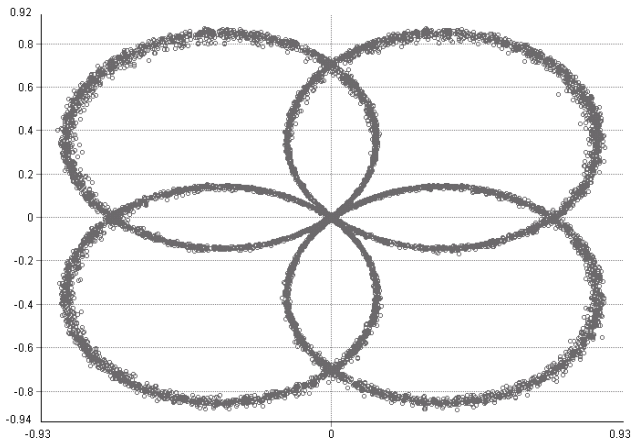

Figure 5.18. Correlated carriers with a frequency drift setup. Received constellation. Linewidth 100 KHz

It is observed the same effect at reception with uncorrelated carriers placed at the same optical frequency and correlated laser sources with a frequency drift (see setup specifications ANNEXES B). We may then analyze the OBI effect mathematically by analogy with the correlated but slightly different wavelengths optical carriers case. This is done in the next section.

5.2.3 Mathematical analysis of carrier-data OBI

Being Δf_2 the frequency spacing, the detected OFDM signal with a slightly spaced optical carrier can be written as follows:

$$\sum_{i=1}^{N_{OFDM}} \sum_{k=0}^{N} C_{ik} \cdot e^{j2\pi(k\Delta f+\Delta f_2)t} p\left(\frac{t-iTOFDM}{TOFDM}\right) \qquad \textbf{(E 5.10)}$$

Where N_{OFDM} is the the number of OFDM frames and N is the number of carriers for each frame. $\Delta f=1/T_{OFDM}$ is the subcarrier spacing, with T_{OFDM} as frame period.

At the receiver end, prior to the FFT application, the received frame (i) is sampled at $t = i \cdot T_{OFDM} + nT_S$, being T_S the symbol period ($T_{OFDM}=N \cdot T_S$) as:

$$X_i(n) \approx e^{j2\pi i v} \sum_{k=0}^{N} C_{ik} \cdot e^{j\frac{2\pi k}{N}n} \qquad \textbf{(E 5.11)}$$

Being $v=\Delta f_2/\Delta f$. As seen, each OFDM frame will be affected by a different phase delay, and when multiple carrier detections occur, constellations such as the one showed in Figure 5.11 will be obtained. This non-desired effect increases with the number of users making the SE approach impractical.

A solution would be to use in detection a new optical carrier (RX carrier) in a different spectral position. The TX carrier could be filtered out in reception, or else (or also) the RX carrier spectral position could be chosen so that its electrical mixing band with the OFDM signal falls in a different electrical band to the one of the mixing of the OFDM signal with the TX carrier.
The constellation obtained will be similar to the one in Fig. 5.16; the ring could then be compensated by temporal training using a few subcarriers as pilot tones.

5.3 Carrier – Carrier OBI. Low-Cost approach. Local Free-Running Sources

This kind of OBI occurs when two or more lasers transmit in different optical channels spaced closely in the frequency domain. See the example in Figure 3.14.

Since the incident optical signal in the RX photodetector is the sum of the fields of the individual carriers, the photocurrent will contain beat signals which are the cross-terms at the difference frequencies that are produced when the optical field interacts in pairs [P5]. If some beat signals appear in an active subcarrier channel, the signal can be significantly degraded. The interference spectrum will be centered at a frequency equal to the difference of the optical frequencies from the two optical sources (laser). The following figures show theoretically and empirically the Carrier-Carrier OBI.

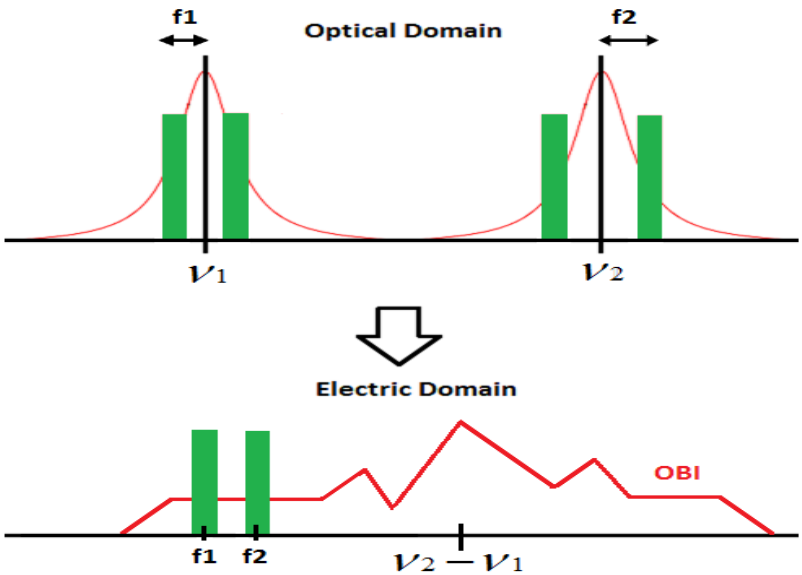

Figure 5.19. OBI due to optical carrier beating graphic

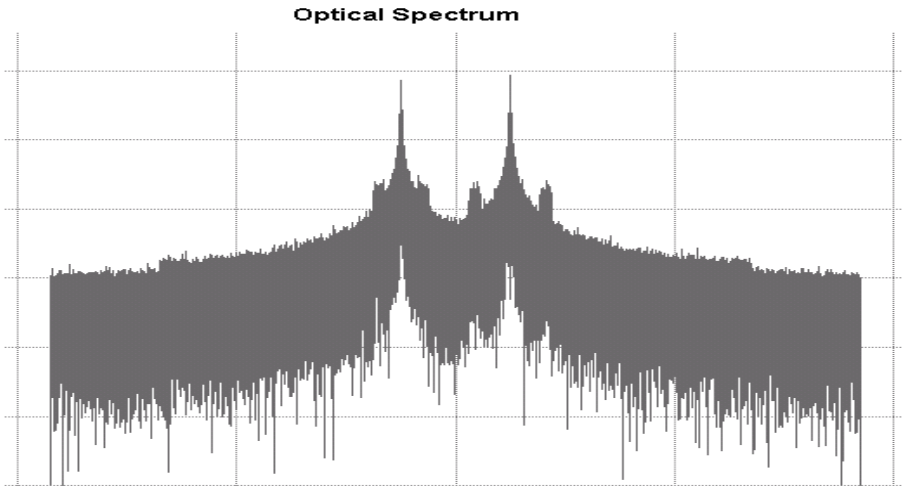

Figure 5.20. OBI due to optical carrier beating. Optical spectrum

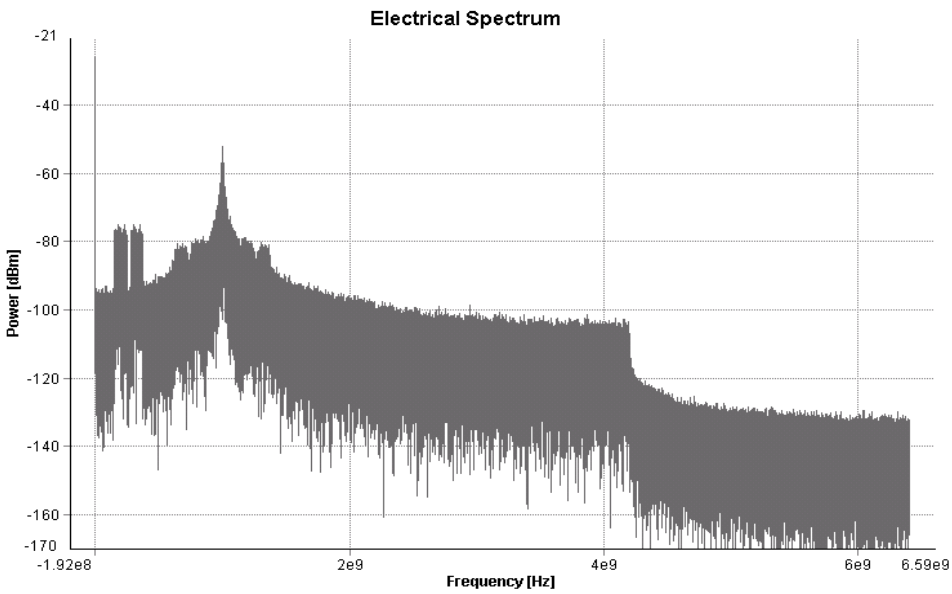

Figure 5.21. OBI due to optical carrier beating. Electrical spectrum

Mathematically, the Carrier-Carrier OBI effect is analyzed below. We assume that the Carrier-to-Interference Ratio (CIR) is the suitable quantity to measure the OBI at the input of the electrical detector [B1]. So, the goal of the further mathematical development is to obtain an expression to evaluate the total OBI effect in terms of CIR in a multiuser scenario.

We consider a total of M users each with an OFDM signal bandwidth B. On the receiver side, an optical signal consisting of a superposition of all transmitter signals is received and converted to electrical form by means of a direct detection. Note that the OFDM subcarriers from all M optical carriers are spaced equally among them. Graphically, we might recall Figure 3.14 and Figure 3.15.

Thus, the combined optical field at the receiver input *ε(t)* is composed by the contributions of the M transmitters as follows:

$$\varepsilon(t) = \sum_{k=0}^{M} \varepsilon_k(t) \qquad \textbf{(E5.12)}$$

Each $\varepsilon_k(t)$ contribution is defined in (E5.13. The following expression is based in the complex representation.

$$\varepsilon_k(t) = \mathrm{Re}\left[E_k(t) e^{j2k\pi v_{ot}}\right] \qquad \textbf{(E5.13)}$$

Being *E(t)* the electrical field of the optical carrier and v_o the nominal optical frequency for all transmissions. At the same time, the electrical field can be expressed as:

$$E_k(t) = Eo\sqrt{1 + m_k \cdot X(t)} \cdot e^{2\pi v_k} \cdot e^{j\Phi_k(t)} \qquad \textbf{(E5.14)}$$

The photocurrent output at the detector *i(t)* is proportional to the total intensity of the incident field.

$$\begin{aligned} i(t) &= \frac{R}{2}\left|\sum_k E_k\right|^2 = \frac{R}{2}\left(\sum_k E_k \cdot \sum_k E_k^*\right) = \\ &= \frac{R}{2}\sum_k \left|E_k\right|^2 + R\sum_k\sum_n E_k \cdot E_n^* = \\ &\frac{R}{2} E_o^2 \sum_k (1 + m_k \cdot x(t)) e^{j2\pi v_k t} e^{j\phi_k(t)} + \\ &+ RE_o \sum_k\sum_n (1 + m_k \cdot x(t)) \cdot (1 + m_k \cdot x(t)) \cdot e^{j2\pi(v_k - v_n)t + j(\phi_k(t) - \phi_n(t))} \end{aligned} \qquad \textbf{(E5.15)}$$

where *R* is the responsivity of the photodetector. The first term of the equation represents the detected signals. The second term represents the OBI effect centered at v_k-v_n. If the energy of this OBI term falls in the signal electrical band it will interfere with the signal, see Figure 5.19 and Figure 5.21. We consider that the quality of transmission is maintained if the CIR is below a certain quality

threshold. The CIR is defined as the average power of one signal over the combined average power of their co-channel adjacent signals.

It is possible to model the OBI if the signal power spectrum and the optical field spectrum are known for each laser. The optical spectrum of the lasers can be modeled as a lorentzian shape (Figure 5.22). The convolution of two lorentzian functions can be approximated by a lorentzian whose width equals the sum of widths of the convolving lorentzians, therefore a lorentzian spectrum has been found empirically to model well the OBI for low values of m [B1].

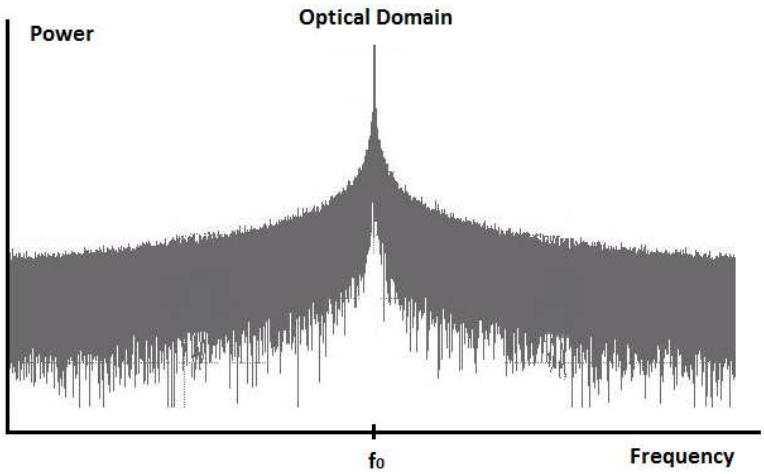

Figure 5.22. Lorentzian Shape optical spectrum

Now, a graphic of two-sided lorentzian PSD function is shown in Figure 5.23. This PSD is centered at f_o; this value represents the difference between the optical frequencies from the two optical sources. So $f_o = v_k - v_n$.

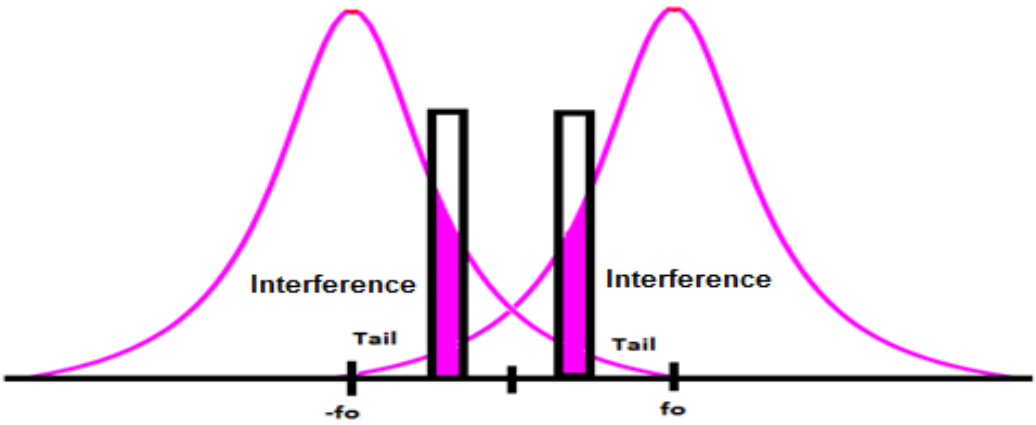

Figure 5.23. Two-sided Lorentzian PSD graphic

Being a the laser spectral width, the mathematical expression that represents the two-sided Lorentzian PSD function is:

$$g(f) = \frac{a}{2\pi(a^2 + (-fo)^2)} + \frac{a}{2\pi(a^2 + (fo)^2)} \qquad \textbf{(E5.16)}$$

Being f_o the optical frequency difference: v_k-v_n or $k \cdot \Delta v$, with k as an integer. Each term of OBI in the electrical domain is the result of convolving the optical spectra from two laser sources. The width of each optical signal spectral component increases with laser linewidth.

Now, in order to fulfill the goal of this analysis (CIR expression) it is necessary to know the total OBI power of the system (P_{OBI}). We need to take into account all the mixing terms between any two laser sources in a multi-transmitter scenario. Being M the number of transmitters the result is shown in the next figure. The factor of the number of beats between any two carriers is ***2(M-k)***. As indicated, f_o can be rewritten as $fo=(k \cdot \Delta v)$.

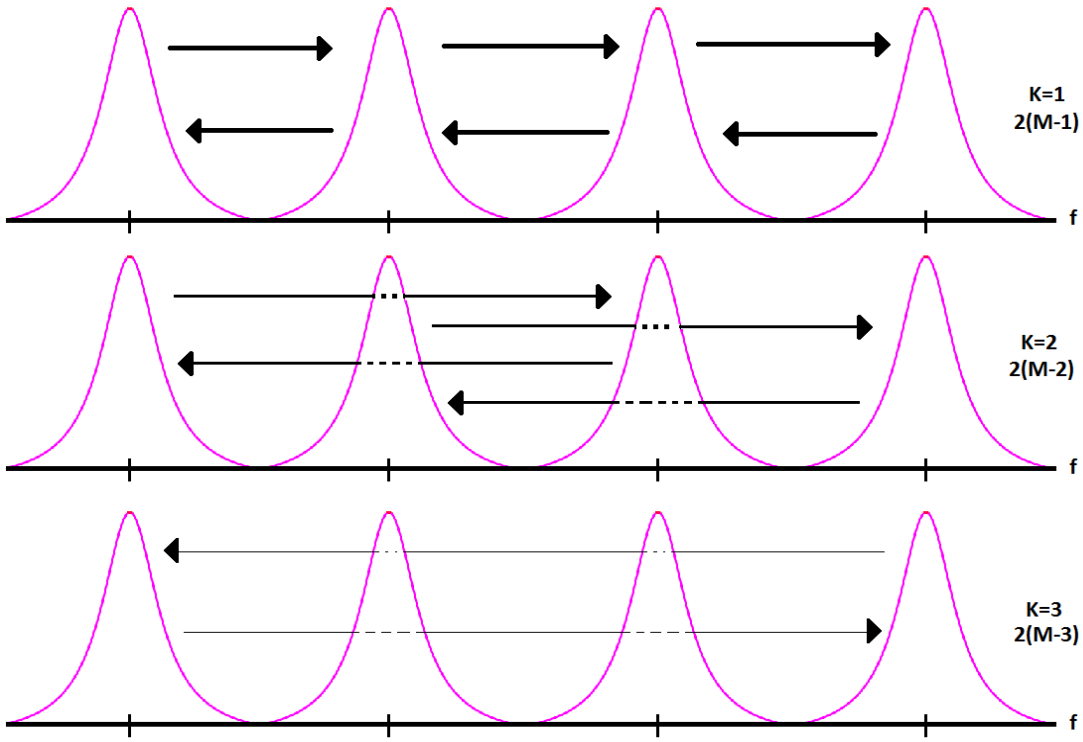

Figure 5.24. Carrier beating graphic

On the other hand, according to [B1], then, the results of the carrier power and the OBI total power in the *i(t)* equation (E5.15) are:

- For the electrical carrier signal (taken as a pure tone signal)

$$P_{signal} = \left(\frac{R}{2} E_o^{\,2}\right)^2 \cdot \frac{m_k^{\,2}}{2} = \frac{R^2 E_o^{\,4} m_k^{\,2}}{8} \qquad \textbf{(E5.17)}$$

- For the OBI power:

$$R^2 E_0^{\,4} \cdot \int_B g(f)\, Interference \cdot df \cong g(0) \cdot B \qquad \textbf{(E 5.18)}$$

When computing the OBI power affecting the useful signal band, it is assumed for simplicity that *Δv>>Bandwidth=M*B*, so, the integral of g(f) over the signal bands can be simply approximated as ***B·g(0)***.

$$g(0) = \frac{a}{\pi(a^2 + fo^2)} \qquad \textbf{(E5.19)}$$

Considering all the previous analysis, in order to find out the OBI power, let:

$$P_{OBI} = \sum_{k=1}^{M} \frac{a}{\pi(a^2 + k^2 \Delta\nu^2)} \cdot R^2 E_o^{\,4} \cdot (M-k) \cdot B = \sum_{k=1}^{M} \frac{a \cdot R^2 E_o^{\,4} \cdot (M-k) \cdot B}{\pi(a^2 + k^2 \Delta\nu^2)} \qquad \textbf{(E5.20)}$$

Finally, once the total OBI power is obtained, the Carrier to Interference Ratio expression can be fulfilled. Note that as a first approximation we will only consider relevant the interference between adjacent optical carrier:

$$CIR = \frac{\text{Average Carrier Power}}{\text{Average co - Channel Interference Power}} = \frac{P_{Carrier}}{P_{OBI}} \qquad \textbf{(E5.21)}$$

The CIR expression that can be used to evaluate the OBI effect is given by:

$$CIR = \frac{\dfrac{R^2 E_o^4 m_k^2}{8}}{\dfrac{a \cdot R^2 E_o^4 \cdot (M-k) \cdot B}{\pi(a^2 + k^2 \Delta\nu^2)}} = \frac{R^2 E_o^4 m_k^2 \cdot \pi(a^2 + k^2 \Delta\nu^2)}{8 \cdot a \cdot R^2 E_o^4 \cdot (M-k) \cdot B} = \frac{m_k^2 \cdot \pi(a^2 + \Delta\nu^2)}{8 \cdot a \cdot (M-1) \cdot B}$$

(E5.22)

5.3.1 Carrier-Carrier OBI simulations

Having the previous expression of the CIR due to the OBI as a result of the theoretical study of the Low-Cost Approach, in this section, the minimum wavelength separation in a multiuser scenario is going to be evaluated by means of a VPI simulation, guaranteeing a good transmission quality according to EVM (see ANNEXES C).

Graphically, the test process is shown in Figure 5.25. The goal of the test is to analyze the effect on EVM value of an OFDM transmission in presence of two optical sources equally spaced upwards and downwards in frequency domain as a function of the spectral gap between the optical sources. First of all, those two lasers are placed closely (400MHz) to the center laser. In each iteration of the simulation, those lasers are going to be separated 50MHz from the reference. Each laser represents an user on an access network.

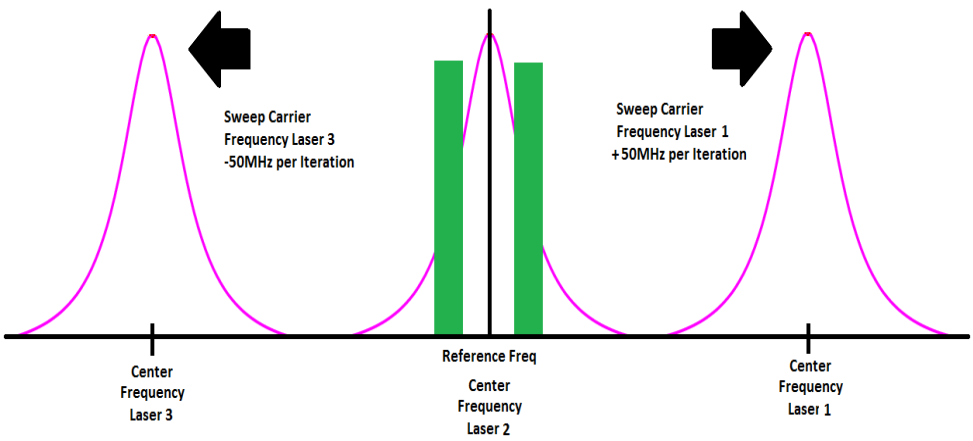

Figure 5.25. Simulation test graphic

Scenario description (see ANNEXES B to know all parameters):

- Laser1: 193,1THz + 400MHz
- Laser2: 193,1THz

- Laser3: 193,1THz - 400MHz
- Iterations: 40
- Ramp value Laser1: 50MHz
- Ramp value Laser3: -50MHz
- Carrier Frequency OFDM signal: 150MHz
- Bandwidth OFDM signal: 100MHz
- OFDM Carriers: 16
- Bit Rate: 200 MHz

In Figure 5.26 a plot of the simulation design is shown. A sweep has been performed following the method explained in 3.7.1. Moreover, in this case, the laser sources number one and three do not have any OFDM coder nor voltage driver installed. Since the goal of this simulation is to study the Carrier-Carrier interference effect, the OFDM data signals are no longer necessary.

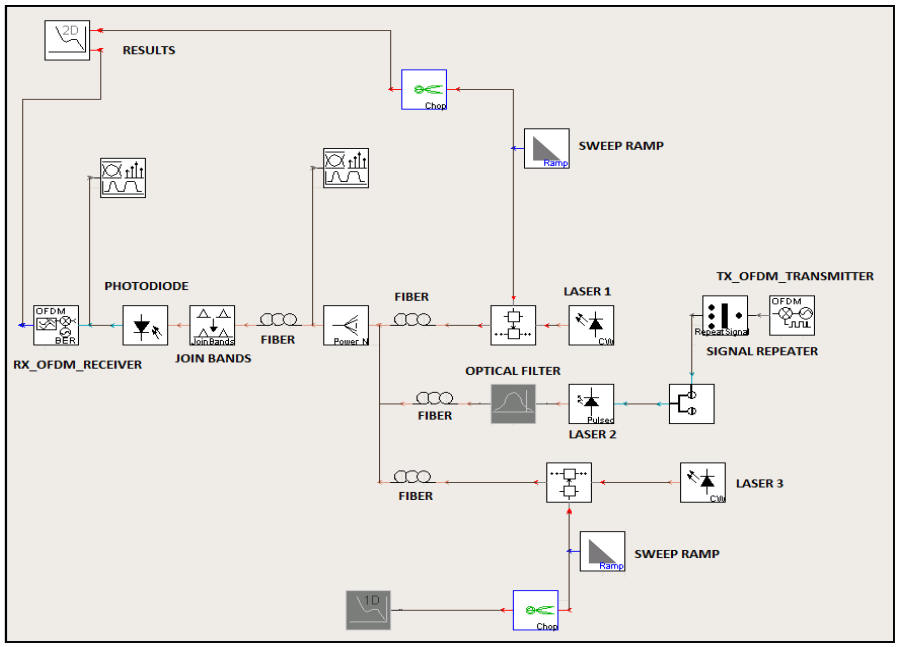

Figure 5.26. OBI analysis scenario

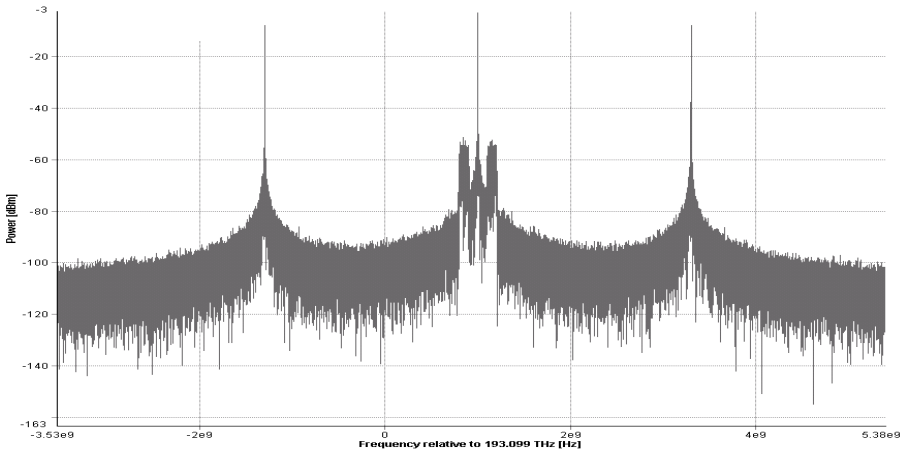

Figure 5.27. Received optical signals at the photo-detector

5.3.2 Results

Due to the fiber length used in the scenario design (Figure 5.26). the optical filter has not been set. Moreover, the isolation of the OBI effect in the system has been another important reason to spare the SSB filter in this simulation.

As it can be seen in the next figures, the OBI effect in the quality of the received constellation decreases as the frequency spacing among the optical carriers increases. Depending on the linewidth of the lasers employed, the minimum space among the laser sources in order to obtain a acceptable performance will vary. Finally, a comparison has been made using different linewidths.

Uncorrelated Lasers with Linewidth = 10KHz:

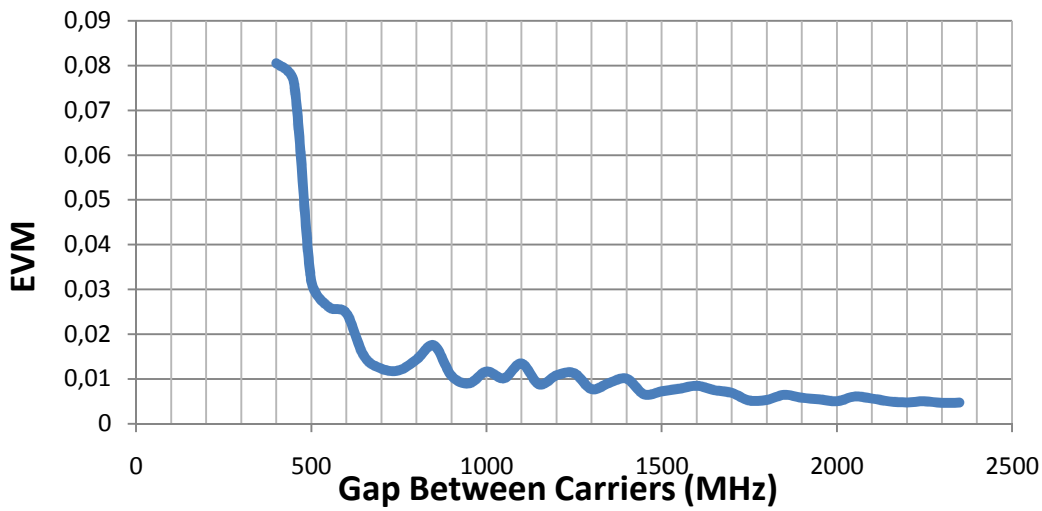

Chart 5.1. EVM evolution due to the gap set among the optical carriers

Uncorrelated Lasers with Linewidth = 1MHz:

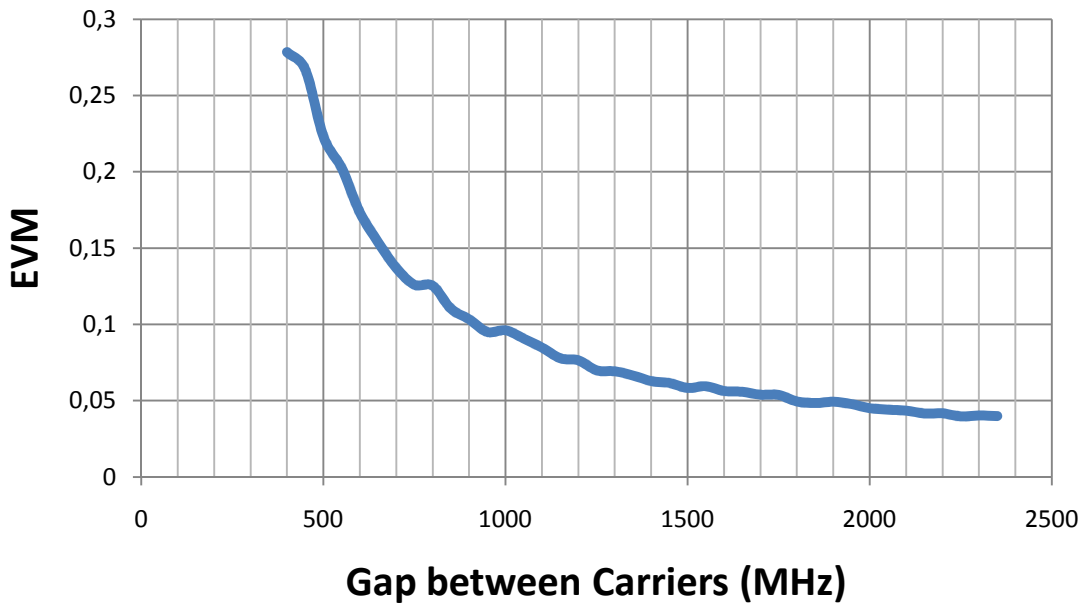

Chart 5.2. EVM evolution due to the gap set among the optical carriers

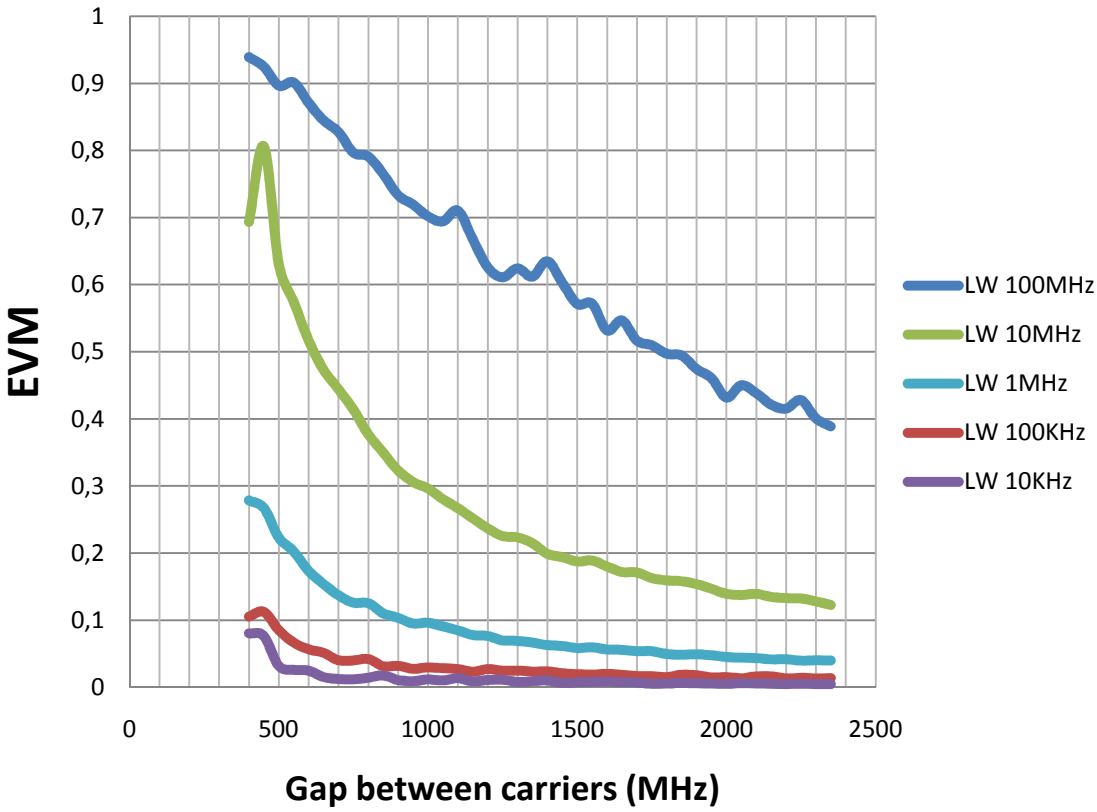

Chart 5.3. Comparison among different linewidths

According to the range of acceptable EVM values for a 4-QAM constellation in ANNEXES C, only the laser sources from 10KHz to 1MHz fulfill the EVM requirements with a gap of at least 1500 MHz.

CHAPTER 6. CONCLUSIONS AND FUTURE LINES

6.1 Conclusions

In this Master Thesis a review of the basic concepts of OFDM modulation and transmission has been carried out with emphasis on applications in fiber optics access. In this sense, the characteristics of fiber optics transmission and in particular the effects of chromatic dispersion have been analyzed. Also, conventional optical modulation and detection techniques have been reviewed with an eye to identify potential modulation and demodulation techniques for the optical transmission of OFDM signals.

A classification of optical OFDM transmission techniques has been formulated and benefits and drawbacks of each one have been highlighted.

From the different optical OFDM transmission options identified, we have chosen as a subject for further study the RF up-conversion and direct detection technique and we have analyzed the requirements of an optical single side band filter and the allocation of guardbands, both through theoretical analysis and with simulations using VPI. The results show that for the typical distances used in access networks (up to 30Km) and data rates up to 10Gbps we could drop the requirement of the SSB filter in some access applications allowing for colorless ONU operation and cost reduction.

As about the required guard band, the result of the tests performed prove that the amount of guardband necessary in systems with the characteristics of Figure 4.7 for fiber lengths up to 30 kilometers need not exceed the 10 percent of the OFDM bandwidth, which means that lower bandwidth (and hence lower cost) electronics could be used in OFDMA-PONs.

Another important contribution of this Master Thesis refers to the study of the user multiplexing strategies. Two strategies based on IM/DD optical OFDM systems have been analyzed which assume different wavelength allocations of the optical carrier of each user. In the SE (Figure 5.1) approach the optical carriers from each ONU share the same wavelength while in the LC (Figure 5.25 and Figure 5.27) approach, enough spectral separation between carriers needs to be guaranteed in order to ensure acceptable CIR levels. The basic problem to deal with is the OBI generated in the joint direct optical detection.

A detailed study of the OBI effect has been carried out. The origin of the OBI concept and it specific meaning in the field of optics has been clarified. In optics, the term OBI has been found to generically refer to all kinds of undesired optical mixing products taking place in the direct detection process. In subcarrier multiplexing networks three basic kinds of OBI have been identified: carrier-to-carrier, carrier-to-data and data-data, this latter is also sometimes referred to intermodulation products.

In the context of the SE uplink multiplexing strategy, the data-carrier OBI is the relevant effect. Several simulations have been performed to see that due to the uncorrelation of the superposed carriers a ring-shaped constellation is obtained that makes this system unpractical. A mathematical derivation has shown the mechanisms that lead to such constellations. A proposal for circumventing the problem is to use a different carrier for detection and to compensate for the phase noise by means of pilot tones. This task is left for future works.

In the context of the LC uplink multiplexing strategy, the carrier-carrier OBI is found to be the most relevant. We have provided a closed mathematical expression to find the CIR values and have determined through simulation the minimum spectral separation between optical carriers that ensure a minimum quality threshold for several scenarios of practical relevance.

6.2 Future Lines

Regarding the modulation and detection schemes used in the simulations of this Master Thesis, it is interesting to study other options for optical detection, such as the coherent detection. In fact, a comparison between the current OBI effect study using direct detection against coherent detection can be an interesting future research line.

Regarding the OBI, our goal has been based on trying to understand in depth this phenomenon, explaining its causes and consequences. This is the first step to try to avoid it. As a factor to take into account for the access network design, further developments need to focus on this research line. Phase noise compensation using pilot tones should be the continuation research line withregard to the multicarrier detection occurred in the Carrier-data OBI.

Note that, the laser chirp feature in DML has not been taken into account in the simulations performed in this Master Thesis. In next studies, the effect of this parameter in the presented studies should be evaluated.

Finally, another important future line to follow would be laboratory tests of the scenarios proposed in the simulations.

CHAPTER 7. ACRONYMS

- ADC - Analogue-to-digital converter
- BER – Bit error rate
- CD – Chromatic dispersion
- CMOS - Complementary Metal Oxide Semiconductor
- CO-D - Coherent detection
- CP - Cyclic prefix
- DAC - Digital-to-analogue converter
- DD- Direct detection
- DFB Laser - Distributed feedback Laser
- DML – Directly Modulated Laser
- (x)DSL – Digital Subscriber Line
- EVM - Error vector magnitude
- FDM - Frequency division multiplexing
- FFT – Fast Fourier transform
- FTTB – Fiber To The Building
- FTTH – Fiber To The House
- GB- Guard Band
- GDD - Group Delay Dispersion
- HS – Hermitian Symmetry
- ICI – Intercarrier interference
- IFFT - Inverse fast Fourier transform
- IM - Intensity modulation
- ISI - Inter-symbol interference
- LO – Local oscillator
- MZM - Mach-Zehnder modulator
- NGPON – New Generation Passive Optical Network
- OBI- Optical Beat Interference
- OFDM – Orthogonal frequency division multiplexing
- OLT – Optical Line Terminal
- ONU – Optical Network Unit
- PD - Photodetector
- PON – Passive Optical Network
- QP - Quadrature point
- QAM – Quadrature amplitude modulation
- SER - Symbol error rate
- SSB – Single Side Band
- TDMA – Time Division Multiplexing Access
- VPI - Virtual Photonics Inc.
- WLAN – Wireless Local Area Network

CHAPTER 8. REFERENCES

8.1 Books

[B1] Thomas E. Stern, Georgios Ellinas and Krishna Bala. *Multiwavelength Optical Networks: A Layered Approach* (Addison-Wesley Professional Computing Series). Cambridge, second Edition

8.2 Papers and tutorials

[P0] Jun Zheng and Nirwan Ansari, "*Optical Access Networks,"* Journal of Optical Networking, Vol. 4, Issue 6, pp. 355-356 (2005)

[P1] Jean Armstrong, *OFDM for Optical Communications* (Journal of Lightwave Technology, vol. 27, 2009)

[P2] Sander L. Jansen, *SC341 OFDM for Optical Communications* (Short Course OFC, 2010)

[P3] N.K.Shankaranarayanan, Stuart D. Elby and Kam Y. Lau*. WDMA/Subcarrier-FDMA Lightwave Networks: Limitations due to the Optical Beat Interference* (Journal of Lightwave Technology, vol. 9, 1991)

[P4] S.L. Woodward, X. Lu, T.E. Darcie and G.E. Bodep. *Reduction of Optical-Beat Interference in Subcarrier Networks*. (IEEE Photonics Technology Letters Vol.8, 1996)

[P5] N. Antoniades, W. Xin, T.E Stern, B.Pathak and E.S. Yang. *Use of Subcarrier Multiplexing/Multiple Access for multipoint Connections in All-Optical Networks*. (EE. Dept. Columbia University)

[P6] Can Desem. *Optical Interference in Subcarrier Multiplexed Systems with Multiple Optical Carriers*. (IEEE Journal on selected Areas in Communication vol.8, 1990)

[P7] Rishad Ahmed, Shafik, Md. Shahriar Rahman and Nabil Shovon Ashraf. *On The Error Vector Magnitude As A Performance Metric And Comparative Analysis* (IEEE--ICET 2006 2nd International Conference on Emerging Technologies)

[P8] Rishad Ahmed Shafik, Md. Shahriar Rahman and Nabil Shovon Ashraf .*On the Extended Relationships Among EVM, VER and SNR as Performance Metrics*.(4th International Conference on Electrical and Computer Engineering ICECE 2006)

[P9] VPI tutorial and Help reference.

[P10] Jun Zheng and Nirwan Ansari, "*Optical Access Networks,"* Journal of Optical Networking, Vol. 4, Issue 6, pp. 355-356 (2005)

[P11] Leonid G. Kazovsky, Wei-Tao Shaw, David Gutierrez, Ning Cheng, and Shing-Wa Wong, *"Next-Generation Optical Access Networks,"* J. Lightwave Technol. 25**, 3428-3442 3428-3442 (2007)**

[P12] S. L. Jansen, D. van den Borne, and S. Adhikari, "Past, Present and Future of Optical OFDM," in *Asia Communications and Photonics Conference and Exhibition*, Technical Digest (CD) (Optical Society of America, 2009)

[P13] Alok Aggarwal, Student Member, IEEE, and Teresa H. Meng, *"Minimizing the Peak-to-Average Power Ratio of OFDM Signals Using Convex Optimization"* IEEE transactions on signal processing, vol. 54, no. 8, august 2006

8.3 UPC Telecommunication Degree Thesis

[T1] Eduardo Heras Miguel, Supervisor: Concepción Santos Blanco. *Fiber-based Orthogonal Frequency Division Multiplexing Transmission Systems* (October 2010)

[T2] Josep Cardona and Lorena Fernández Campos. Supervisor: Concepción Santos Blanco. *Estudio de técnicas de modulación para enlaces ópticos* (February 2009)

[T3] Cristobal Manuel Romero Vidal and Edurne Garcia Villar. Supervisor: Concepción Santos Blanco*. Técnicas avanzadas de medida de dispersion cromática a frecuencias ópticas*. (January 2009)

[T4] Edurne García Villar. Supervisor: Concepción Santos Blanco*. Cost-effective optical transmission systems based on Orthogonal Frequency Division Multiplexing.*

8.4 Internet Sources

[I1] EE Times. James Chen. IEEE 802.11a - *Speeding Up Wireless Connectivity in the Home.*

http://www.eetimes.com/electronics-news/4139996/IEEE-802-11a--Speeding-Up-Wireless-Connectivity-in-the-Home

[I2] Connexions. Ha Ta-Hong, Tuan Do-Hong. *Pulse Shaping to reduce ISI*.

http://cnx.org/content/m15520/latest/

[I3] VPI Photonics official website.

http://www.vpiphotonics.com/

[I4] Wikipedia

http://en.wikipedia.org/

[I5] Accordance

http://ict-accordance.eu/Eng

[I6] IncoAx grafico paises

http://www.incoax.com/index.php?lang=en&cat=about

Escola d'Enginyeria de Telecomunicació i Aeroespacial de Castelldefels

UNIVERSITAT POLITÈCNICA DE CATALUNYA

ANNEXES

TITLE: Next-Generation Optical Access Networks Based on Orthogonal Frequency Division Multiplexing

MASTER DEGREE: Master of Science in Telecommunication Engineering and Management

AUTHOR: Marçal de las Heras Mandome

DIRECTOR: Concepción Santos Blanco

DATE: September 30th 2011

ANNEXES A. FREQUENCY OFFSET MATHEMATICAL STUDY

ANNEXES A.1 Ideal Case

OFDM original signal:

$$X_{OFDM}(t) = \sum_{K=0}^{N-1} a_k \cdot e^{j2\pi k\Delta f t}$$

At Rx sample each t at $t = \frac{n}{N\Delta f}$

$$X_{OFDM}(n) = \sum_{K=0}^{N-1} a_k \cdot e^{j\frac{2\pi kn}{N}}$$

Performing the IFFT of the given OFDM signal:

$$\Gamma_{OFDM}(m) = \frac{1}{N}\sum_{K=0}^{N-1} X_{OFDM}(n) \cdot e^{-j\frac{2\pi nm}{N}} = \sum_{n=0}^{N-1}\sum_{k=0}^{N-1} a_k \cdot e^{j\frac{2\pi n}{N}(k-m)} = a_m$$

Now, with a certain frequency offset:

$$\Delta\nu \rightarrow \delta = \frac{\Delta\nu}{\Delta f} \qquad X_{OFDM}(t) = \sum_{K=0}^{N-1} a_k \cdot e^{j2\pi(k\cdot\Delta f + \Delta\nu)t}$$

Sampled:

$$X_{OFDM}(n) = \sum_{K=0}^{N-1} a_k \cdot e^{j2\pi(k\cdot\Delta f+\Delta\nu)\frac{n}{N\cdot\Delta f}} = \sum_{k=0}^{N-1} a_k \cdot e^{j\frac{2\pi kn}{N}} \cdot e^{j\frac{2\pi n\Delta\nu}{N\cdot\Delta f}}$$

Perform the IFFT:

$$\Gamma_{OFDM}(m) = \sum_{n=0}^{N-1} e^{j\frac{2\pi n}{N}\cdot\delta} = \sum_{k=0}^{N-1} a_k \cdot e^{j\frac{2\pi kn}{N}} \cdot e^{-j\frac{2\pi nm}{N}}$$

$$= \sum_{k=0}^{N-1} a_k \cdot \underbrace{\sum_{n=0}^{N-1} e^{j\frac{2\pi n}{N}(k-m+\delta)}}_{\frac{1-e^{j2\pi(k-m+\delta)}}{1-e^{j2\pi/N(k-m+\delta)}} = \frac{e^{j\pi(k-m+\delta)}}{e^{j\pi/N(k-m+\delta)}} = \frac{\sin(\pi(k-m+\delta))}{\sin(\pi/N(k-m+\delta))}}$$

$$\Gamma(m) = \sum_{k=0}^{N-1} a_k \cdot \frac{\sin(\pi(k-m+\delta))}{\sin(\pi/N(k-m+\delta))} \cdot e^{j\pi(k-m+\delta)\frac{N-1}{N}}$$

If:

$$\sin(\pi(k-m+\delta))\cdot\cos(\pi\delta) + \cos(\pi(k-m+\delta))\cdot\sin(\pi\delta) = e^{j\pi(k-m)}\cdot\sin(\pi\delta)$$

$$\Gamma(m) = \sum_{k=0}^{N-1} a_k \cdot \frac{\sin(\pi(k-m+\delta))}{\sin(\pi/N(k-m+\delta))} \cdot e^{j\pi(k-m+\delta)\frac{N-1}{N}}$$

Then:

$$\Gamma(m) = \sum_{k=0}^{N-1} a_k \cdot \frac{\sin(\pi\delta)}{\sin(\pi/N(k-m+\delta))} \cdot e^{-j\frac{\pi(k-m)}{N}} \cdot e^{j\pi\delta\frac{N-1}{N}} = \sin(\pi\delta)\cdot e^{j\pi\delta\frac{N-1}{N}} \cdot \sum_{k=0}^{N-1} \frac{a_k \cdot e^{-j\frac{\pi(k-m)}{N}}}{\sin(\pi/N(k-m+\delta))} \cdot$$

$$\Gamma(m) = \sum_{k=0}^{N-1} a_k \cdot \frac{\sin(\pi\delta)}{\sin(\pi/N(k-m+\delta))} \cdot e^{j2\pi(k-m)} \cdot e^{-j\frac{\pi(k-m)}{N}} \cdot e^{j\pi\delta\frac{N-1}{N}}$$

$$k = m \rightarrow \Gamma(m) = a_m \cdot \frac{\sin(\pi\delta)}{\sin(\pi\delta/N)} e^{j\pi\delta\frac{N-1}{N}}$$

ANNEXES B. SETUP SPECIFICATIONS

In this annexes chapter, all the parameters and its values of the simulations performed in this Master Thesis are shown. First of all, the parameters and values of the VPI Long-Haul simulation template are indicated as a reference, then, the rest of simulations show only the different parameters regard the original template.

VPI template Long-Haul Simulation

- Laser CW Emission Frequency: 193,1THz
- Laser Average power: 5.0e-3
- Laser Linewidth: 1e6
- Drive amplitude: 0.17 A,V
- Bias: 0.5 A,V
- Carrier Frequency OFDM signal: 7.5 e9 Hz
- Bandwidth OFDM signal: 5 GHz
- OFDM Carriers: 64
- Roll Off: 0.2
- Bit Rate: 10 Gbps
- Time window: 8*1024/Bit rate (spectral resolution)
- Sample rate: 4*Bit rate (max frequency simulatable, Hz)
- Modulation: 4-QAM
- Cyclic Prefix: 0.125
- Chirp: No option configurable
- Fiber length: 1000 Km
- Op filter BW: 18e9
- Op filter Gaussian order: 3
- Op filter central freq: 193.1e12+7.5e9

Simulation setup 1: VPI template Adaptation Simulation (Figure 4.5)

- Fiber length: 20 Km
- Op filter Disabled
- Bit Rate: 1Gbps
- Bandwidth OFDM signal: 500 MHz
- Chirp: 0

Simulation setup 2: Optical filter analysis scenario 1 (Figure 4.7) With Filter

- Laser central frequency: 193.1THz

- Value to sweep: fiber length
- Iterations: 40
- Ramp value fiber: 1.75Km
- Fiber length starting value : 1m
- Carrier Frequency OFDM signal: 1GHz
- Bandwidth OFDM signal: 100 MHz
- OFDM Carriers: 16
- Bit Rate: 200 Mbps
- Time window: 8*256/Bit rate (spectral resolution)
- Sample rate: 128*Bit rate (max frequency simulatable, Hz)
- Modulation: 4-QAM
- Roll-off factor= 0.18
- Op SSB filter center Frequency: 193.1e12+1e9
- Op SSB filter bandwidth: 150e6 Hz
- Op SSB filter Gaussian order: 3

Simulation setup 3: Optical filter analysis scenario 2 (Figure 4.7) without filter

- Laser central frequency: 193.1THz
- Value to sweep: fiber length
- Iterations: 40
- Ramp value fiber: 1.75Km
- Fiber length starting value : 1m
- Carrier Frequency OFDM signal: 1GHz
- Bandwidth OFDM signal: 100 MHz
- OFDM Carriers: 16
- Bit Rate: 200 Mbps
- Time window: 8*256/Bit rate (spectral resolution)
- Sample rate: 128*Bit rate (max frequency simulatable, Hz)
- Modulation: 4-QAM
- Roll-off factor= 0.18
- No Op SSB filter

Simulation setup 4: Optical filter analysis scenario 2 (Figure 4.7) 1 Gbps

- With filter:

- Laser central frequency: 193.1THz
- Value to sweep: fiber length
- Iterations: 40
- Ramp value fiber: 1.75Km
- Fiber length starting value : 1m
- Carrier Frequency OFDM signal: 1GHz
- Bandwidth OFDM signal: 500 MHz
- OFDM Carriers: 16

- Bit Rate: 1 Gbps
- Time window: 8*256/Bit rate (spectral resolution)
- Sample rate: 128*Bit rate (max frequency simulatable, Hz)
- Modulation: 4-QAM
- Roll-off factor= 0.18
- Op SSB filter center Frequency: 193.1e12+1e9
- Op SSB filter bandwidth: 600e6 Hz
- Op SSB filter Gaussian order: 3

- <u>Without filter:</u>

- Laser central frequency: 193.1THz
- Value to sweep: fiber length
- Iterations: 40
- Ramp value fiber: 1.75Km
- Fiber length starting value : 1m
- Carrier Frequency OFDM signal: 1GHz
- Bandwidth OFDM signal: 500 MHz
- OFDM Carriers: 16
- Bit Rate: 1 Gbps
- Time window: 8*256/Bit rate (spectral resolution)
- Sample rate: 128*Bit rate (max frequency simulatable, Hz)
- Modulation: 4-QAM
- Roll-off factor= 0.18
- No Op SSB filter

<u>Simulation setup 5: Optical filter analysis scenario 2 (Figure 4.7) 10 Gbps</u>

- <u>With filter:</u>

- Laser central frequency: 193.1THz
- Value to sweep: fiber length
- Iterations: 40
- Ramp value fiber: 1.75Km
- Fiber length starting value : 1m
- Carrier Frequency OFDM signal: 10GHz
- Bandwidth OFDM signal: 5 GHz
- OFDM Carriers: 16
- Bit Rate: 10 Gbps
- Time window: 8*256/Bit rate (spectral resolution)
- Sample rate: 128*Bit rate (max frequency simulatable, Hz)
- Modulation: 4-QAM
- Roll-off factor= 0.18
- Op SSB filter center Frequency: 193.1e12+10e9
- Op SSB filter bandwidth: 6 GHz

- Op SSB filter Gaussian order: 3

- <u>Without filter:</u>

- Laser central frequency: 193.1THz
- Value to sweep: fiber length
- Iterations: 40
- Ramp value fiber: 1.75Km
- Fiber length starting value : 1m
- Carrier Frequency OFDM signal: 10GHz
- Bandwidth OFDM signal: 5 GHz
- OFDM Carriers: 16
- Bit Rate: 10 Gbps
- Time window: 8*256/Bit rate (spectral resolution)
- Sample rate: 128*Bit rate (max frequency simulatable, Hz)
- Modulation: 4-QAM
- Roll-off factor= 0.18
- No Op SSB filter

<u>Simulation setup 6: Guard Band analysis scenario 1 (Figure 4.5 and Chart 4.6)</u>

- Laser1 CW: 193,1THz
- Laser Peak power: 3*1.0e-3
- Laser Linewidth: 100e3
- Sweep Carrier Frequency starting value: 1e9 Hz
- Sweep Carrier Frequency end value: 7.5e9 Hz
- Sweep Carrier Frequency step:10e6 Hz
- Bandwidth OFDM signal: 2 GHz
- OFDM Carriers: 16
- Bit Rate: 4 Gbps
- Time window: 8*1024/BitRate (spectral resolution)
- Sample rate: 8*BitRate (max frequency simulatable, Hz)
- Cyclic Prefix: 0
- Chirp: 0
- Fiber length: 20 Km
- No Op SSB filter

<u>Simulation setup 7: Guard Band analysis scenario 2 (Figure 4.5 and Chart 4.7)</u>

- Laser1 CW: 193,1THz
- Laser Peak power: 3*1.0e-3
- Laser Linewidth: 100e3
- Sweep Carrier Frequency starting value: 2.5e9 Hz

- Sweep Carrier Frequency end value: 9e9 Hz
- Sweep Carrier Frequency step: 10e6 Hz
- Bandwidth OFDM signal: 5 GHz
- OFDM Carriers: 16
- Bit Rate: 10 Gbps
- Time window: 8*1024/BitRate (spectral resolution)
- Sample rate: 8*BitRate (max frequency simulatable, Hz)
- Cyclic Prefix: 0
- Chirp: 0
- Fiber length: 20 Km
- No Op SSB filter

Simulation setup 8: Guard Band analysis scenario 3 (Figure 4.5 and Chart 4.8)

- Laser1 CW: 193,1THz
- Laser Peak power: 3*1.0e-3
- Laser Linewidth: 100e3
- Sweep Carrier Frequency starting value: 1e9 Hz
- Sweep Carrier Frequency end value: 9e9 Hz
- Sweep Carrier Frequency step: 10 e6
- Bandwidth OFDM signal: 5 GHz
- OFDM Carriers: 16
- Bit Rate: 10 Gbps
- Time window: 8*1024/BitRate (spectral resolution)
- Sample rate: 8*BitRate (max frequency simulatable, Hz)
- Cyclic Prefix: 0
- Chirp: 0
- Fiber length: 60 Km
- No Op SSB filter

Simulation setup 9: SE analysis scenario 1 (Figure 5.9 and Figure 5.10)

- Laser1 CW: 193,1THz
- Laser2 pulsed: 193,1THz

- Lasers Peak power: 3*1.0e-3
- Laser Linewidth: 100e3
- Random number seed: 1,5

- Carrier Frequency OFDM signal: 1e9 MHz

- Bandwidth OFDM signal: 100 MHz
- OFDM Carriers: 16
- Bit Rate: 200 Mbps
- Time window: 16*1024/BitRate (spectral resolution)

- Sample rate: 32*BitRate (max frequency simulatable, Hz)
- Cyclic Prefix: 0
- Chirp: 0
- Fiber length: 1m
- No Op SSB filter

Simulation setup 10: SE analysis scenario 2 (Figure 5.10 and Figure 5.14)

- Laser1 CW: 193,1THz + 100 KHz
- Laser2 pulsed: 193,1THz

- Lasers Peak power: 3*1.0e-3
- Laser Linewidth: 100e3
- Random number seed: 1,5

- Carrier Frequency OFDM signal TX: 500 MHz
- Carrier Frequency OFDM signal RX: 400e6 MHz

- Bandwidth OFDM signal: 100 MHz
- OFDM Carriers: 16
- Bit Rate: 200 Mbps
- Time window: 16*1024/BitRate (spectral resolution)
- Sample rate: 32*BitRate (max frequency simulatable, Hz)
- Cyclic Prefix: 0
- Chirp: 0
- Fiber length: 1m
- No Op SSB filter

Simulation setup 11: SE analysis scenario 3 (Figure 5.10 and Figure 5.17)

- Laser1 CW: 193,1THz + 10 KHz
- Laser2 pulsed: 193,1THz

- Lasers Peak power: 3*1.0e-3
- Laser Linewidth: 0
- Random number seed: 0,0

- Carrier Frequency OFDM signal: 500e6 MHz

- Bandwidth OFDM signal: 100 MHz
- OFDM Carriers: 16
- Bit Rate: 200 Mbps
- Time window: 16*1024/BitRate (spectral resolution)
- Sample rate: 32*BitRate (max frequency simulatable, Hz)
- Cyclic Prefix: 0
- Chirp: 0

- Fiber length: 1m

Simulation setup 12: LC analysis scenario (Figure 5.10 and Figure 5.26)

- Laser1 CW: 193,1THz + 400MHz
- Laser2 pulsed: 193,1THz
- Laser3 CW: 193,1THz - 400MHz
- Iterations: 40
- Ramp value Laser1: 50MHz
- Ramp value Laser3: -50MHz

- Lasers Peak power: 3*1.0e-3
- Laser Linewidth: variable.
- Random number seed: variable
- Carrier Frequency OFDM signal: 150e6 MHz
- Bandwidth OFDM signal: 100 MHz
- OFDM Carriers: 16
- Bit Rate: 200e6 bps
- Time window: 8*256/BitRate (spectral resolution)
- Sample rate: 64*BitRateDefault (max frequency simulatable, Hz)
- Modulation: 4-QAM
- Cyclic Prefix: 0
- Chirp: 0
- Fiber length: 1 m
- Op filter BW: dissabled
- Op filter Gaussian order: dissabled
- Op filter central freq: dissabled

ANNEXES C. THE ERROR VECTOR MAGNITUDE

Mostly, the results which are presented in this project have been evaluated by means of the analysis of the received 4-QAM constellation. So, to evaluate the results of the simulations it is necessary a quantitative measurement of the received constellations.

The Error Vector Magnitude (EVM) is the measurement used to evaluate the quality of the transmission in the simulations. Basically, the error vector is the difference between the measured signal at the receiver side and an ideal reference signal. EVM is a performance metric to evaluate the quality of communication. EVM expresses the difference between the expected complex value of a demodulated symbol and the value of the actual received symbol [P7].

Each different modulation format such as BPSK, 4-QAM or 16-QAM has different amplitude levels. To calculate and compare EVM measurements effectively a normalization is necessary.

EVM is defined as the root-mean-square (RMS) value of the difference between a set of measured symbols and ideal symbols. The differences among them are averaged over a given large number of symbols. Figure C 1 shows the procedure:

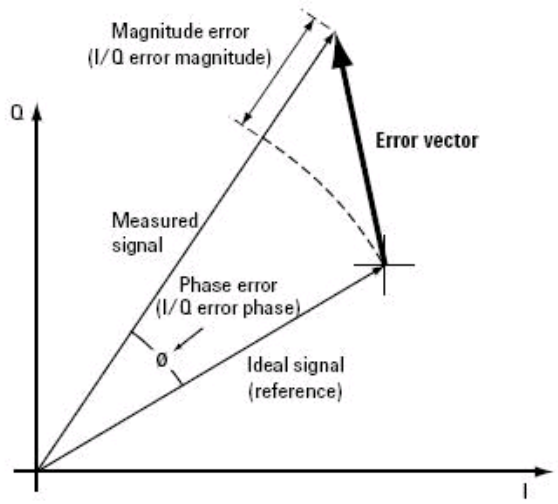

Figure C 1. EVM calculation schematic

The receiver modules used in the simulations estimate the EVM for m-QAM signals. They use decoded electrical I and Q signals. Those modules perform clock recovery and data and phase correction by multiplying the received signal

expressed in the complex domain as *IRx* + *iQRx* (*IRx* and *QRx* are the in-phase and quadrature signals) with the following factor [P9]:

$$C = \frac{1}{N}\sum_{k=1}^{N}\frac{I_{TXk} + iQ_{TXk}}{I_{RXk} + iQ_{RXk}} \qquad \textbf{(E C. 1)}$$

where *N* is the number of transmitted symbols. *ITx* and *QTx* stand for the in-phase and quadrature coded symbols at the transmitter Depending the order of the modulation, *m*.The following values for *ITx* and *QTx* are generated [P9]:

- 4-QAM (m=2) Output amplitudes = -1+1
- 16-QAM (m=4) Output amplitudes = -3 -1 +1 3
- 64-QAM (m=6) Output amplitudes = -7 -5 -3 -1 +1 3 5 7
- 256-QAM (m=8) Output amplitudes = -15 -13 -11 -9 -7 -5 -3 -1 +1 3 5 7 9 11 13 15

The relative constellation root-mean-square error (EVM) is calculated as [P9]:

$$EVM = \sqrt{\frac{\sum_{i=1}^{N}(I_{TXi} - I_{RXi})^2 + (Q_{TXi} - Q_{RXi})^2}{\sum_{i=1}^{N}(I^2{}_{TXi} + Q^2{}_{TXi})}} \qquad \textbf{(E C. 2)}$$

In our simulations the EVM calculations are performed by the EVM estimator VPI module. Once the method to calculate the EVM is explained, it is necessary to establish certain thresholds and acceptable values of EVM to evaluate the quality of the received constellation. According to [P13], a range between -10dB and -13dB for 4-QAM (QPSK) constellation has been considered. The equivalent dimensionless values for the previous range are (0.05 – 0.08).

Carrier Modulation	Maximum EVM (dB)
BPSK	−5
BPSK	−8
QPSK	−10
QPSK	−13
16-QAM	−16
16-QAM	−19
64-QAM	−22
64-QAM	−25

Figure C 2. Maximum EVM values related to the modulation scheme